UNIVERSITY OF SOUTHAMPTON

FACULTY OF ENGINEERING, SCIENCE AND MATHEMATICS

School of Ocean and Earth Science

Bacterioplankton community composition and activity in the Atlantic Ocean

By

Jane Louise Heywood

Thesis for the degree of Doctor of Philosophy

October 2007

Graduate School of the
Southampton Oceanography Centre

This PhD dissertation by

Jane Louise Heywood

has been produced under the supervision of the following persons

Supervisor/s

Dr. Mikhail Zubkov, Prof. Patrick Holligan

Chair of Advisory Panel

Dr. Rachel Mills

Member/s of Advisory Panel

UNIVERSITY OF SOUTHAMPTON

ABSTRACT

FACULTY OF ENGINEERING, SCIENCE AND MATHEMATICS
SCHOOL OF OCEAN AND EARTH SCIENCES

Doctor of Philosophy

BACTERIOPLANKTON COMMUNITY COMPOSITION AND ACTIVITY IN THE ATLANTIC OCEAN

By Jane Louise Heywood

Temporal and spatial patterns of bacterioplankton in six different provinces of the Atlantic Ocean were examined between 1996 and 2004. The abundance and integrated biomass of three prokaryote groups (*Prochlorococcus* spp.*, Synechococcus* spp. and heterotrophic bacteria) were used to detect standing stock changes and characterise community structure in the Northern and Southern oligotrophic gyres and in the equatorial region. There was no statistically significant inter-annual variability in *Prochlorococcus* or *Synechococcus* abundance or integrated biomass in any of the provinces. The abundance and biomass of the remaining prokaryoplankton was variable but this variation could not be ascribed to seasonal differences and did not follow a clear inter-annual trend.

The importance of the microbial loop in recycling organic nutrients in the upper Atlantic Ocean was also studied by comparing ratios of bacterial to primary production in different oceanic provinces. A proportionately higher rate of photosynthetically fixed carbon flowed through the microbial loop in the Northern oligotrophic gyre (22 – 55 %) compared to the other provinces studied. This indicates a difference in energy flow through the ecosystem in different oceanic regions with a greater emphasis on energy flow through the microbial loop in the Northern oligotrophic gyre probably due to reduced grazing of phytoplankton and reduced export production compared to other Atlantic Ocean provinces.

The role of defined groups of bacteria in the cycling of nutrients was identified using a combination of flow cytometric sorting with radiotracer uptake and CARD-FISH. The SAR11 clade of bacteria were found to dominate the low nucleic acid group of bacterioplankton and as such it was possible to quantify the activity and abundance of these cells in the Atlantic Ocean. Despite their small genome size, SAR11 bacteria were found to be generally as active as an average bacterioplankton cell and were responsible for between 30 and 50 % of the total community methionine uptake.

This research has characterised bacterioplankton composition and activity in Atlantic Ocean provinces thus enabling further understanding of the function and importance of the microbial loop in the upper ocean.

Contents

List of Tables

List of Figures

ACKNOWLEDGEMENTS

I would firstly like to thank my supervisors, Dr Mikhail Zubkov (NOC) and Prof Patrick Holligan (NOC) for their support and guidance throughout this project.

Secondly I would like to thank Dr Bernhard Fuchs (MPI) and Martha Schattenhoffer (MPI) for help and advice with fluorescence *in situ* techniques and for the provision of the probes used in this study. Also to Dr Glen Tarran (PML) for the use of flow cytometry facilities and to the post-doctoral researchers and technicians who have given advice and assistance in analysing samples; Dr Isabelle Mary, Dr Juliette Topping and Ross Holland (NOC).

I would also like to acknowledge and thank all the participants of the Atlantic Meridional Transect Programme who collected, analysed samples and conducted experiments during the AMT cruises. In particular, Dr Alex Poulton (NOC) for providing me with primary production data, Katie Chamberlain (PML) and Malcolm Woodward (PML) for supplying nitrate concentrations and Dr Mike Zubkov for providing me with samples and data from earlier AMT cruises. I also thank the British Oceanographic Data Centre for providing data from past and present AMT cruises. I would also like to thank Dr Peter Ward (BAS) for providing me with samples from the Scotia Sea.

In addition, I would like to thank all the principal scientists for their help during the work at sea, as well as the captain, crew, UKORS engineers and of course all the other scientists on board *RRS James Clark Ross* and *RRS Discovery* for their excellent support.

This work was supported by the Natural Environmental Research Council through the Atlantic Meridional Transect consortium (NER/0/5/2001/00680),

Finally, I thank my friends and family for their continual encouragement and support.

Abbreviations

AAnP	Aerobic anoxygenic phototrophs
ACC	Antarctic Circumpolar Current
ADCP	Acoustic doppler current profiler
AMT	Atlantic Meridional Transect
ANOVA	Analysis of variance
BATS	Bermuda Atlantic time-series
BCD	Bacterial carbon demand
BP	Bacterial production
BSi	Boron silicon
C	Carbon
CARD	Catalysed reporter deposition
CDOM	Coloured dissolved organic matter
CH_4	Methane
CO_2	Carbon dioxide
CTD	Conductivity, temperature, depth profiler
DCM	Deep chlorophyll maximum
DMS	Dimethyl sulphide
DOC	Dissolved organic carbon
DOM	Dissolved organic matter
DON	Dissolved organic nitrogen
EQ	Equatorial upwelling
FISH	Fluorescence *in situ* hybridisation
f_{max}	Fluorescence maximum (equal to the chlorophyll maximum)
FRFF	Fast repetition rate fluorometer
GMT	Greenwich mean time
HB	Heterotrophic bacteria
HCl	Hydrochloric acid
HNLC	High nutrient low chlorophyll
HOT	Hawaii Ocean time-series
HPLC	High performance liquid chromatography
leu	Leucine
met	Methionine
N	Nitrogen
N_2O	Nitrous oxide
NAG	North Atlantic gyre

NEC	North Equatorial Current
NECC	North Equatorial Countercurrent
NH_3	Ammonia
NO_2	Nitrite
NO_3	Nitrate
NT	Northern temperate region
P	Phosphorus
PAR	Photosynthetically active radiation
pCO_2	Partial pressure carbon dioxide
PCR	Polymerase chain reaction
PF	Polar Front
PFA	Paraformaldehyde
PIC	Particulate inorganic carbon
PO_4	Phosphate
POC	Particulate organic carbon
PON	Particulate organic nitrogen
PP	Primary production
Pro	*Prochlorococcus*
rRNA	Ribosomal ribonucleic acid
RFLP	Restriction fragment length polymorphism
SACCF	Southern Antarctic Circumpolar Current Front
SAF	Subantarctic Front
SAG	South Atlantic gyre
SAPS	Stand alone pump system
SBACC	Southern Boundary of the Antarctic Circumpolar Current
Sc	Scotia Sea
SeaWiFs	Sea-viewing wide field-of-view sensor
SEC	South Equatorial Current
SiO_4	Silicate
SSU	Small subunit
ST	Southern temperate region
Syn	*Synechococcus*
TCA	Trichloroacetic acid
TCO_2	Total carbon dioxide
UP	North West African upwelling

Chapter 1

Introduction

1.1 Prokaryotes

Prokaryotes encompass the two domains; Bacteria and Archaea. The first prokaryotes appeared approximately 3.8 billion years ago (Mojzsis et al., 1996) and this combined with their high growth rates has facilitated great evolutionary changes. Consequently the Bacteria domain has the greatest diversity of any of the three domains of life. Prokaryotes have evolved to exist in many, often extreme, environments where other forms of life cannot survive (Edwards et al., 2000; Thomas and Dieckmann, 2002). Prokaryotes are the most abundant and ubiquitous organisms on the planet with an estimated 4 - 6 x 10^{30} cells of which 1.2 x 10^{29} cells are found in the global ocean (Whitman et al., 1998). Although prokaryotic cells are very small (typically 0.2 – 1 µm diameter in the open ocean), their high global abundance results in estimates of the global prokaryotic carbon biomass between 60 – 100 % that of the estimated total plant carbon biomass (Whitman et al., 1998).

1.2 Bacterioplankton diversity

Prior to the study of marine prokaryotic community composition, bacterioplankton measurements were made on the community as a whole. It has since been determined that there is great diversity in community composition as well as the function of different bacteria and archaea with prokaryotic plankton consisting of phylogenetically and metabolically diverse groups (Giovannoni and Rappe, 2000). The majority of marine bacteria fall into one of the following phylogenetic branches of the Bacteria domain: alpha, gamma or beta proteobacteria, *Cytophaga-Flavobacterium-Bacteroides* group, *Planctomycetales* or the cyanobacteria (Giovannoni and Rappe, 2000; Fig. 1.1). Archaeal diversity is less well known but members of the two major clades, Crenarchaeota and Euryarchaeota are present in the water column (Giovannoni and Rappe, 2000; Fig. 1.1). Until relatively recently, Archaea were thought to only be important in extreme environments such as deep-sea hydrothermal vents and high saline environments and were not considered to be present in significant numbers in the water column (Woese et al., 1990). It was not until 1992 when archaeal rDNA sequences were found in samples from the Pacific and Atlantic Oceans (DeLong, 1992; Fuhrman et al., 1992). The prokaryotic plankton community was therefore

referred to as bacterioplankton and this term is still used in many studies, including this one, to refer to both planktonic bacteria and archaea.

Figure 1.1: Phylogeny of the major marine and freshwater prokaryotes. (Adapted from Giovannoni and Sting, 2005).

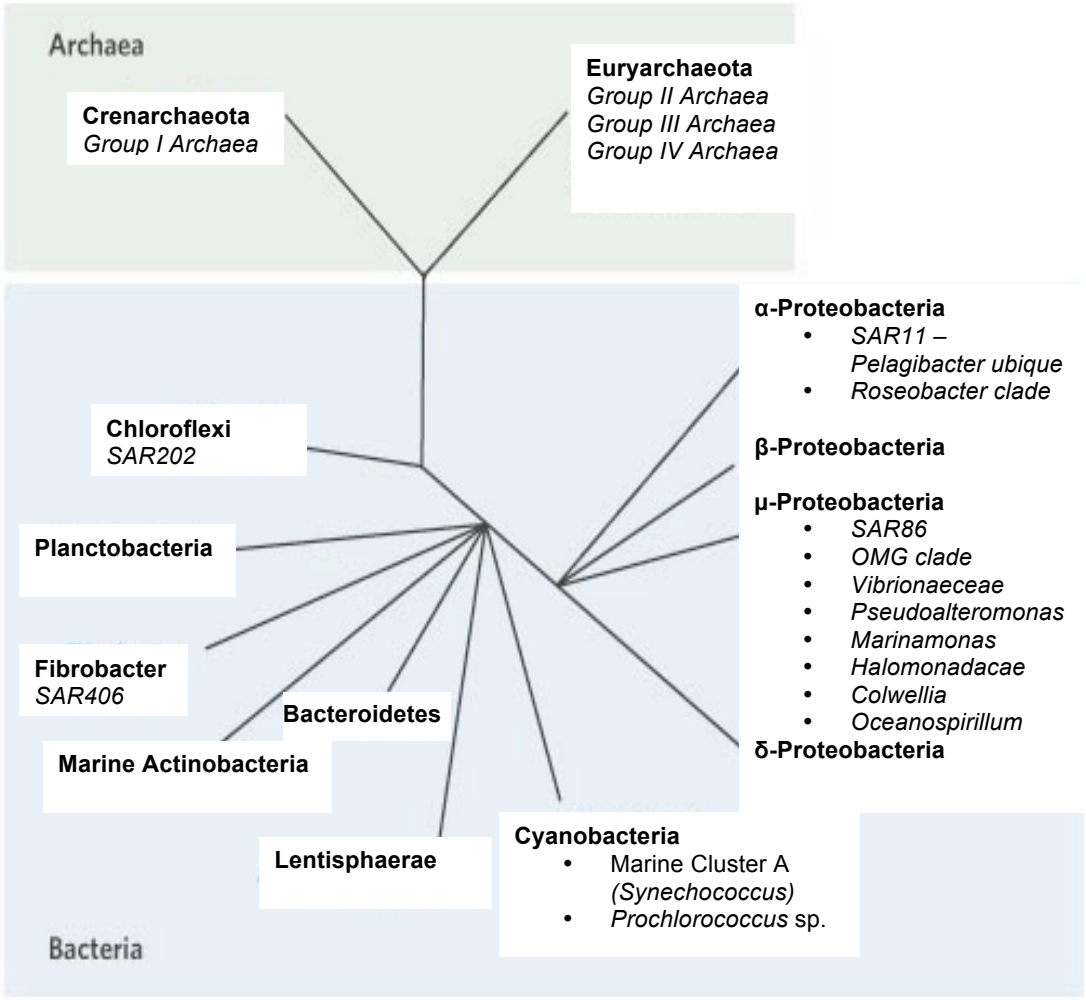

Although molecular analysis of mixed bacterial communities has led to the identification of several novel groups, gene clusters obtained from the environment exhibit high genetic variability within the groups and as many of the sequences are not found in culture, the exact number of species present in seawater samples is unknown (Curtis *et al.*, 2002). As a result, research has focused on determining metabolic diversity in the marine microbial community rather than identifying individual species. For example, members of the *Planctomycetales* group have been shown to be important anaerobic

oxidizers of ammonium to N_2 in anoxic waters (Kuypers *et al.*, 2003). Methane oxidising bacteria or methanotrophs have also been identified in the gamma and alpha *Proteobacteria* groups (Hanson and Hanson, 1996) some of which are capable of nitrogen fixation (Auman *et al.*, 2001).

Bacteria have been considered as heterotrophs as part of the marine microbial loop, however, autotrophic bacteria can be abundant in the microbial community of oceanic waters. The two dominant groups of oceanic phototrophic bacteria are the coccoid cyanobacteria *Synechococcus* and the prochlorophyte *Prochlorococcus* which have since been shown to contribute up to 45% of phytoplankton carbon biomass (Campbell and Vaulot, 1993). Two genetically distinct populations of *Prochlorococcus* have been identified, one that is common in water with high light intensities and one that is common in low light intensities. These two populations have adapted to their respective niches by varying the ratio of chlorophyll b_2/a_2, therefore altering the efficiency of photosynthesis (Moore *et al.*, 1998).

The classical view of marine microbes being either heterotrophic or phototrophic is changing with the discovery of mixotrophic bacteria that can obtain energy from both photosynthesis and heterotrophic respiration. For example, *Prochlorococcus*, was traditionally considered to be entirely phototrophic but has recently been found to take up amino acids at high rates, particularly the low-light adapted species (Zubkov *et al.*, 2004).

Some obligate heterotrophic bacteria have been found to contain photosynthetic pigments such as carotenoids, bacteriochlorophyll a (Kolber *et al.*, 2001) and proteorhodopsin and are capable of phototrophy (Beja *et al.*, 2001). Bacteriochlorophyll-containing aerobic anoxygenic phototrophs (AAnPs), although not capable of photosynthesis, do have the ability to harvest light energy thus reducing the energy required from heterotrophic metabolism, giving them an ecological advantage in photic, oligotrophic environments (Yurkov and Beatty, 1998). Until recently the energetic role of proteorhodopsin was uncertain, however experiments using *E. coli* have found that this light-driven proton pump is activated during periods of respiratory inhibition, thereby facilitating bacterial survival in oxygen depleted illuminated waters (Walter et al., 2007).

1.3 Prokaryote physiology

A typical prokaryote cell contains approximately 50 % carbon and 12 % nitrogen (dry weight). Some bacteria are capable of utilising CO_2 via photosynthesis however the majority of prokaryotes must obtain carbon in other forms from the environment. This is usually in the form of amino acids, fatty acids, organic acids, sugars or aromatic compounds (Madigan and Martinko, 2006). Some bacteria are able to fix N_2 but most prokaryotes take up nitrogen in the form of ammonia (NH_3) and some are able to assimilate nitrate (NO_3). Organic nitrogen compounds are also a source for many prokaryotes e.g. amino acids and nitrogen bases of nucleotides (Giovannoni and Rappe, 2000).

Other macronutrients needed for cell growth are phosphorus (for nucleic acid and phospholipids synthesis), sulphur (for methionine, cysteine and vitamin synthesis), potassium (for enzymes involved in protein synthesis), magnesium (for cell structure and enzyme function), calcium (for bacterial cell wall stabilisation) and sodium (required for the growth of marine prokaryotes). Iron is also required for the proteins and cytochromes involved in electron transport in respiration (Madigan and Martinko, 2006).

1.4 Bacterioplankton distribution

Abiotic factors that may influence the distribution of bacteria include temperature, light and availability of organic nutrients. For example, studies in the Atlantic Ocean have shown that water temperature is positively correlated with the ratio of bacterial production to primary production, and, more strongly, with the ratio of bacterial carbon demand to primary production (Hoppe *et al.*, 2002). The abundance of bacteria in the western North Atlantic is correlated with the concentration of soluble reactive phosphorus, however the same study showed that the distribution of *Prochlorococcus* was independent of nutrient concentrations but unlike other prokaryotic groups, was correlated with temperature (Cavender-Bares *et al.*, 2001).

Bacterial distribution has been examined at millimetre (Seymour *et al.*, 2000; Long and Azam, 2001), centimetre (Mitchell and Fuhrman, 1989; Duarte and Vaque, 1992) and metre scales (Ducklow, 2000). Vertical stratification of bacterial communities exists in the water column, with alpha *Proteobacteria* dominating in the upper surface layer (the most abundant clades are the *Roseobacter,* SAR11 and SAR116 clades) and the

SAR202, SAR324 and Marine Group A clades dominating bacterial communities in the aphotic zone (Giovannoni and Rappe, 2000).

1.5 The microbial loop

Heterotrophic bacterioplankton transport low molecular weight organic molecules across the cell wall into the cell and obtain energy for growth through the respiration of these organic molecules. Between 5 and 50% of carbon fixed by phytoplankton is released as dissolved organic matter (DOM) (Larsson and Hagstrom, 1982). Several studies have indicated that the majority of this DOM is taken up by heterotrophic bacterioplankton (Azam, 1998; Azam et al., 1983; Ducklow, 2000). Bacteria are grazed upon by heterotrophic flagellates which are in turn preyed upon by microzooplankton thus forming a 'microbial loop' (Fig. 1.2) that returns carbon to the food web that would have otherwise been lost via DOM (Azam *et al.*, 1983).

The rate of bacterioplankton biomass production quantifies the role of prokaryotes in the carbon cycle of the open ocean. In order to study the amount of carbon flowing through the microbial loop and hence the importance of it in marine food webs, the growth rate and bacterial carbon demand (BCD) of bacteria must be determined. The incorporation of radiolabelled metabolic precursors into cells along with measurements of growth rates has enabled the rate of production of bacterial organic matter to be determined (Fuhrman and Azam, 1980; Kirchman *et al.*, 1985). This measure of bacterial production reflects the amount of organic matter available to other trophic levels in the food web. Heterotrophic bacteria obtain energy from the respiration of organic matter and therefore the BCD is greater than the rate of bacterial production. However, the BCD can be calculated if the efficiency of bacterial growth is known (Ducklow, 2000).

Bacterial production is commonly determined by measuring the uptake of labile organic molecules, for example, thymidine or leucine (Fuhrman and Azam, 1982; Kirchman, 1993)(Zubkov et al., 2000). Thymidine is incorporated into DNA and is therefore a measure of DNA synthesis whereas leucine is incorporated into protein and is therefore a measure of protein synthesis. The rates of either DNA or protein synthesis are related to cell growth and could be converted into the rate of new biomass production using conversion factors.

The rate of net primary production by phytoplankton is a key element of the global carbon cycle and has been estimated for the global ocean to be 45 to 50 Pg C per annum (Field et al., 1998; Longhurst et al, 1995). In recent years, the importance of the microbial loop in returning carbon to the marine food web has been studied by comparing the rate of primary production to the rate of bacterial production. Studies in the subarctic Pacific (Kirchman *et al.*, 1993), subarctic NE Atlantic (Ducklow *et al.*, 1993), Southern Ocean (Bjornsen and Kuparinen, 1991) and Arabian Sea (Pomroy and Joint, 1999) have examined bacterial production (BP) as a percentage of primary production (PP) and produced values ranging from 3 to 50 %. However, more recent estimates of BP/PP in non-polar oceanic regions are between 8 and 13% (Ducklow, 2003).

Figure 1.2: Sources and pathways of nutrients through the marine ecosystem and the microbial loop.

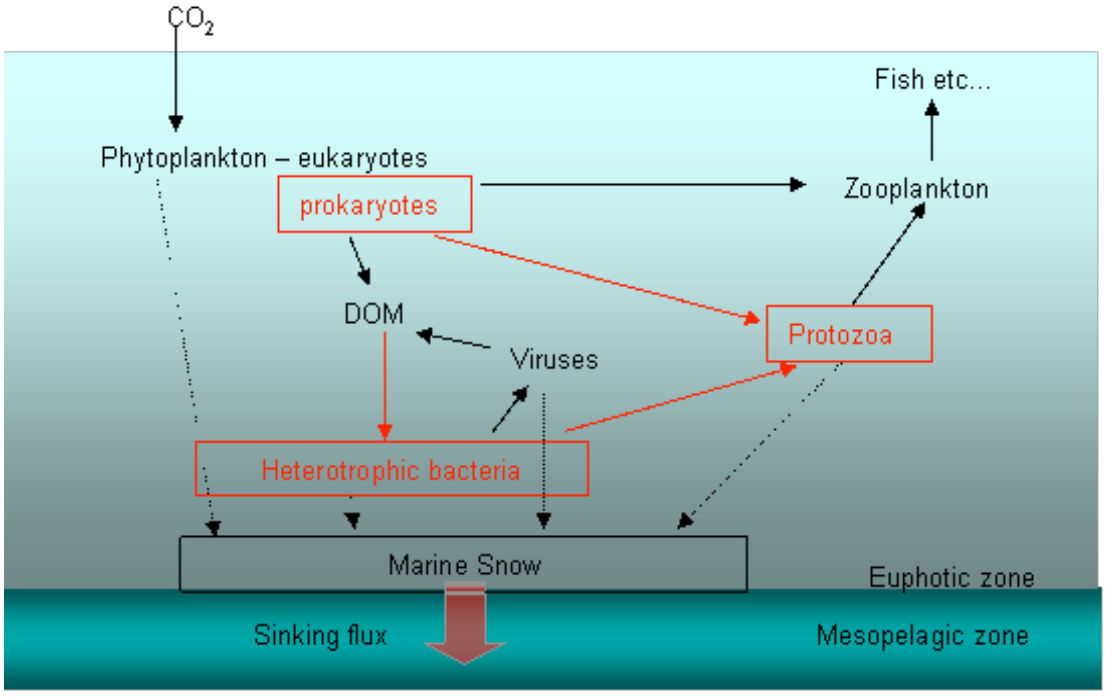

1.6 Recent developments in marine microbial ecology

Prior to the 1970s the primary role of bacterioplankton in oceanic food webs was thought to be as decomposers of organic matter. This view has changed considerably during the past twenty years with heterotrophic bacteria now shown to dominate the cycling of organic matter via the 'microbial loop' (Azam *et al.*, 1983; Ducklow *et al.*,

2000). This recent turnaround in opinion is a result of technological advances in marine microbial ecology.

In 1977, Hobbie *et al*. reported bacterial concentrations measured using epifluorescence microscopy that were several orders of magnitude greater than those measured previously using traditional culture-based techniques (e.g. ZoBell, 1946). The discrepancy between bacterial numbers obtained from microscopy and cell-culturing was highlighted many years earlier and at the time was explained by the majority of cells visible by microscopy being dormant or dead (Jannasch and Jones, 1959). This theory was strengthened by the identification of nongrowing 'ghosts' in seawater i.e. bacterial cells without nucleiods (Zweifel and Hagstrom, 1995) although later studies showed that these ghosts were able to grow and in fact contained nucleiods that were too small to detect (Choi *et al.*, 1996).

The main reason for the 'great plate count anomaly' (Staley and Konopka, 1985) is an inability or impaired ability of many marine bacteria to form colonies under the standard culture conditions used. However, contrary to previous belief, this was largely due to an inability to mimic, *in vitro*, a natural environment conducive to the growth of many bacteria, a problem still facing marine microbiologists today. Growing bacteria *in vitro* enables isolation of specific strains and the subsequent study of cell physiology not possible by other methods. The inability to culture and study the physiology and metabolism of many marine bacterioplankton groups led to the assumption that they were relatively unimportant in marine food webs. Despite recent advances in cell-culture techniques that have enabled the cultivation of previously uncultivable bacteria (Zengler *et al.*, 2002), it was the earlier development of alternative methods for studying microbial community metabolism and respiration that emphasised bacteria as important carbon recyclers (Pomeroy, 1974).

Up until the mid-1980s it was virtually impossible to determine the species, genus or order of a bacterium using light or epifluorescent microscopy due to the small size and usually undistinguishable morphological characteristics of bacterial cells. An important technological advancement in the field of microbial ecology was the application of molecular biology techniques, principally the extraction of DNA from mixed communities followed by cloning and sequencing of the small subunit (SSU) rRNA gene (Olsen *et al.*, 1986). Restriction fragment length polymorphism (RFLP) has been used to assess the diversity of prokaryotic 16S rDNA sequences from both coastal and oceanic samples (e.g. Acinas *et al.*, 1997; Gallagher *et al.*, 2004 and Rappe *et al.*,

2000). This technique provides a measure of the frequency of certain cloned sequences but as the primers used in the DNA amplification step may bind preferentially to some species over others, the number of clones obtained may not accurately represent the community composition.

In the past five years the fields of genomics and proteomics have been applied to the study of marine microbes. The sequencing and annotation of genomes from cultivable marine bacteria has revealed valuable insights into the metabolism and adaptation of these microbes to their environment. For example, analysis of the genome sequence from the planctomycete, *Pirellula* sp., revealed genes encoding a holdfast polymer to attach the cells to sinking, nutrient-rich marine snow particles; genes coding for nitrate transporters to support growth under nitrogen-limiting conditions; sulphatase genes for the cleavage of sulphated algal polymers prior to aerobic oxidation and the potential ability of *Pirellula* sp. to survive anoxic conditions by obtaining energy from heterolactic acid fermentation. The evolution of a large genome in *Pirellula* sp. (7.145 Mb) enables it to adapt to varying environmental conditions and stresses such as anoxia, nutrient limitation and even periods of starvation (Glockner, 2003). In contrast, sequencing and annotation of *Prochlorococcus marinus* genotypes have revealed that the small genomes (1.66 to 1.75 Mb) of these photosynthetic organisms lack many genes coding for proteins involved in photosynthetic pathways and the low-light SS120 genotype is missing genes for nitrate or nitrite transporters and therefore must rely on reduced forms of nitrogen such as NH_4^+ and amino acids (Dufresne et al., 2003). *Prochlorococcus marinus* is adapted to survive in nutrient-limited waters and therefore has evolved a streamlined genome, with the minimum number of genes necessary for phototrophic growth and survival.

Of particular interest is the ability to obtain DNA sequences directly from environmental samples, eliminating the need for culturing and permitting studies on the diversity and distribution of uncultivable prokaryotes. This has been achieved using whole-genome shotgun sequencing (Venter et al., 2004). The abundance of certain genes encoding proteins important in biogeochemical cycles, (for example the *nif* family of genes involved in N_2 fixation) can be estimated using quantitative PCR (qPCR). This method has also been used to examine bacterial diversity and abundance. QPCR has also been to study the distribution and abundance of *Prochlorococcus* and *Synechococcus* ecotypes by exploiting differences in the 16S-23S rDNA internal transcribed spacer (Ahlgren et al., 2006; Coleman et al., 2006).

However, the amplification of mixed community DNA by PCR introduces biases as described previously where primers may preferentially bind to one species or group of bacteria over another, making truly quantitative measurements from mixed community samples impossible. Methods to reduce the effect of this PCR-bias include the recent development of whole genome amplification, using a rolling circle DNA amplification step (Hutchinson et al., 2005 and Stepanauskas and Sieracki, 2007). This method amplifies the whole genomic DNA in the sample prior to amplification of the target genes of interest, thus reducing the number of cycles or PCR reactions and therefore reducing inter-specific primer-binding biases.

To obtain a direct measurement of microbial community composition, fluorescent *in situ* hybridisation (FISH) has been used (see review: Amann *et al.*, 1995) where fluorescent labelled 16s rRNA probes bind to target sequences in the cell allowing enumeration of labelled cells using epifluorescence microscopy. This technique has been further developed to increase the detection of probe-labelled cells by using a signal amplification step (CARD-FISH, Pernthaler *et al.*, 2002b). Unlike PCR primer pairs, FISH probes target only short (approximately 20 bases) nucleic acid sequences so they cannot usually be designed to detect fine-scale differences between closely related 'species' without becoming unspecific to the target group. However, this method remains the only way of quantifying prokaryotic clades in mixed community environmental samples.

In addition to molecular-based methods for studying microbial community composition, the development of flow cytometry has enabled rapid quantification of cells from marine environments. Flow cytometry also provides the ability to separate the mixed community based upon cell characteristics using stains specific for nucleic acids (Marie et al., 1997), protein (Zubkov et al., 1999), cell activity (Lopez-Amoros et al., 1998; Sieracki et al., 1999) and viability (Tyndall et al., 1985). By combining flow cytometric cell sorting with molecular techniques or radiotracer uptake methods, community composition or activity respectively can be more accurately defined in mixed bacterioplankton communities (Mary et al., 2006; Zubkov et al., 2001).

Despite the technological advancements in community characterisation and enumeration, there is still a lack of knowledge regarding the activity and functioning of the majority of specific groups of marine prokaryotes. A recent development combining microautoradiography and FISH has enabled the identification of prokaryotes that actively take up specific substrates (Ouverney and Fuhrman, 1999). However, this

method is at best only semi-quantative (Sintes and Herndl, 2006) and the majority of measurements have been made on coastal bacteria (e.g. (Alonso and Pernthaler, 2005; Elifantz et al., 2005; Vila et al., 2004).

1.7 Biogeochemical cycles

Many elements on the planet can be transformed between various chemical forms, both biotic and abiotic. These transformations can occur through chemical reactions with other elements or compounds or through biologically mediated processes such as respiration and metabolism. Understanding the various processes, sources and sinks involved in these biogeochemical cycles is important in order to be able to predict the effects of anthropogenic activities on the environment such as climate change and pollution (Behrenfeld et al., 2006; Beman et al., 2005; del Giorgio and Duarte, 2002; Karl, 1997). As prokaryotes are responsible for many of the biologically-mediated processes involved in biogeochemical cycling (Arrigo, 2005), research into the activity and distribution of these organisms is crucial as anthropogenic environmental impacts become more significant.

The carbon cycle involves the fixation of CO_2 from the atmosphere into organic matter via photosynthesis in plants and phytoplankton (primary production). Global net primary production (NPP; the amount of photosynthetically fixed carbon available for transfer to other trophic levels after respiration and other metabolic utilisation) has been estimated using satellite-based measurements to be 104.9 Pg C per annum (Field et al., 1998). Following carbon fixation, the resulting organic compounds can be respired by photosynthetic or heterotrophic organisms, thus producing new biomass and CO_2.

Aquatic and terrestrial environments contribute approximately 50 % each to global carbon fixation (Field et al, 1998). Organic matter produced in the surface ocean can sink from the photic zone into deeper waters and become incorporated into sediments. This drawdown and sequestration of atmospheric CO_2 is termed the biological pump and may be an important sink for anthropogenic CO_2. However, the majority of fixed carbon remains in the upper ocean and is metabolised and respired by heterotrophs, thus flowing through the food web and being available for higher trophic levels.

Furthermore, in the context of the oceanic carbon cycle it is also necessary to consider physical and chemical processes. The majority of atmospheric CO_2 dissolves in the oceans and due to physical processes, some of this may be transported to deep water

where it cannot usually escape back into the atmosphere for long timescales (the solubility pump) apart from in upwelling regions. The dissolution of CO_2 in the oceans lowers the seawater pH and this can have a detrimental effect on calcification, carried out for example by coccolithophorid phytoplankton and corals (Riebesell et al., 2000). Although the oceans can be a sink of atmospheric CO_2, they are also a source through respiration, calcification and diffusion. Figure 1.3 depicts the major pathways in the oceanic carbon cycle.

Figure 1.3: The oceanic carbon cycle (Chisholm 2000)

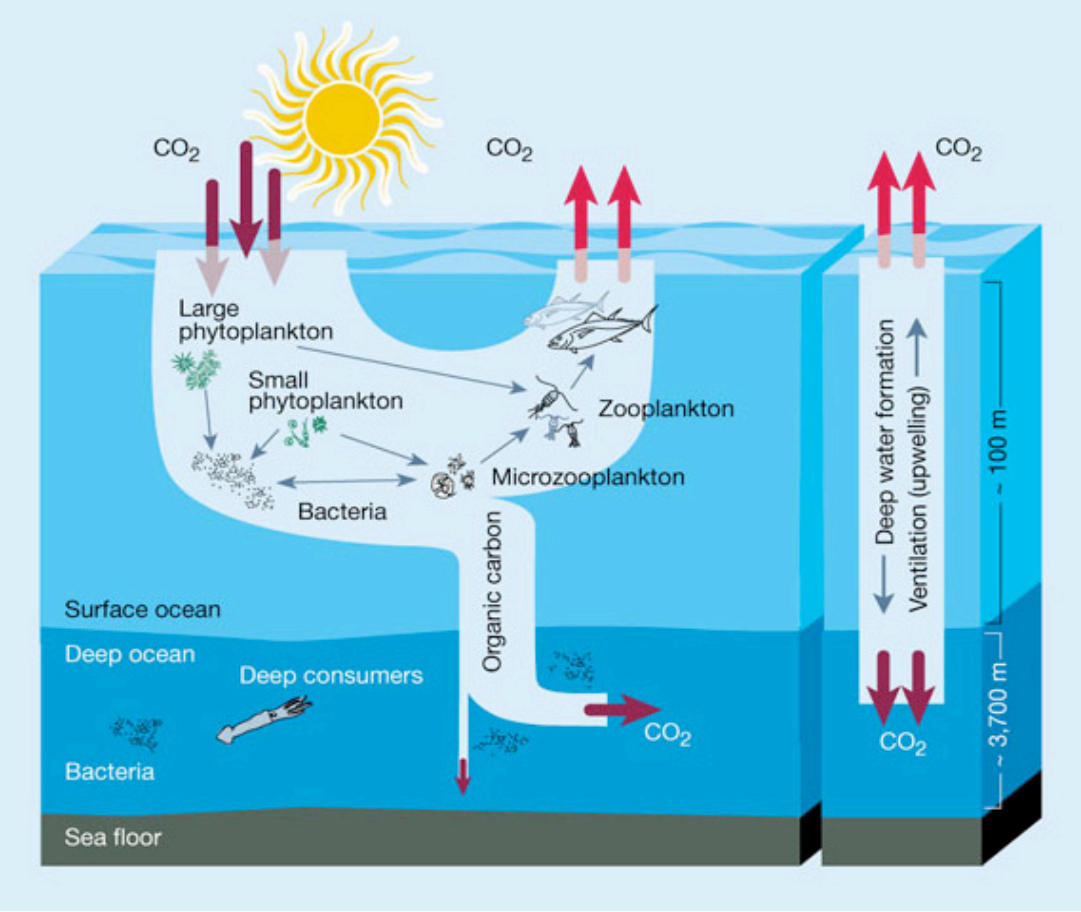

Bacteria are responsible for the majority of organic matter respiration (Ducklow, 1999; Williams, 1981) in the oceans and also contribute to carbon export via the sinking flux (Legendre and Fevre, 1995; Legendre and Rassoulzadegan, 1996; Richardson and Jackson, 2007). Bacteria and Archaea have vital roles in the flow of carbon to higher trophic levels via the microbial loop (Azam and Worden, 2004) and picophytoplankton (< 2 µm size fraction), including the cyanobacteria have also been shown to dominate primary production in oligotrophic waters (Maranon et al., 2001). Hence, knowledge of

the abundance, distribution and rates of carbon flow through the prokaryotic community are essential components in studies of the carbon cycle and ecosystem functioning.

In addition to the importance of prokaryotes in the carbon cycle, they also mediate processes in many other biogeochemical cycles, for example the nitrogen (Capone et al., 1997; LaRoche and Breitbarth, 2005; Zehr and Ward, 2002), sulphur (Bates, 1994; Kiene et al., 1999), phosphorus (Ammerman, 1993; Michaels, 1996; Zubkov et al., 2007) and iron (Barbeau et al., 2001) cycles.

1.8 Objectives

Four objectives and hypotheses have been identified to examine the importance of prokaryotic plankton and the controls upon the community in the Atlantic Ocean. The main pathways and the corresponding objectives are highlighted on the simplified food web diagram shown below.

Figure 1.4: Simplified food web diagram with the pathways and constituents examined in this thesis are highlighted in red. The numbered boxes correspond to the objectives and hypotheses to be tested as described below.

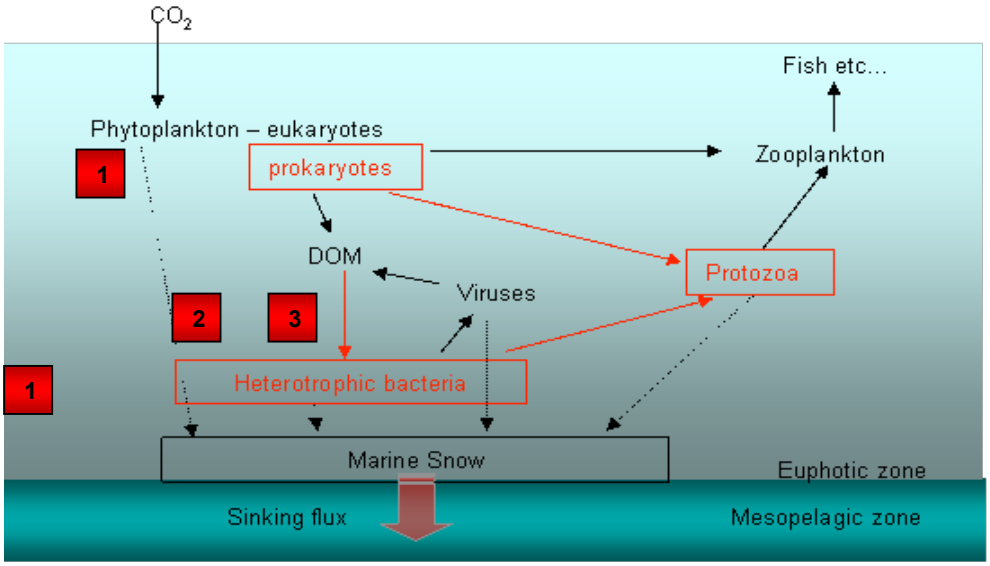

1. **To determine the microbial community composition and how this varies both vertically in the water column and latitudinally along each transect. (Chapters 3 and 4)**

Biannual sampling along the AMT enables the study of a wide range of environments, for example the 5 different oceanic provinces and sampling through different layers of the water column. Additional sampling in the Scotia Sea has also provided another contrasting physical environment for comparison. The hypotheses to be tested is that microbial community composition varies spatially and temporally in parallel with changes in physical parameters such as light and with changes in organic nutrient concentrations. It is also proposed that different provinces can be identified along both the AMT transects and in the Scotia Sea using the abundance and distribution of prokaryotes.

2. **To examine the flow of carbon through the microbial loop. (Chapter 5)**

Photosynthesis by both prokaryotic and eukaryotic phytoplankton produces new biomass in the oceans. This biomass can be re-mineralised in the photic zone via zooplankton grazing or by the uptake of DOM by heterotrophic prokaryotes or is removed out of the photic zone via the sinking flux. The importance of the microbial loop in retaining this organic matter in the photic zone is examined in this chapter by looking at the proportion of photosynthetically fixed carbon used by heterotrophic prokaryotes, i.e. the relationship between bacterial and primary production. Due to low primary production rates in the oligotrophic gyres, the hypothesis to be tested is that relatively more of the photosynthetically fixed C flows through the microbial loop in the oligotrophic gyres than in more nutrient rich waters where there would be a greater export of biomass and/or higher grazing rates.

3. **To determine the metabolic activities of dominant bacterial groups in order to assess the influence of microbial community composition on biogeochemical cycles. (Chapter 6)**

Recent research has highlighted specific activities for certain bacterial groups in specialised environments however, the activity and diversity of heterotrophic bacteria in oceanic environments remains largely unknown. Chapter 6 focuses on linking the activity of defined bacterioplankton groups in terms of amino acid uptake to the community composition. It is hypothesised that the rate of amino acid uptake differs for different bacterial taxonomic groups and is related to the availability of these organic nutrients.

Chapter 2

Hydrographic features of the sampling sites and an overview of the Atlantic Meridional Transect Programme

2.1 The Atlantic Ocean

The northern and southern Atlantic Ocean is dominated by large anticyclonic convergent gyres that act to deepen the pycnocline and prevent nutrients from the deep water coming up to the euphotic zone. In the northern hemisphere, northeast trade winds in combination with the Coriolis force and increased solar heating close to the equator result in a westward flowing North Equatorial Current, generating a clockwise circulation in the northern gyre. Similarly, south of the equator, southeast winds force water westwards to form the South Equatorial Current, contributing to the anti-clockwise circulation of the southern gyre (Fig. 2.1; Niiler, 2001).

Balance between the Coriolis force and the gravity gradient produced by Ekman transport result in geostrophic currents around the gyre. These boundary currents are intensified in the west, characterised by sharp boundaries and fast flow (the Gulf Stream and the North Atlantic current in the northern hemisphere and the Brazil current in the southern hemisphere). In contrast, the eastern boundary currents (the Canary current in the north and the Benguela current in the south) are slower, have more diffuse boundaries and typically cooler waters originating from mid-latitudes (Tomczak and Godfrey, 2003).

Several currents exist around the equator; the two persistent dominant currents in surface waters flow westwards, forming the North Equatorial Current (NEC; > 10 ºN) and the South Equatorial Current (SEC; from approximately 3 ºN to 15 ºS). Eastward flowing sub-surface countercurrents also exist in this region, north and south of the equator. The North Equatorial Countercurrent (NECC) exhibits strong seasonality, inhibited by strong trade winds in the boreal spring. Deeper in the water column, equatorial undercurrents also flow eastwards at depths greater than 100 m (Tomczak and Godfrey, 2003).

The deep pycnocline in the northern and southern gyres limits the input of nutrients from deep water to the photic zone. This results in typically oligotrophic conditions in the gyres with sources of nutrient inputs limited to eddy-induced upwelling (McGillicuddy et al., 1998; Oschlies and Garcon, 1998), atmospheric deposition

(Sarthou et al., 2007) and lateral transport and diffusion close to the boundaries (Palter et al., 2005; Williams et al., 2006). At the equator and in the eastern boundary currents, upwelling occurs in regions of divergence and due to coastal processes, providing inputs of nutrient-rich deep water into the photic zone.

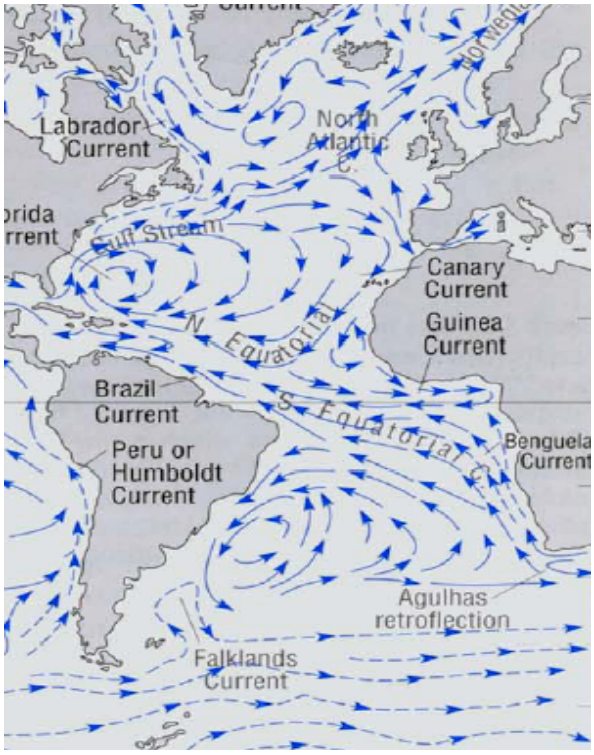

Figure 2.1: Schematic diagram of Atlantic Ocean currents and circulation (Lalli and Parsons, 1997)

2.2 The Scotia Sea

The Scotia Sea was included in this study as an extension southwards from the AMT sampling sites. Located between the South Atlantic and the Weddell Sea, the Scotia Sea is dominated by the eastward flow of the Antarctic Circumpolar Current (ACC; (Rintoul et al., 2001). The ACC consists of four strong currents between 54 and 63 ºS. The northernmost of these currents is the Subantarctic Front (SAF) followed by the Polar Front (PF), the Southern Antarctic Circumpolar Current Front (SACCF) and the Southern Boundary of the Antarctic Circumpolar Current (SBACC)(Brandon et al., 2004; Orsi et al., 1995). It has been suggested that the interaction of internal waves and tides with topography may be the cause of the high rate of mixing of deep nutrient-rich waters with surface waters observed in this region (Heywood et al., 2002).

Samples were collected during cruise JR82 which consisted of 8 north-south transects crossing the ACC in January 2003 (Fig. 2.2; Ward et al., 2006).

2.3 The Atlantic Meridional Transect (AMT) programme

Oligotrophic gyres cover vast areas of the world's oceans and several research programmes have focused on the study of biologically-mediated processes in these waters. These programmes are in the form of fixed point time-series such as the Bermuda Atlantic Time-series (BATS; DuRand et al., 2001; Michaels, 1994) and the Hawaii Ocean Time-series (HOT; Karl and Lukas, 1996) or sampling along single transects (e.g. as part of the JGOFS programme; Hoppe et al., 2002) and the global sampling strategy of the IMBER-endorsed Galathea 3 cruises; www.galathea3.dk). The majority of biological oceanographic research in oligotrophic gyres has been concentrated in the northern gyres of the Pacific and Atlantic Oceans. In contrast to other research programmes, the AMT programme combines repeated sampling over 10 years with a large spatial coverage including both the northern and southern Atlantic gyres.

The aim of the AMT programme is to conduct biological, chemical and physical research, sampling biannually on cruises along a transect between the UK and either the Falkland Islands or South Africa. Eighteen cruises have been carried out (AMT-1-17) between 1995 and 2005 as part of 2 phases of the programme (AMT 1-11 and AMT 12-17). During the second phase of the AMT programme, southbound cruises in the boreal autumn sampled the NW African upwelling region, whereas northbound cruises in the boreal spring sampled waters farther west into the N. Atlantic gyre. This thesis includes data from seven AMT cruises. The dates, start and end locations of each of these cruises are shown in Table 2.1.

Table 2.1: AMT cruise dates and locations. The cruises shown in bold (AMT-14 and 15) were the cruises directly participated in during the course of this Ph.D. research. For the remaining cruises, either samples were provided for processing post-cruise (AMT-12 and 13), or data were provided for analysis (AMT-3, 4 and 6).

Cruise	Dates	Start location	End location
AMT-3	16/09 – 25/10/1996	U.K.	Falkland Islands
AMT-4	21/04 – 27/05/1997	Falkland Islands	U.K.
AMT-6	14/05 – 16/06/1998	South Africa	U.K.
AMT-12	12/05 – 17/06/2003	Falkland Islands	U.K.
AMT-13	10/09 – 14/10/2003	U.K.	Falkland Islands
AMT-14	**28/04 – 02/06/2004**	**Falkland Islands**	**U.K.**
AMT-15	**17/09 – 29/10/2004**	**U.K.**	**South Africa**

Previous research has identified 5 distinct oceanic provinces along the Atlantic Meridional Transect. These are the oligotrophic Northern (NAG) and Southern (SAG) gyres, temperate regions at the high latitude Northern (NT) and Southern (ST) ends of the transect and an upwelling region around the equator (EQ) (Zubkov *et al.*, 1998b). The cruise tracks are shown in Fig. 2.2.

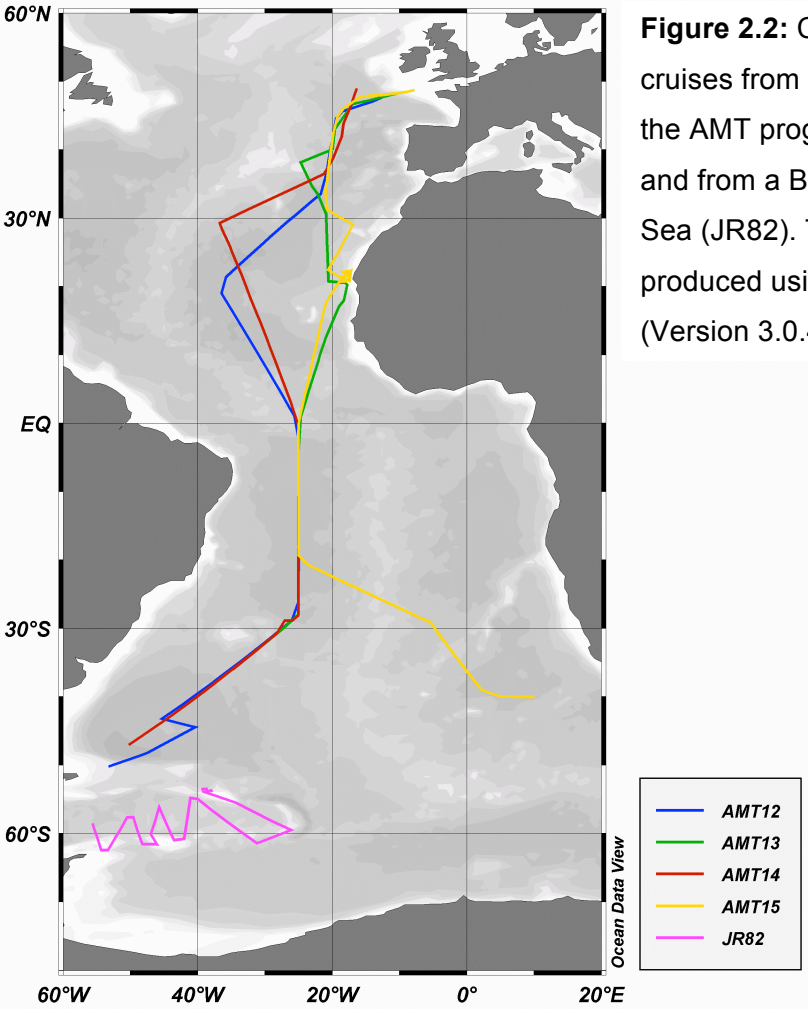

Figure 2.2: Cruise tracks for AMT cruises from the second phase of the AMT programme (AMT12 to 15) and from a BAS cruise in the Scotia Sea (JR82). The map was produced using Ocean Data View (Version 3.0.4; Schlitzer, 2006).

The following three objectives were identified for the second phase of the AMT programme.

1: To determine how the structure, functional properties and trophic status of the major planktonic ecosystems vary in space and time.

2: To determine the role of physical processes in controlling the rates of nutrient supply, including DOM, to the planktonic ecosystem.

3: To determine the role of atmosphere-ocean exchange and photo-degradation in the formation and fate of organic matter.

Objective 1 contains the following four hypotheses.

1. The size spectra, and mineralization capacity of planktonic organisms are major determinants of CO_2 and organic matter export to the atmosphere and deep water.
2. Growth rates of phytoplankton in tropical and subtropical waters are correlated with the *f* ratio and, for the surface layer, with the relative contribution of nanoplankton.
3. The biodiversity of the microbial planktonic community significantly influences C, N and P recycling and ecosystem trophic state.
4. Basin scale variability in photosynthetic growth rates and pCO_2 flux can be derived from remotely sensed data.

This research specifically addresses hypothesis 3 of objective 1 of the AMT programme however data presented here have been used in conjunction with other AMT data to test hypotheses 1 and 2, shown above (San Martin et al., 2006; Hickman, 2007).

Many biological, chemical and physical parameters were measured during the second phase of the AMT programme. These parameters, along with the frequency and method of sampling used are summarized in Table 2.2.

Table 2.2: Typical daily sampling schedule (AMT12–17) (adapted from (Robinson et al., 2006).

Time	Operation	Research area
Pre-dawn ~03:00 GMT	Bongo nets (200 µm, 50 µm; 200–0 m, 50–0 m)	Mesozooplankton abundance, diversity and size distribution
	CTD(s) (0–300 m)+fluorescence, oxygen, transmission, ADCP, FRRF	Plankton community structure including picoplankton abundance and community structure, bacterial production, primary production, chlorophyll a and other photosynthetic pigments, respiration, calcification, N_2 fixation, new and regenerated production, nutrients (NO_3, NO_2, PO_4, SiO_4) CDOM, DOC/N, POC/N, PIC, BSi, climate reactive gases (DMS, N_2O, CH_4), carbon species, oxygen
05:00 GMT	SAPS (~every 3rd day)	Export production, isotopic composition of particulate organic nitrogen
11:00 GMT	CTD (0–1000 m)+fluorescence, oxygen, transmission, ADCP	Picoplankton abundance and community structure, bacterial production, iron speciation, nutrients (NO_3, NO_2, PO_4, SiO_4), CDOM
	Optics rig+FRRF	Optical properties, satellite algorithm development
	Single net (200 µm; 100–0 m)	Mesozooplankton diversity and activity
Continuous	Thermosalinograph, fluorescence, pCO_2	Province determination, source and sink regions of CO_2
Continual	Water sampling from non-toxic supply	Alkalinity, TCO_2, ammonia, DMS, CDOM, calibration samples for salinity, HPLC pigments, POC/N, PIC, picoplankton community structure and abundance
Continual	Atmospheric sampling when wind conditions permit and rainfall when possible	Air–sea exchange

2.4 Sample collection and measurement of physical, chemical and biological parameters

2.4.1 Sample collection and hydrographic measurements

Water samples from the upper 300 m of the water column were collected in Niskin bottles attached to a rosette sampler with a conductivity, temperature, depth profiler (CTD, SeaBird 911*plus* instrument); a fluorometer (Chelsea MKIII Aquatracka) and a PAR sensor (Chelsea) fitted. Temperature, salinity and PAR were measured at 0.5 m depth intervals.

Samples were collected from up to 24 depths twice daily at pre-dawn and mid-morning stations. Further details of the sampling frequency used for each set of measurements or experiments are described in the methods section of each chapter. Sub-samples for flow cytometry were collected directly from the Niskin bottles into acid washed (10 % HCl) 50 ml polypropylene screw-top tubes. Sub-samples for radiotracer incubations and CARD-FISH were collected via acid-washed silicone tubing into 1 L acid-washed Thermos flasks to maintain the ambient water temperature and store samples in the dark until processing (within one hour of collection).

2.4.2 Inorganic nutrient and chlorophyll-a measurements

Dissolved inorganic nutrients and total chlorophyll-*a* were measured at up to 10 depths from each station. Nitrate and nitrite concentrations above 0.1 µM were measured using a 5-channel Technicon segmented flow colorimetric autoanalyser (Bran+Luebbe AAII; (Brewer and Riley, 1965; Grasshoff, 1976). Lower (nM) concentrations of nitrate and nitrite were measured using a colourimetric segmented flow analytical system with liquid waveguide capillary cell (World Guide Precision; Woodward and Rees, 2001). The concentration of total chlorophyll-*a* was determined by filtering 250 – 500 mls seawater through glass fibre filters (Whatman, GF/F). Chlorophyll was then extracted from the filters by submersion in 10 mls 90 % acetone for 18 – 20 hours in the dark and was measured using a TD-700 fluorometer (Turner Designs).

2.4.3 Primary production measurements

Primary production rates were measured using a ^{14}C fixation method on water samples from 5 – 6 depths from the pre-dawn CTD cast. The depths chosen for sampling

corresponded with the light irradiance levels, 97 %, 55 %, 33 %, 14 %, 1 % and 0.1 % of the surface irradiance. Triplicate sub-samples (125 mls) were incubated with radiolabelled sodium bicarbonate (18 - 20 μCi $NaH^{14}CO_3$) in the dark and light from local dawn until dusk; 10 – 16 h duration in temperature-regulated on-deck incubators fitted with light filters to simulate the *in situ* irradiance levels. Following incubation, samples were collected on 0.2 μm polycarbonate filters and fumed over hydrochloric acid for 30 – 40 mins. Filters were subsequently submerged in 5 mls liquid scintillation cocktail (Optiphase HiSafe-3) and the radioactivity counted on a TriCarb 3100TR liquid scintillation counter. A more detailed description of the method is presented in Poulton et al. (2006).

2.4.4 Data analysis

Due to differences in the treatment of data derived from different experiments, specific analyses and statistical tests used are described in the methods sections of each chapter. In general, provinces were determined using Bray-Curtis similarity tests followed by hierarchical agglomerative cluster analysis (Clarke and Warwick, 2001) performed with PRIMER 5 software (PRIMER-E Ltd., Plymouth, U.K.). Comparison between provinces was made using either one-way ANOVAs and / or paired or 2 sample t-tests. Other statistics used include Pearson's correlations and regression analysis to compare amino acid uptake rates and to derive biomass and bacterial production conversion factors. All these statistics were performed using either Minitab or SPSS software.

2.5 Hydrographic and biological characteristics along the AMT

2.5.1 Temperature

Surface water temperatures along the AMT range from approximately 14 ºC in the higher latitudes to 26 ºC in the subtropics and around the equator (Fig. 2.3). There are clear temperature differences in the northern tropics and sub-tropics (10 to 35 ºN) between AMT-12 and 14 and AMT-13 and 15. Although surface temperatures are similar at these latitudes between cruises, the difference in cruise tracks is reflected in the depth of the thermocline. In the northwest African upwelling region (between 15 and 22 ºN), sampled on AMT-13 and 15, the thermocline shoaled to approximately 50 metres. Farther northwards on these cruises, as sampling stations were located farther from the coast, the thermocline deepened. In the northern gyre between 10 to 35 ºN

during AMT-12 and 14, warmer waters extended deeper in the water column than in the upwelling region. In the southern gyre, there was a clearly defined sharp thermocline; however the decrease in temperature with increasing depth was more gradual in the NAG and warmer waters extended deeper in the water column (Fig. 2.3).

Seasonal differences in water temperature were evident in the higher latitude northern and southern ends of the transects. Surface waters north of 40 ºN were warmer in autumn (AMT-13 and 15) compared to spring (AMT-12 and 14) as increased solar radiation during summer promoted stratification and increased water temperatures. In the austral spring, despite a difference in cruise track between AMT-13 and AMT-15, a sharp horizontal front was observed around 30 ºS during both cruises. This front was absent or less distinct in the austral autumn, with warmer surface waters in the southern temperate regions (Fig. 2.3). Surface water temperatures in the southern temperate regions were also slightly higher during autumn 2004 (13 – 15 ºC; AMT-14) compared to similar latitudes in autumn 2003 (9 – 11 ºC; AMT-12). AMT-14 started 12 days earlier in the year than AMT-12, and this is reflected in the stratification of surface waters in the southern high latitudes during AMT-14 indicated by the higher temperatures relative to AMT-12.

2.5.2 Salinity

The deepening of the thermocline in the northern and southern oligotrophic gyres is also associated with a deepening of the halocline producing a w-shaped distribution along the transects (Fig. 2.4). The highest salinities of 37.1 PSU, were located between 20 and 100 m in both the northern and southern gyres. Higher salinities extended deeper into the water column in the northern gyre compared to the southern gyre.

The difference in cruise tracks between the gyre cruises and the upwelling cruises is also reflected in the salinity profiles in the northern tropics and sub-tropics with lower salinity water sampled during the upwelling cruises (AMT-13 and 15) compared to the gyre cruises (AMT-12 and 14). As was observed in the thermocline depth, there is also a shoaling of the halocline around the equator. The decreased salinity observed in surface waters between the equator and 10 ºN during the boreal autumn (AMT-13 and 15) compared to spring (AMT-12 and 14) is due to inputs of freshwater originating from the Amazon, carried by the NECC (Fig. 2.4; Robinson et al., 2006)

Figure 2.3: Temperatures (ºC) in the upper 300 m of the water column along 4 consecutive AMT transects. The gyre cruises, AMT-12 and 14 were in the boreal spring and the upwelling cruises, AMT-13 and 15 were in the austral spring.

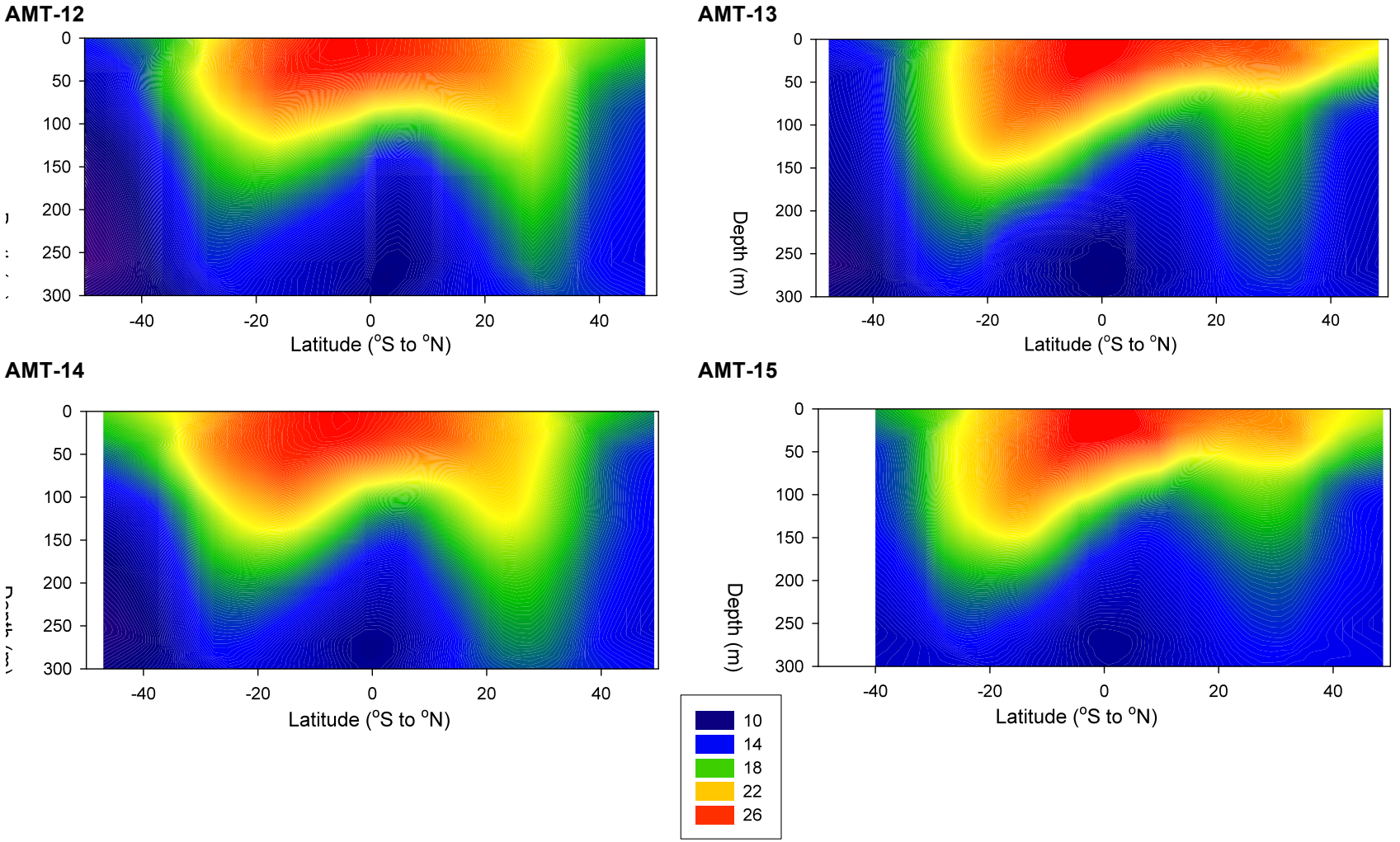

Figure 2.4: Salinity (PSU) in the upper 300 m of the water column along 4 consecutive AMT transects. The gyre cruises, AMT-12 and 14 were in the boreal spring and the upwelling cruises, AMT-13 and 15 were in the austral spring.

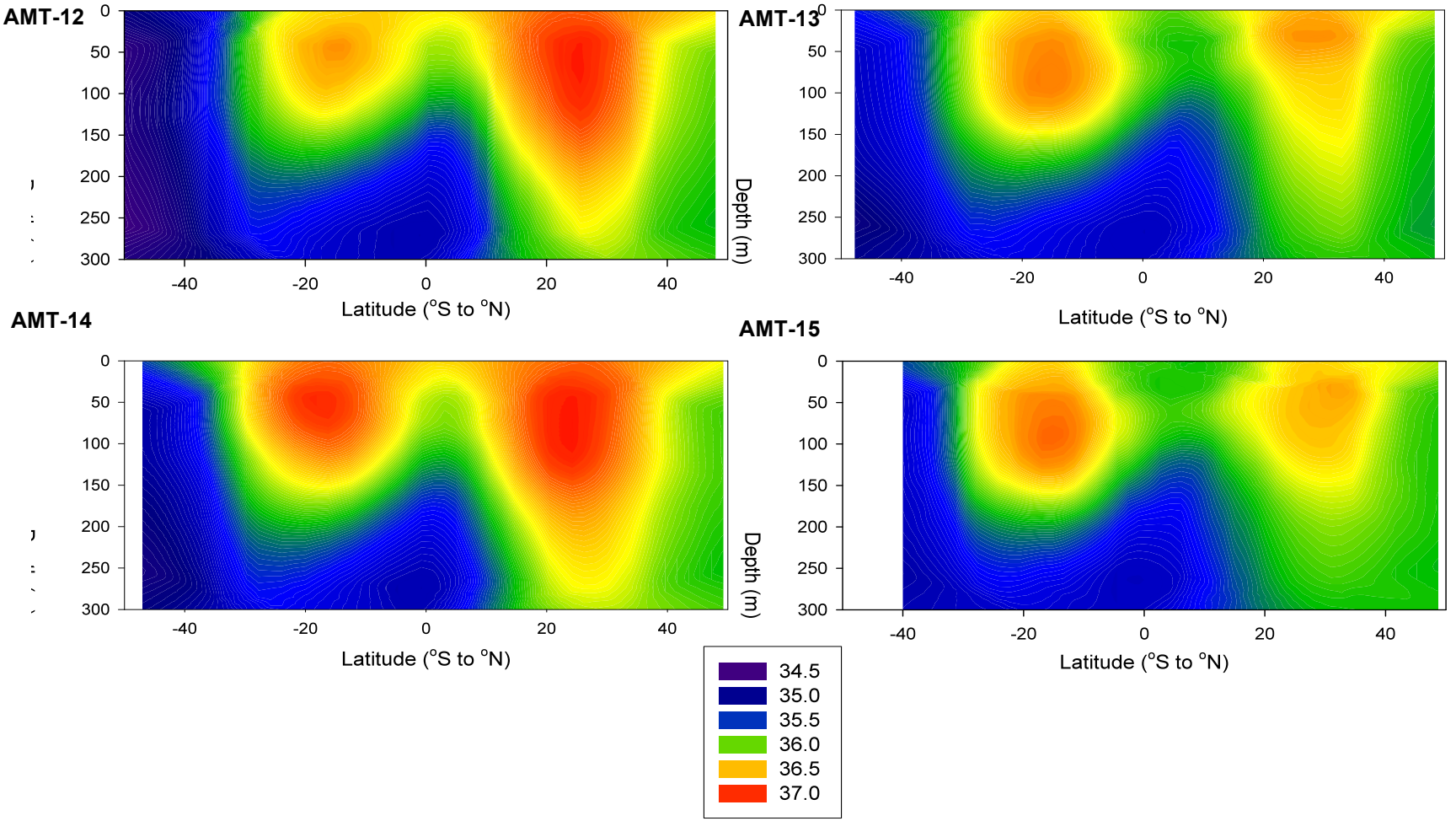

2.5.3 Density

Density is a function of temperature and salinity, however, differences are observed between the density profiles and the profiles of the determining factors along all four AMT cruises (Fig. 2.5). The high temperature of surface waters around the equator result in the lowest density water along the transects (23 -24) despite a higher salinity in this region compared to the subtropical gyres. Shoaling of the pycnocline in the northwest African upwelling region during AMT-13 and 15 is also more pronounced than shoaling of the halocline.

2.5.4 Inorganic nutrients (NO_3 +NO_2)

The total concentration of nitrate and nitrite in surface waters of the Atlantic gyres is typically below 0.1 µM. These low-nutrient waters can extend to depths of greater than 100 m in the southern gyre (AMT-14 and 15; Fig. 2.6). Downwelling effects of the gyres, preventing mixing with deep, nutrient-rich waters can be seen down to 300 m where the concentration of nitrate and nitrite rarely exceeded 15 µM. Higher concentrations, reaching 30 µM in the equatorial region and 20 µM in the southern temperate region were observed at a similar depth of 300 m. Upwelling of nutrient-rich, deeper waters is apparent by the maintenance of concentrations exceeding 15 µM at depths of around 100 m in the equatorial, southern temperate and the NW African upwelling region around 18 ºN (AMT-13 and 15; Fig. 2.6).

Seasonal differences in nutrient concentrations are emphasised in the southern temperate region along the AMT transect with higher nitrate and nitrite concentrations in the austral autumn (AMT-12 and 14) compared to spring (AMT-13 and 15; Fig.2.6).

2.5.5 Chlorophyll-a

The northern and southern gyre regions contain very low surface chlorophyll-*a* concentrations (< 0.1 $mg.m^{-3}$), as determined fluorometric measurements (Fig. 2.7). Vertical distributions of chlorophyll-*a* along the transects show a sub-surface chlorophyll maximum located deeper in the NAG and SAG of between 0.1 and 0.2 $mg.m^{-3}$ (up to 180 m) and shoaling to approximately 80 m around the EQ and towards higher latitudes. This w-shaped distribution of the deep chlorophyll maximum (DCM) corresponds to the lower boundary of warmer, high salinity waters in the gyres and the equator and is co-located with the depth of the nitracline (Fig. 2.3, 2.4 and 2.6).

Higher chlorophyll concentrations were found in the northwest African upwelling and in the northern and southern temperate regions with peak concentrations located in the upper 50 to 80 m of the water column. Spring blooms of phytoplankton were identified by generally higher chlorophyll-*a* concentrations in the temperate regions compared to autumn (Fig. 2.7).

Figure 2.5: Water density (Sigma-t) in the upper 300 m of the water column along 4 consecutive AMT transects. The gyre cruises, AMT-12 and 14 were in the boreal spring and the upwelling cruises, AMT-13 and 15 were in the austral spring.

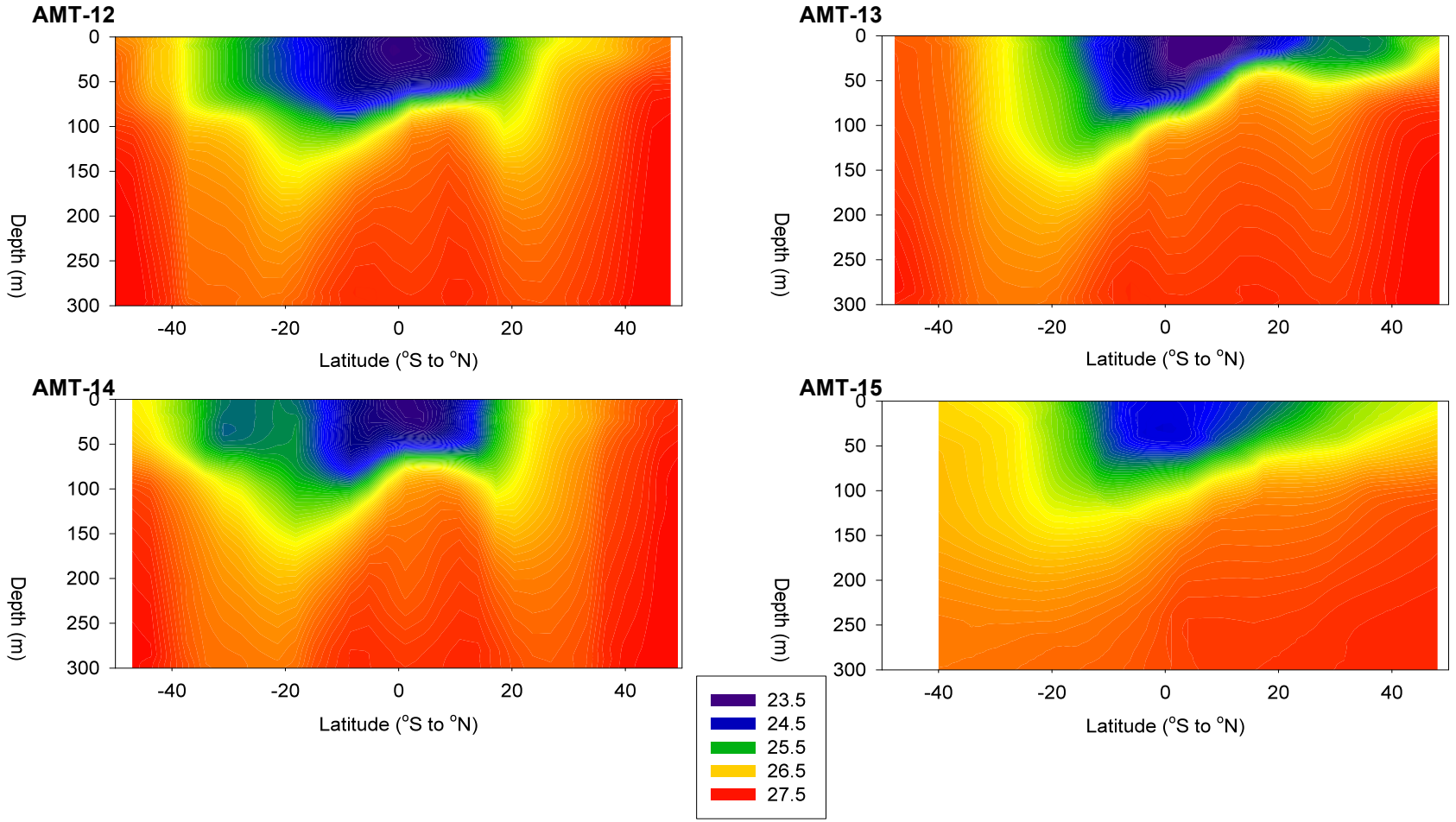

Figure 2.6: Concentration of nitrate + nitrite (μM) in the upper 300 m of the water column along 4 consecutive AMT transects. The dotted white lines are the 0.1 μM contours and the solid black lines represent the 1 μM contours. The gyre cruises, AMT-12 and 14 were in the boreal spring and the upwelling cruises, AMT-13 and 15 were in the austral spring.

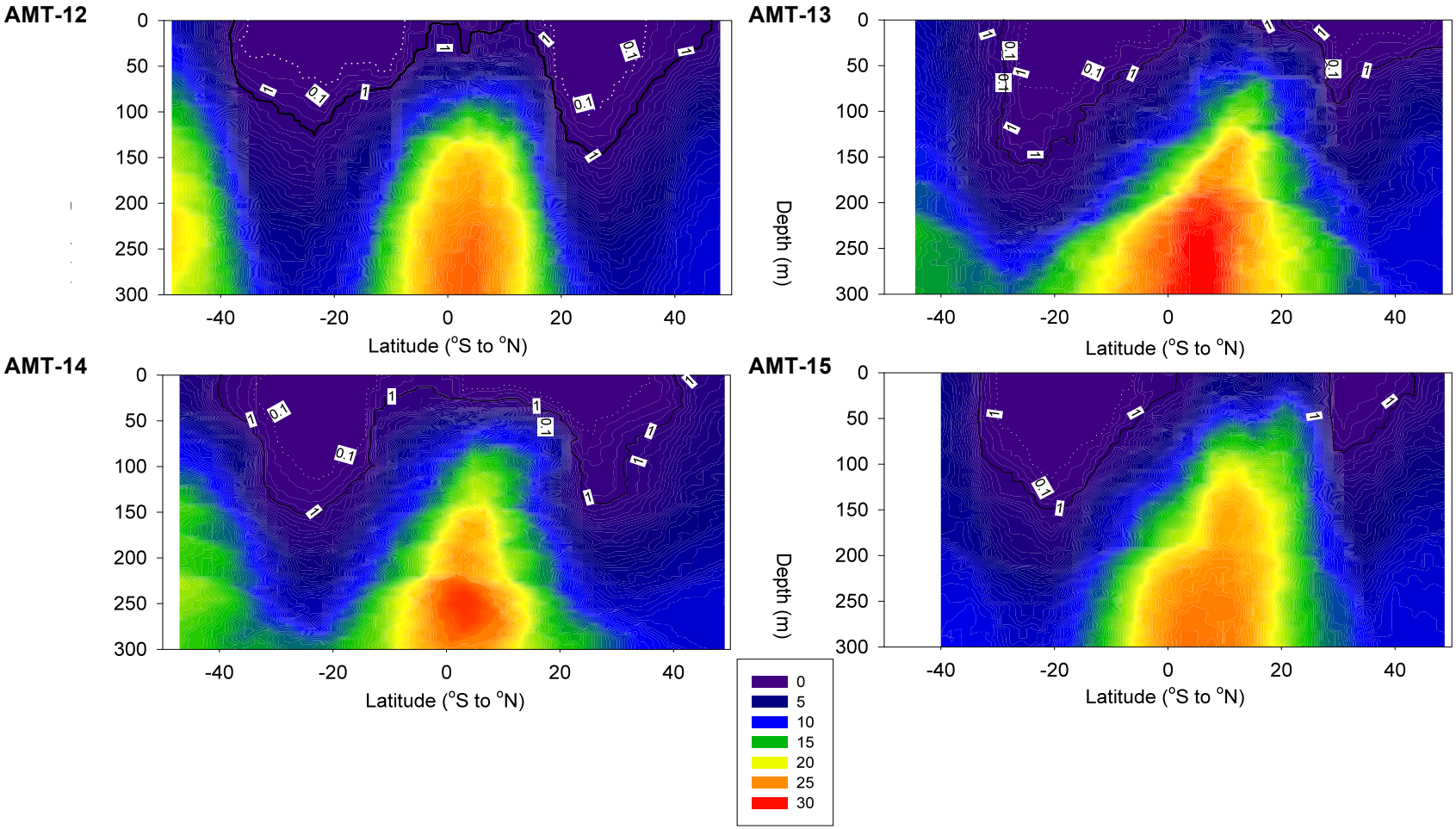

Figure 2.7: Chlorophyll-*a* concentrations (mg.m^{-3}) in the upper 200 m of the water column along 4 consecutive AMT transects. The gyre cruises, AMT-12 and 14 were in the boreal spring and the upwelling cruises, AMT-13 and 15 were in the austral spring. Note the different scale used for AMT-12 and 14 shown on the left compared to AMT-13 and 15 shown on the right.

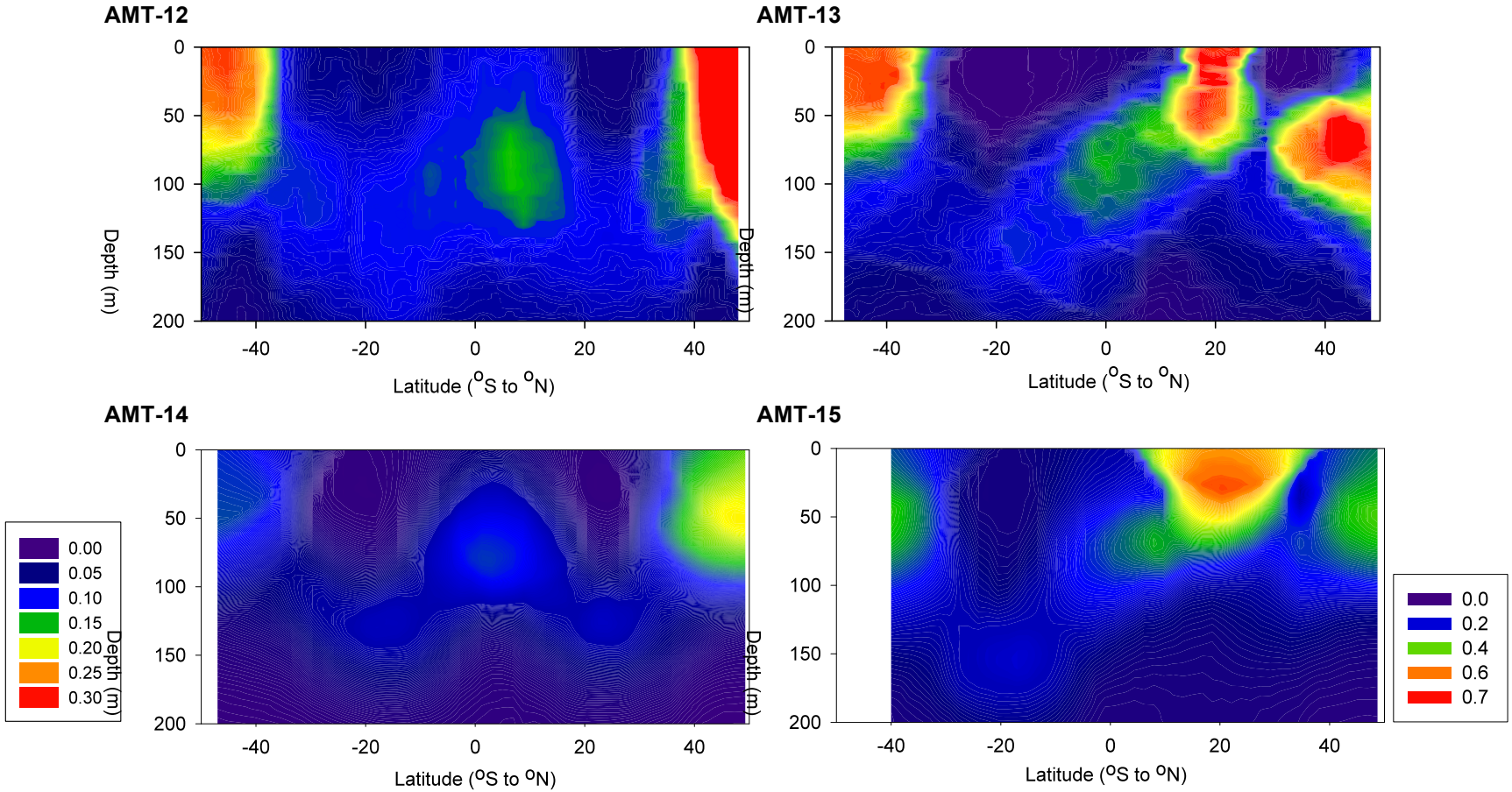

Chapter 3

Bacterioplankton abundance and distribution in the Atlantic Ocean and the Scotia Sea

3.1. Introduction

In the euphotic zone of oligotrophic waters the small cyanobacterium, *Prochlorococcus* is abundant and numerically dominates the phytoplankton (Buck et al., 1996; Campbell and Vaulot, 1993; Chisholm et al., 1988). In 1994 Li reported that *Prochlorococcus* were responsible for between 11 and 57 % of the total primary production. *Synechococcus* are also present although considerably less abundant in the oligotrophic gyres than in more mesotrophic waters (Dandonneau et al., 2004; Zubkov et al., 1998, 2000). It is important to note that the group of cells referred to as *Synechococcus* in this and other published work may include several species (Honda et al., 1999) although are unlikely to contain any other phycoerythrin-containing cells such as *Synechocystis* (Sherry and Wood, 2001) and *Cyanothece* (Zehr et al., 2001) due to the larger size of these other cells (Neveux et al., 1999).

Phototrophic cyanobacteria such as *Prochlorococcus* and *Synechococcus* can be easily identified by flow cytometry and as such were chosen along with the heterotrophic bacteria to investigate temporal and spatial variability in the Atlantic Ocean.

Zubkov et al. (1998 and 2000) reported seasonal and spatial variability in the picoplankton community along an Atlantic Meridional Transect (AMT) between 1996 and 1997. Data presented here were collected during five further AMT cruises between 1998 and 2004 and a British Antarctic Survey (BAS) cruise in the Scotia Sea in the austral summer of 2003. The aims of this study are to examine the spatial and temporal distribution and abundance of bacterioplankton along several AMT transects. In addition, data from a cruise in the Scotia Sea have also been included as an extension of the AMT transect into cooler more nutrient rich waters to the South. The hypothesis to be tested is that variations in the abundances of different groups of prokaryotes along the AMT transect and in the Scotia Sea are sufficient to identify different regions, harbouring characteristic communities.

3.2. Methods

3.2.1 Sample collection

Samples were collected during five AMT cruises (AMT-6, 12, 13, 14 and 15) and a cruise in the Scotia Sea (JR82) as described in chapter 2. The cruise tracks are shown in chapters 2 and 4.

Samples were collected from 5-9 depths at 27 stations on AMT-6; 10-12 depths at 35 stations on AMT-12; 12 depths at 25 stations on AMT-13; 12-24 depths at 37 stations on AMT-14; 6-24 depths at 43 stations on AMT-15 and 8-11 depths at 21 stations on JR82 (Figs. 4.2 and 4.3). The majority of samples from AMT-12 and 13 were collected pre-dawn, however some samples from AMT-14 and 15 and all the samples from AMT-6 were collected at approximately 11 am local time. Samples from JR82 were collected at various times throughout the day.

Sub-samples for flow cytometry were fixed using paraformaldehyde (1 % final concentration on AMT-12, 13, 14, 15 and JR82) or glutaraldehyde (1% final concentration on AMT-6) within an hour of collection and stored at 4 ºC overnight before freezing at -80 ºC (AMT-12, 13, 14, 15 and JR82) or -20 ºC (AMT-6) until analysed post-cruise. In order to examine the effects of freezing on cells, flow cytometry was also performed daily on board the ship during AMT-14. Duplicate sub-samples were fixed within an hour of collection and analysed the same day. Nutrient concentrations (nitrate plus nitrite) were measured according to Woodward and Rees (2001) as described in chapter 2.

3.2.2 Flow Cytometry

Bacterioplankton including phototrophic cyanobacteria were enumerated using flow cytometry (FACSort, Beckton Dickinson, Oxford, U.K.). The flow rate was calculated by adding a known concentration of 0.5 µm yellow-green fluorescent latex beads (Polysciences, Eppelheim, Germany) as an internal standard. Bead concentrations were measured by counting the number of beads analysed on the flow cytometer during five different time points (between 1 and 5 minutes) and dividing this by the volume of bead

solution analysed (measured by the difference in weight before and after analysis). Flow cytometry data was processed using CellQuest software (Beckton Dickinson, Oxford, U.K).

In samples from the AMT cruises, two groups of picophytoplankton (*Prochlorococcus* spp.; Pro and *Synechococcus* spp.; Syn) were identified by their characteristic autofluorescence (Fig. 3.1; Olson et al., 1993). Pro cells were separated into surface and deep populations according to differences in autofluorescence and side scattering properties of the two populations (Fig. 3.2; Partensky et al., 1996).

Several groups (up to four) of picophytoplankton were visualised based on chlorophyll autofluorescence in samples from the JR82 cruise (Fig. 3.1). Pro was absent or at a concentration below detection by flow cytometry in all the samples from this cruise, however a few Syn cells were observed in some samples. As there were only a small number of Syn and the remaining groups of picophytoplankton were unidentified, cell numbers from all the picophytoplankton groups from the JR82 cruise were combined to give a total picophytoplankton estimate.

Another sub-sample was stained with the nucleic acid stain SYBR Green I, enabling the visualisation of all bacterioplankton (Marie et al., 1997). In the majority of AMT samples, *Prochlorococcus* and *Synechococcus* could be easily separated from the remaining stained bacteria due to their autofluorescence and side scatter properties; subtraction of these groups from the total number of stained cells enabled the enumeration of heterotrophic bacteria.

Figure 3.1: Typical density plots produced by flow cytometry from samples taken from AMT cruises (a and b) and from JR82 (c and d). Arrows indicate the position of beads added to samples as an internal standard and the cell groups identified with similar properties.

a: SYBR Green stained sample (typical AMT sample)

b: Unstained AMT sample showing both *Synechococcus* and *Prochlorococcus*

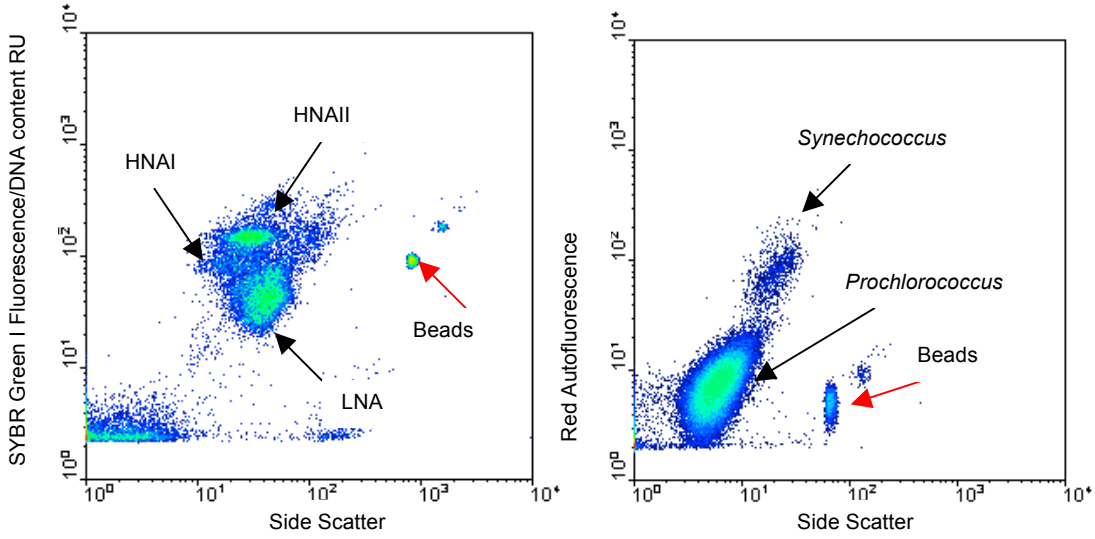

c: SYBR Green stained sample (JR82)

d: Unstained sample from JR82

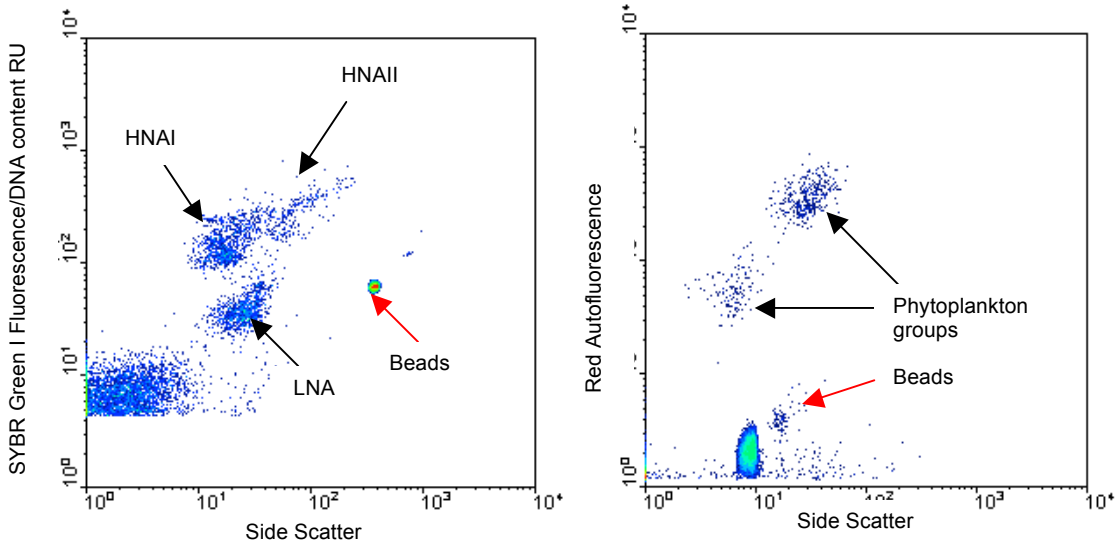

In some samples from the upper water column, *Prochlorococcus* cells contained too little chlorophyll to be detected by autofluorescence emission (Fig. 3.2a) thus the concentration was estimated using SYBR Green I stained samples. The side scatter of *Prochlorococcus* is greater than the HB in deeper water and appears as a separate population on a side scatter versus SYBR Green I fluorescence plot (Fig. 3.2b). However, further up in the water column, the side scatter decreases and the population is co-located with HB (Fig. 3.2c). Previous studies have estimated the abundance of *Prochlorococcus* in surface waters by either counting only the cells with detectable chlorophyll fluorescence emission thus underestimating the population or by counting stained *Prochlorococcus* cells along with the heterotrophic bacteria that have a similar flow cytometry signature, thus overestimating the population (Zubkov et al., 2000).

For the purpose of this study, an alternative method for estimating the abundance of *Prochlorococcus* with low chlorophyll-*a* fluorescence was used. This method assumes a constant ratio between the number of heterotrophic bacteria occurring within a defined region on the flow cytometry plots and the total number of HB. The number of heterotrophic bacteria co-located with *Prochlorococcus* in SYBR Green I stained samples was estimated and subtracted from the number of total events counted in this region. The number of HB in this region was calculated as a percentage of the total HB in deeper samples where *Prochlorococcus* was either not present or could be separated based on higher side scatter or autofluorescence. This percentage of the total HB was then used to estimate the numbers of HB that would be co-located with *Prochlorococcus* on a flow cytometry plot in surface samples.

Figure 3.2: Flow cytometry dotplots showing both chlorophyll autofluorescence in unstained samples (a - c) and SYBR Green I stained samples (d – f) in the southern gyre. At 100 m, deep *Prochlorococcus* (Pro) are visualised in unstained samples (a) and appear as a distinct population in stained samples (d). At 70 m, both surface and deep Pro are seen in unstained samples (b) and remain distinct from the heterotrophic bacteria (HB) in stained samples (e). Near the surface at 4 m, the deep Pro population is absent from the unstained samples and only part of the surface Pro population is visible above the counting threshold (c). In the corresponding stained sample, the Pro are co-located with the HB (f).

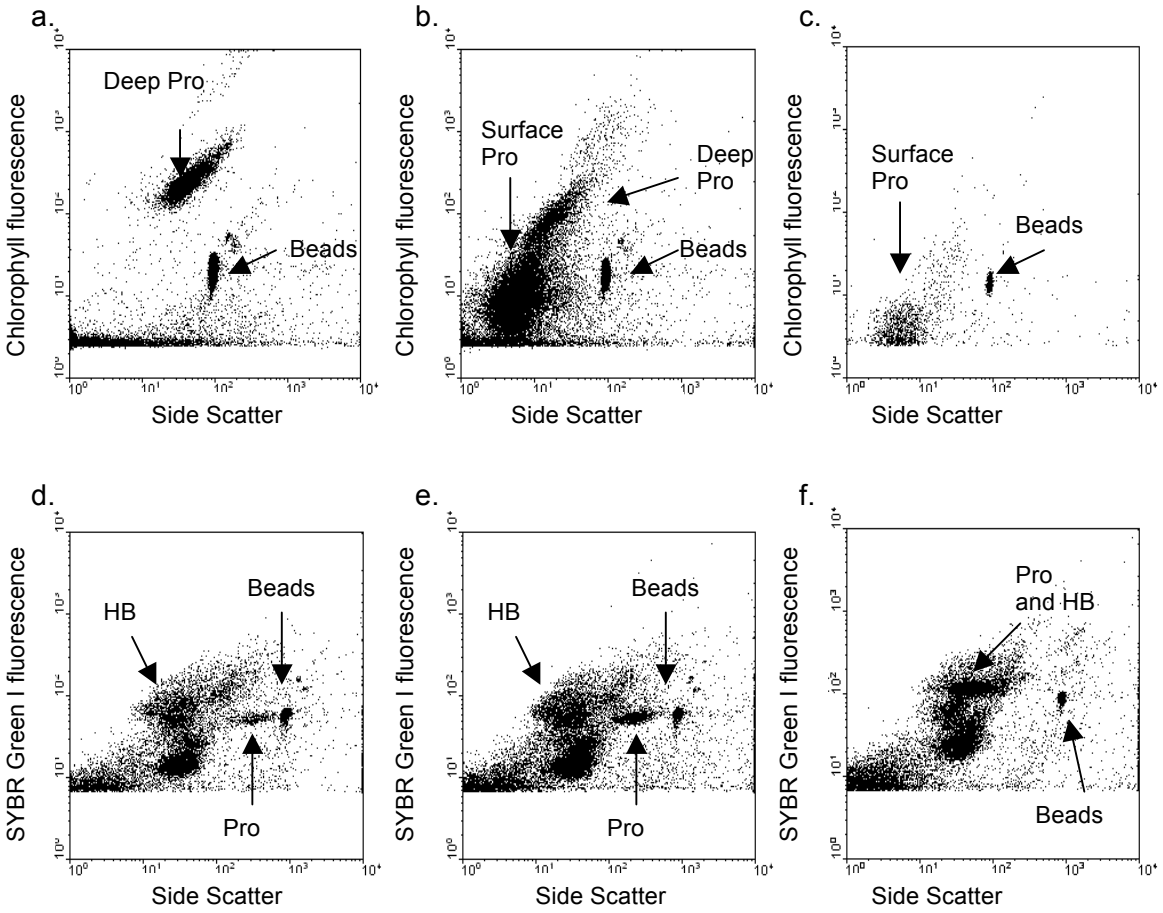

3.3. Results

3.3.1 Physical and chemical properties of the Atlantic Ocean

Isopycnals followed a w-shaped distribution along the AMT, deepening towards the centre of both oligotrophic gyres and shoaling in higher latitude temperate waters and at the equator where there was a steep vertical pycnocline (Fig. 3.3). The SAG was not sampled during AMT-6, therefore there was no deepening of the pycnocline at subtropical latitudes. The pycnocline shoaled around 15 to 25ºN during AMT-13 and 15, this again reflects a difference in cruise track, sampling the Mauritanian upwelling region closer to the NW coast of Africa during these cruises (Fig. 4.2). Seasonal variability is observed in the SAG, with a deeper surface mixed layer during the austral spring (AMT-13 and 15) compared to the austral autumn (AMT-12 and 14).

The depth of the nitracline (defined as 50 nM nitrate + nitrite) followed a similar pattern to the pycnocline, deepening in the gyres and shoaling at the equator (Fig. 3.3). However, the nitracline depth differed considerably between some adjacent stations. The nitracline only exceeded 50 m at one station in the NAG on AMT-14 in contrast to AMT-12, 13 and 15 and the SAG on all four cruises, where deeper nitraclines were observed at the majority of stations.

3.3.2 Cell loss due to freezing

The concentration of cells in samples that were frozen prior to flow cytometric analysis significantly correlated with the concentration in samples that were not frozen for all three cell groups ($p < 0.001$). A higher concentration was measured in a few of the frozen samples compared to the concentration measured in unfrozen samples measured on the day of collection for all cell groups (Fig. 3.4). However, freezing had a detrimental effect on cell concentration for the majority of samples with most of the data lying below the 1:1 ratio line. Linear regressions of all the samples show that following freezing and storage at -80 ºC, 21 % of HB, 30 % of *Prochlorococcus* and 20 % of *Synechococcus* cells were lost (Fig. 3.4).

Figure 3.3: Water density (Sigma-t), 50 nM nitracline depth (solid black line) and location of samples (black dots) during AMT cruises.

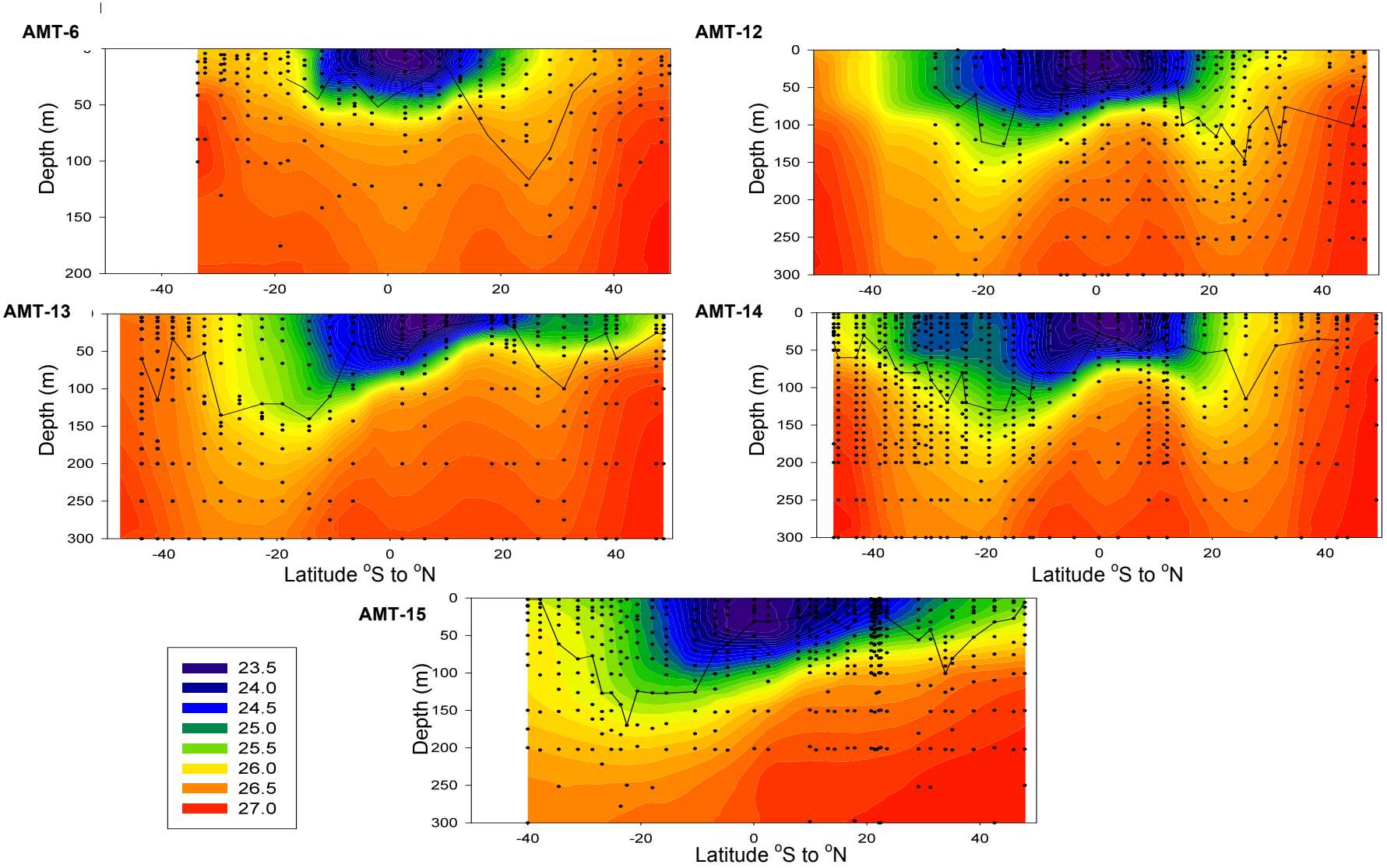

Figure 3.4: Linear regressions between the concentrations of cells measured by flow cytometry on frozen (*y*) and unfrozen samples (*x*) during AMT-14. The equation relating the two measurements is shown on each graph along with the r^2 value and the number of samples (n). The solid line indicates the regression and the dotted line indicates a 1:1 relationship.

a. Heterotrophic bacteria

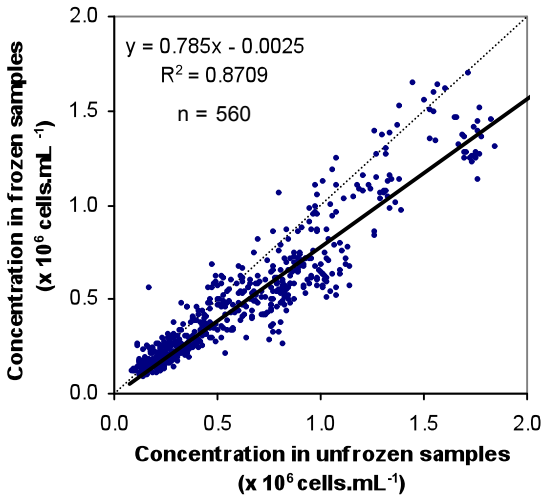

b. *Prochlorococcus*

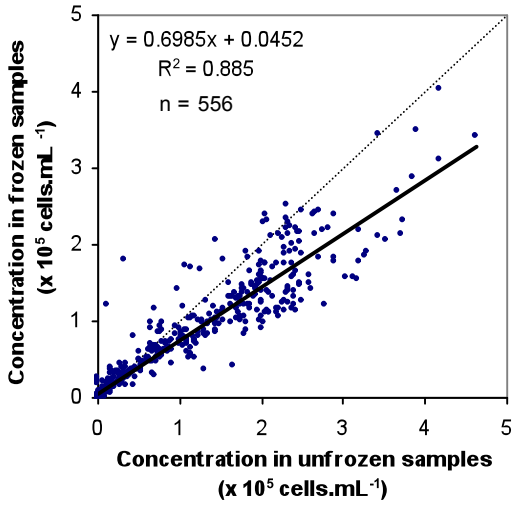

c. *Synechococcus*

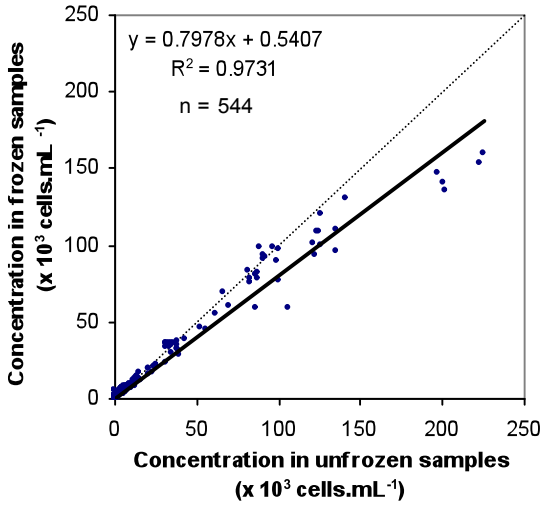

3.3.3 Vertical distribution of bacterioplankton

Heterotrophic bacteria

The vertical distribution of heterotrophic bacteria (HB) in the water column was similar in the equatorial upwelling (EQ), the southern temperate region (ST) and the Scotia Sea (Sc) with a high abundance above the nitracline in the surface mixed waters (up to 50 m). The concentration of HB then decreased rapidly with increasing depth and corresponds to a sharp pycnocline in these provinces (Fig. 3.5). Stations sampled in the Scotia Sea on the JR82 cruise were located close to stations in the ST during AMT-14 however, the abundance of HB in surface waters was higher in the Sc than in the ST (3.5×10^6 cells.mL-1 compared to 1.4×10^6 cells.ml-1).

Despite similar physical and chemical properties of the water column in the NT compared to the ST, the distribution of HB differed with an increase in cell concentration below the nitracline and the surface mixed layer at 60 to 70 m. There was also less light penetration into deeper waters (> 25 m) compared to other provinces.

In both the southern (SAG) and northern (NAG) gyres, the upper 110 to 120 m of the water column had high light penetration and low nitrate concentrations. In the SAG, a clearly defined mixed layer to approx. 100 m could be identified at all stations, this was similar at some stations in the NAG, however at certain stations in this province, no clear mixed layer could be identified (Fig. 3.5). Despite the differences in density profiles between the two gyres, the vertical distribution of HB was similar. Cell concentrations were either relatively stable above the nitracline (SAG) or exhibited a slight increase with depth towards the depth of the nitracline (NAG) followed by a decrease below the nitracline in both gyres (Fig. 3.5).

Prochlorococcus

A similar vertical distribution of *Prochlorococcus* (Pro) was found in the EQ, the ST and the NT with a high concentration in the surface waters followed by a decrease below the shallow nitracline (Fig. 3.6). In the EQ, the SAG and the NAG, both the surface and deep populations of Pro were identified using flow cytometry whereas in the temperate

Figure 3.5: Typical vertical profiles of heterotrophic bacterial abundance (HB; red circles), density (solid black lines) and photosynthetically available radiation (PAR; blue lines) in different provinces along AMT-14 and in the Scotia Sea (Sc). The dashed lines on the AMT-14 graphs indicate the depth of the nitracline. Note the different scales used for HB.

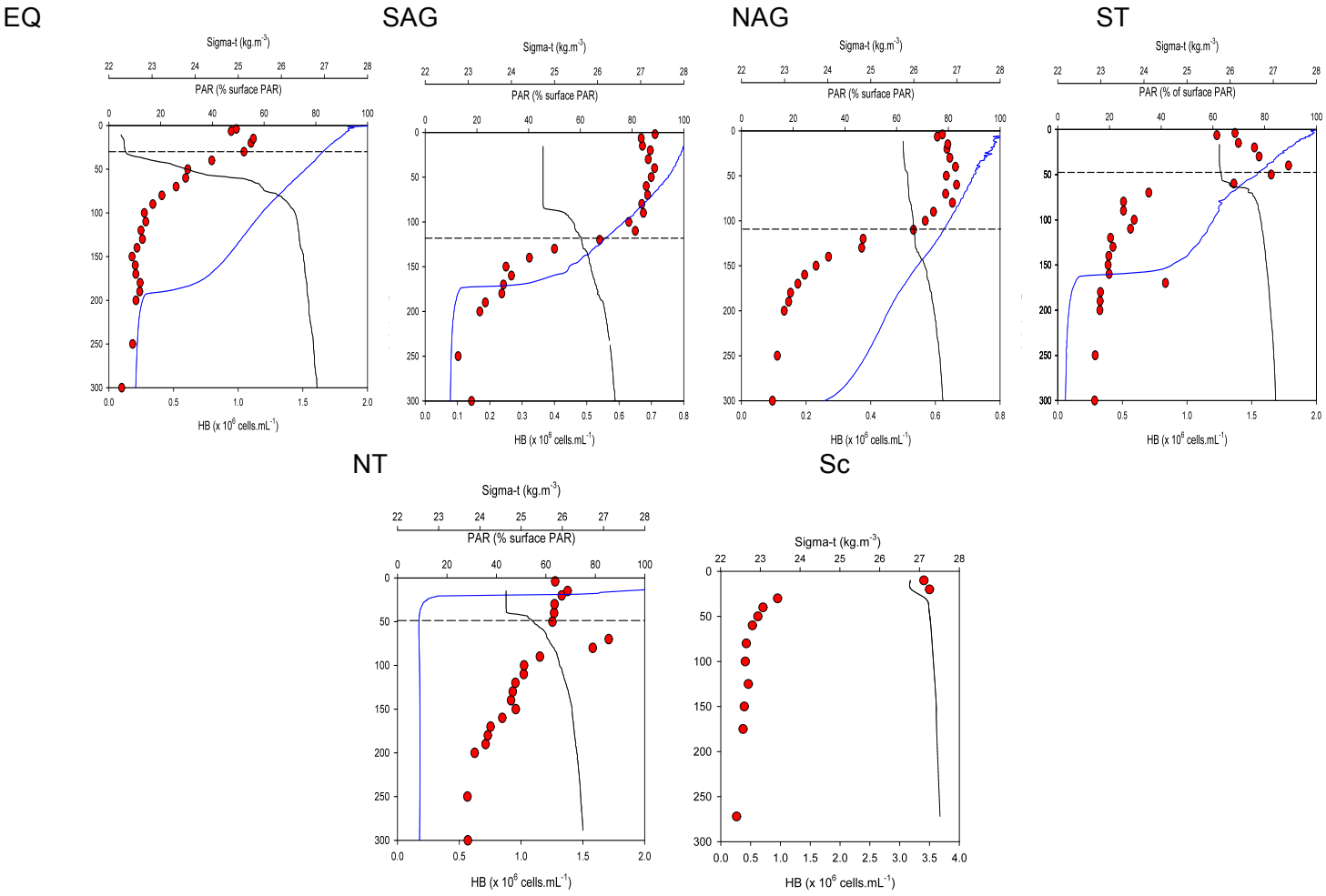

Figure 3.6: Typical vertical profiles of surface (open circles) and deep (solid circles) *Prochlorococcus* (Pro) abundance, density (solid black lines) and photosynthetically available radiation (PAR; blue lines) in different provinces along AMT-14. The dashed lines indicate the depth of the nitracline. Note the different scales used for Pro abundance.

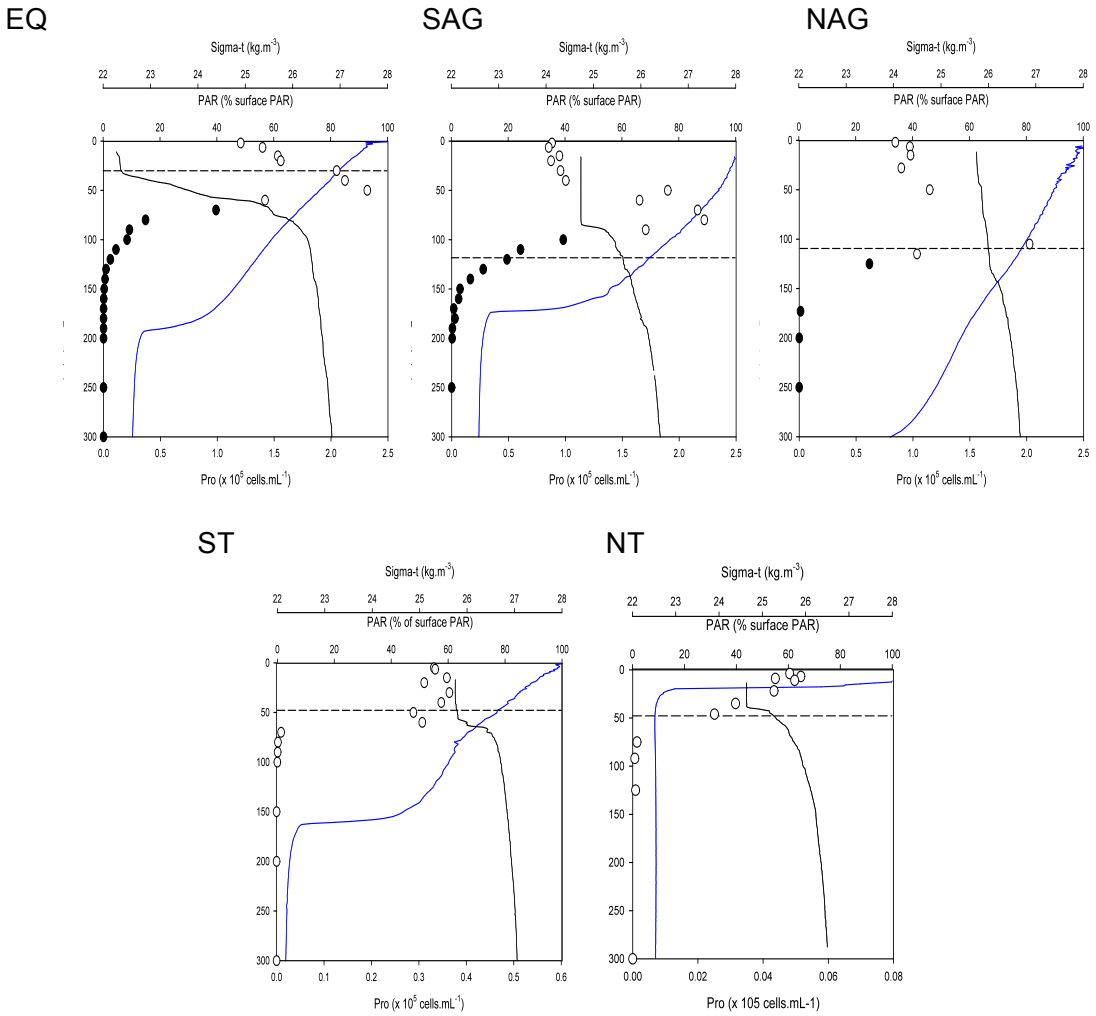

provinces, the flow cytometry signature of the Pro population did not change with depth. In the gyres, surface Pro contained very low and relatively constant amounts of chlorophyll with only a slight increase towards the deepest part of their range. In contrast, the deep Pro population possessed considerably higher average chlorophyll content per cell and this increased with increasing depth (Fig. 3.7).

Figure 3.7: Vertical profile of average *Prochlorococcus* abundance (a) and cellular chlorophyll content (b) at a typical station in the southern Atlantic gyre.

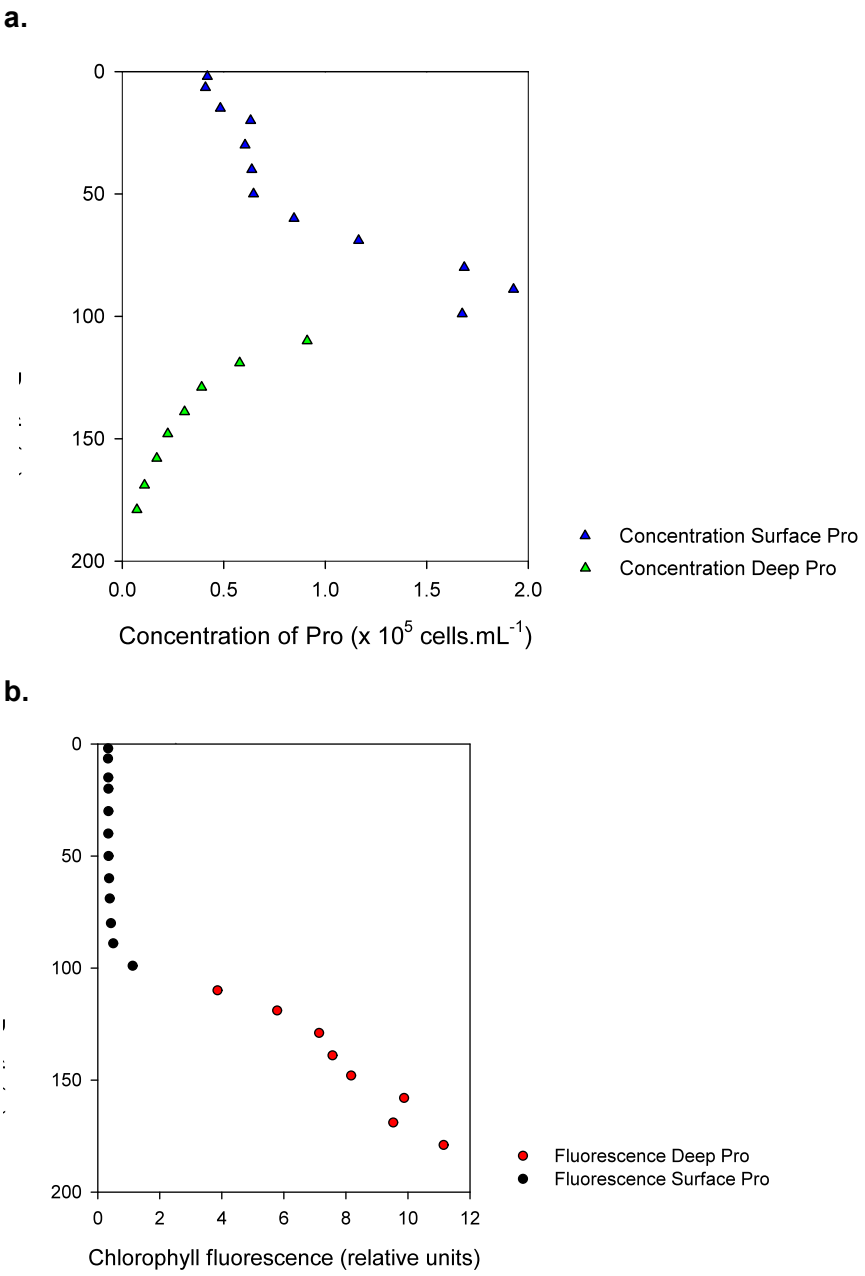

In both the SAG and the NAG there was a sub-surface Pro maximum cell concentration typically located between 100 and 150 m. This peak in Pro abundance often exceeded thrice the surface concentration and was entirely comprised of the surface Pro population as determined by the flow cytometry signature. Below this sub-surface Pro abundance maximum, the cell concentration decreased and the deep Pro dominated at light levels of less than 1 % of the surface irradiation (Figs. 3.6 and 3.7).

Synechococcus

The distribution of *Synechococcus* (Syn) in the water column was similar to that of *Prochlorococcus* (Pro) in the equatorial upwelling (EQ), the southern (ST) and the northern temperate (NT) regions with a high concentration above the nitracline and a decrease with depth below. However, in the SAG and the NAG, Syn did not extend as deep in the water column as the Pro and either the concentration was very low or the cells were absent below the nitracline (Fig. 3.8).

Total picophytoplankton in the Scotia Sea

The vertical distribution of picophytoplankton followed a similar pattern to the distribution of heterotrophic bacteria in the Scotia Sea. High concentrations in excess of 4×10^3 cells.mL^{-1} were found in the shallow surface layers and the concentration then decreased sharply with depth following the sharp pycnocline (Fig. 3.9). The picophytoplankton community in this region was mainly comprised of picoeukaryotes rather than prokaryotes as determined by the flow cytometry signature.

Figure 3.8: Typical vertical profiles of Syn abundance (solid circles), density (solid black lines) and photosynthetically available radiation (PAR; blue lines) as a percentage of the surface PAR in different provinces along AMT-14. The dashed lines indicate the depth of the nitracline. Note the different scales used for Syn abundance.

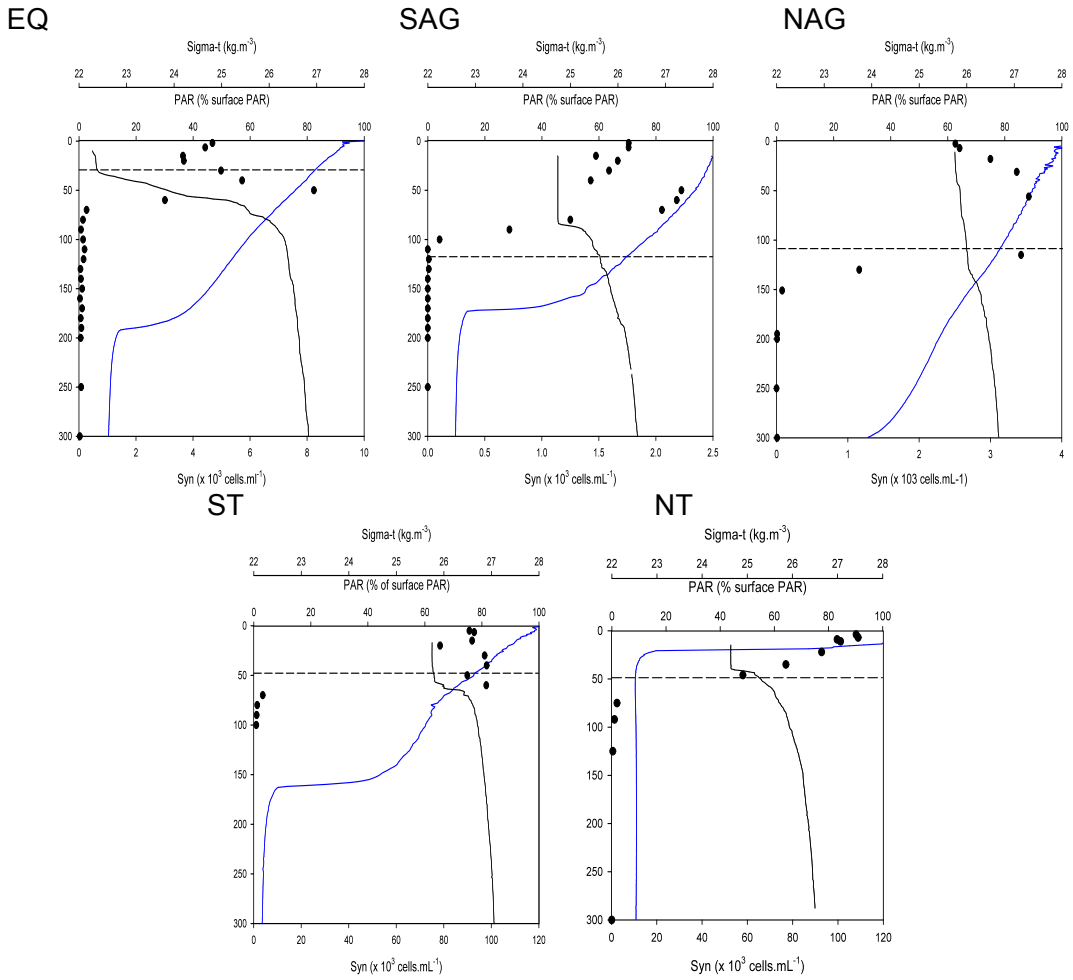

Figure 3.9: Typical vertical profiles of total phytoplankton abundance and density (sigma-t) in the offshore region of the Scotia Sea.

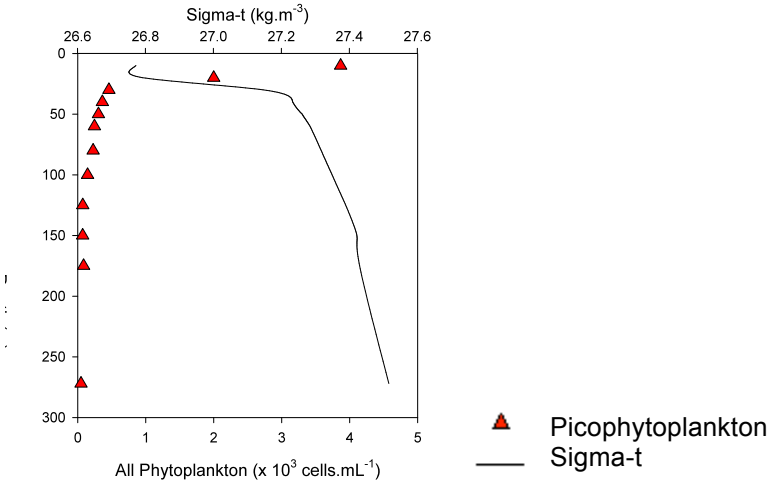

3.3.4 Picoplankton abundance and distribution on cruises AMT-6, 12, 13, 14 and 15.

Heterotrophic bacteria

Heterotrophic bacteria (HB) were most abundant in the surface 20 m of the water column around the equator and at high latitudes (> 35º) at the southern and northern ends of the transect on all cruises (Fig. 3.10). During AMT-6, 13 and 15, surface waters in the upwelling region around 15 to 25 ºN also contained high numbers of HB (1.2 to 2.0 x 10^6 cells mL^{-1}). In contrast, stations at similar latitudes on AMT-12 and 14 were located closer to the centre of the NAG (Fig. 4.2) and contained fewer heterotrophic bacteria (0.74 to 0.89 x 10^6 cells mL^{-1} during AMT-12 and 0.47 to 0.55 x 10^6 cells mL^{-1} during AMT-14). In surface waters south of the equator during AMT-6, HB were also abundant.

The distribution of different heterotrophic bacterial (HB) cell sizes and cellular DNA content were examined during AMT-14. The average DNA content of HB cells varied by almost a factor of 2 both horizontally and vertically along the transect (Fig. 3.11). Cells located in deeper waters generally had a higher DNA content than cells in the upper 100 m of the water column. Unlike HB abundance, the DNA content of cells was higher in the SAG than in the NAG. There was also a difference in the temperate, high latitude ends of the transect with a higher cellular DNA content in the ST than the NT (Fig. 3.11).

Figure 3.10: Concentration of heterotrophic bacteria x 10^6 cells mL^{-1} during AMT cruises.

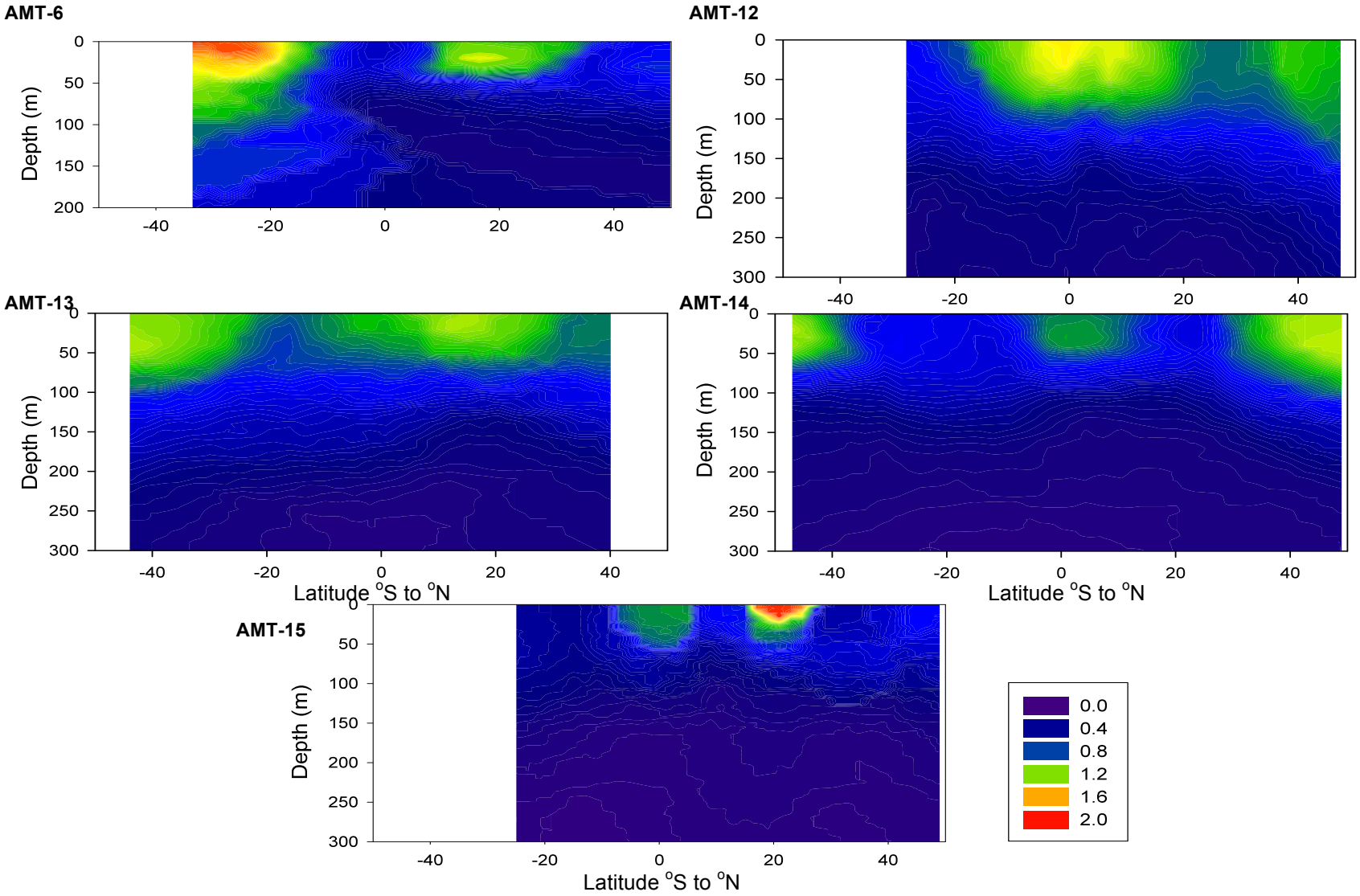

Figure 3.11: Average cellular DNA content of HB during AMT-14 (relative units). SYBR Green I fluorescence values were calibrated using standard reference fluorescent beads.

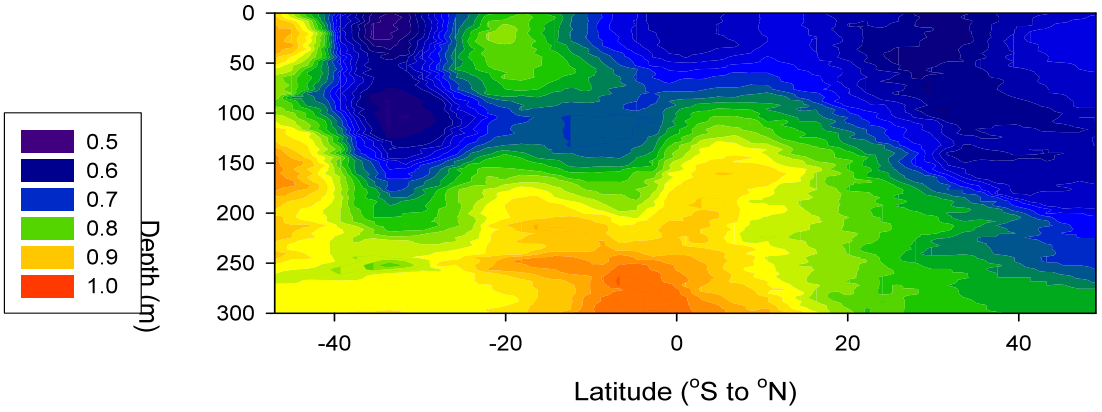

Figure 3.12: Average cell diameter of HB during AMT-14 (µm). Cell diameters were calculated using side scatter values obtained from flow cytometry as described in chapter 4.

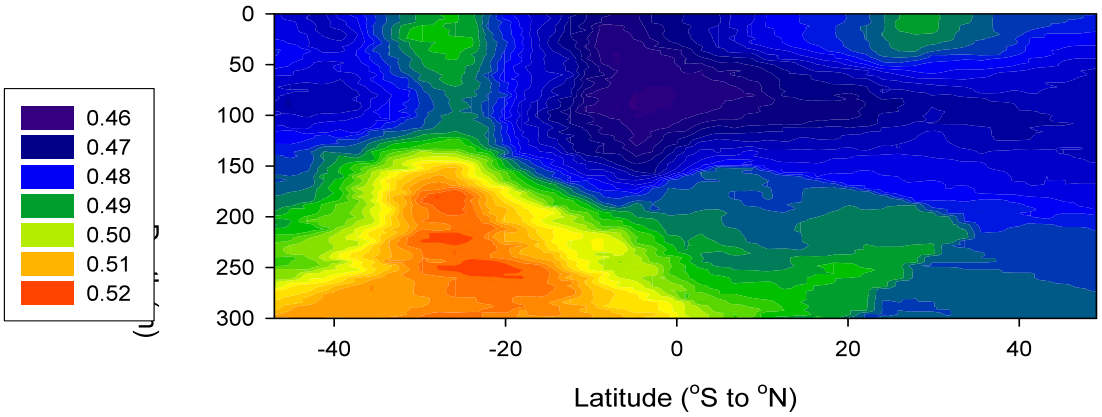

Despite the large differences in DNA content, cell size distribution did not follow the same pattern. Cell diameters varied little both horizontally and vertically during AMT-14 and the largest cells did not have the greatest DNA content. However, as for DNA content, cell size generally increased with depth (Fig. 3.12).

Figure 3.13: *Prochlorococcus* concentration x 10^5 cells mL^{-1} during AMT cruises.

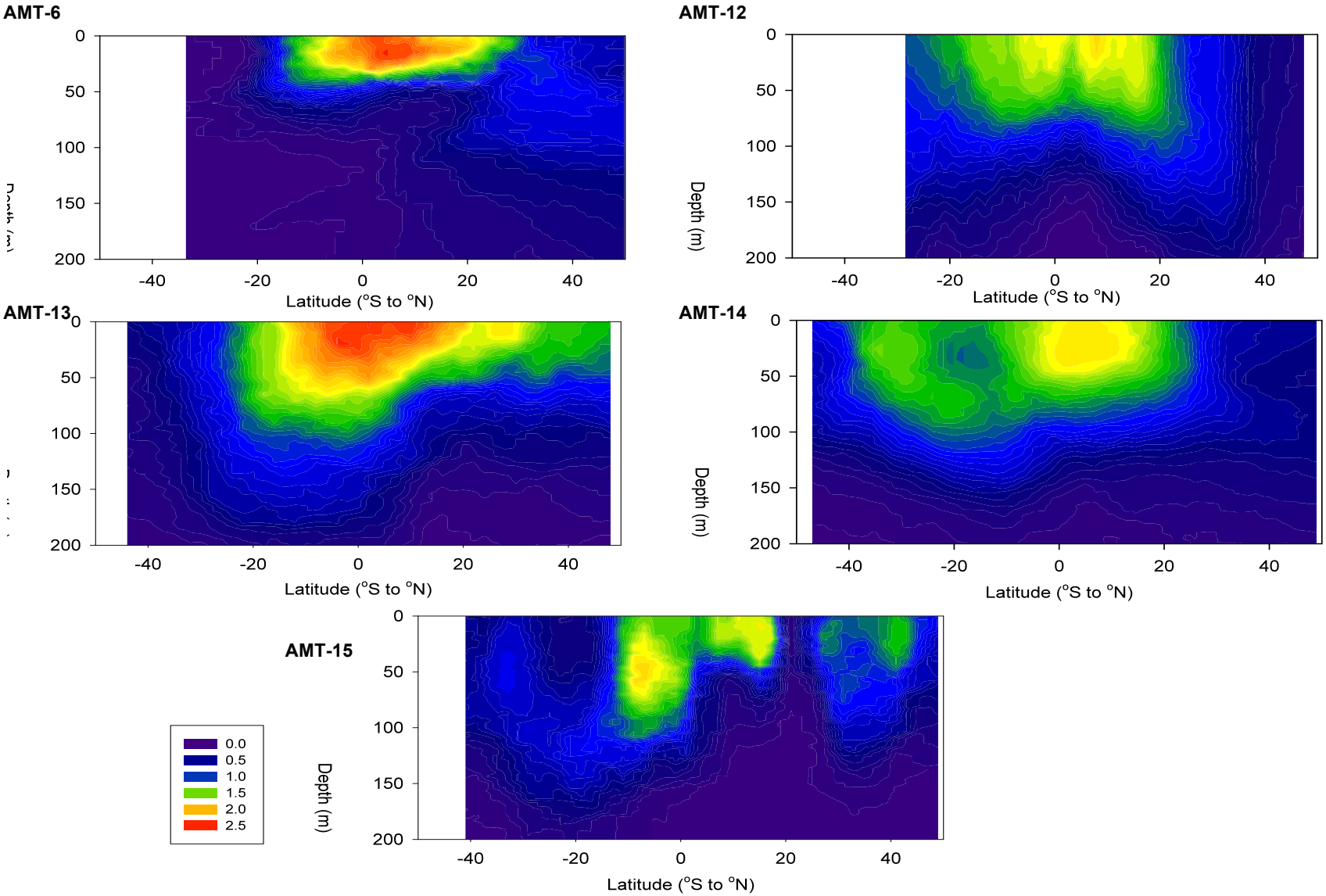

Prochlorococcus

Prochlorococcus (Pro) numerically dominated the picophytoplankton over the majority of the transect with the peak abundance on all cruises (1.75 to 2.5 x 10^5 cells mL^{-1}) located in the upper 40 m of the water column around the equator (Fig. 3.13). Cells extended deeper in the water column in the oligotrophic gyres than at the equator or at high latitudes (150 to 200 m in the gyres compared to 50 to 100 m at the equator and high latitude regions), following a similar latitudinal pattern to the pycnocline and the nitracline. Approximately 70 to 75 % of total Pro cells were located above the nitracline and there was a steady decline in cell concentration with depth below the nitracline.

As already stated, the two *Prochlorococcus* populations have different cellular contents of chlorophyll as determined by relative fluorescence measurements obtained from flow cytometry. However, the horizontal distribution of cellular fluorescence along the AMT transect shows little variance in the surface 50 m. Greater diversity in cellular chlorophyll fluorescence was observed in deeper waters with the highest values located between 150 and 200 m in the SAG between 20 and 30 ºS (Fig. 3.14).

Figure 3.14: Average chlorophyll fluorescence per *Prochlorococcus* cell during AMT-14. Fluorescence values were calibrated using standard reference fluorescent beads.

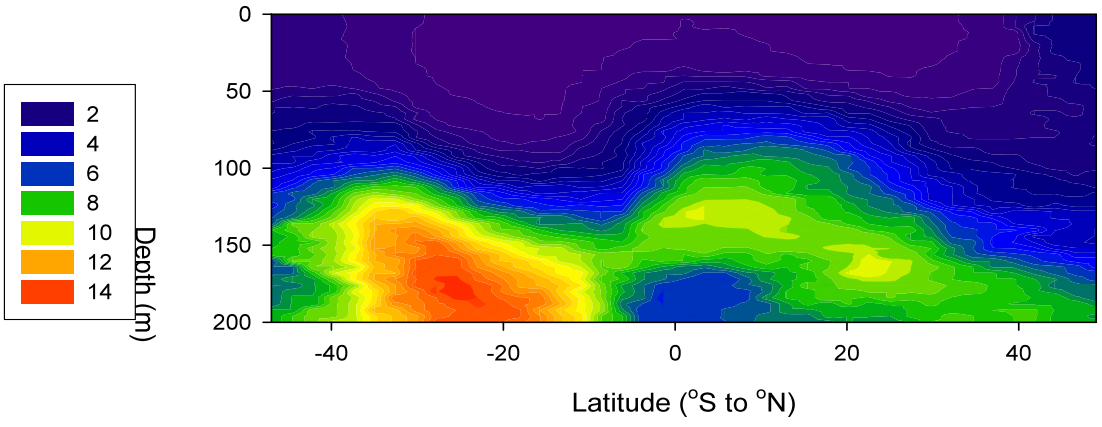

Figure 3.15: Log. *Synechococcus* concentration x 10^3 cells mL^{-1} during AMT cruises. Note the different scale used for AMT-12, all other cruises are plotted on the same scale.

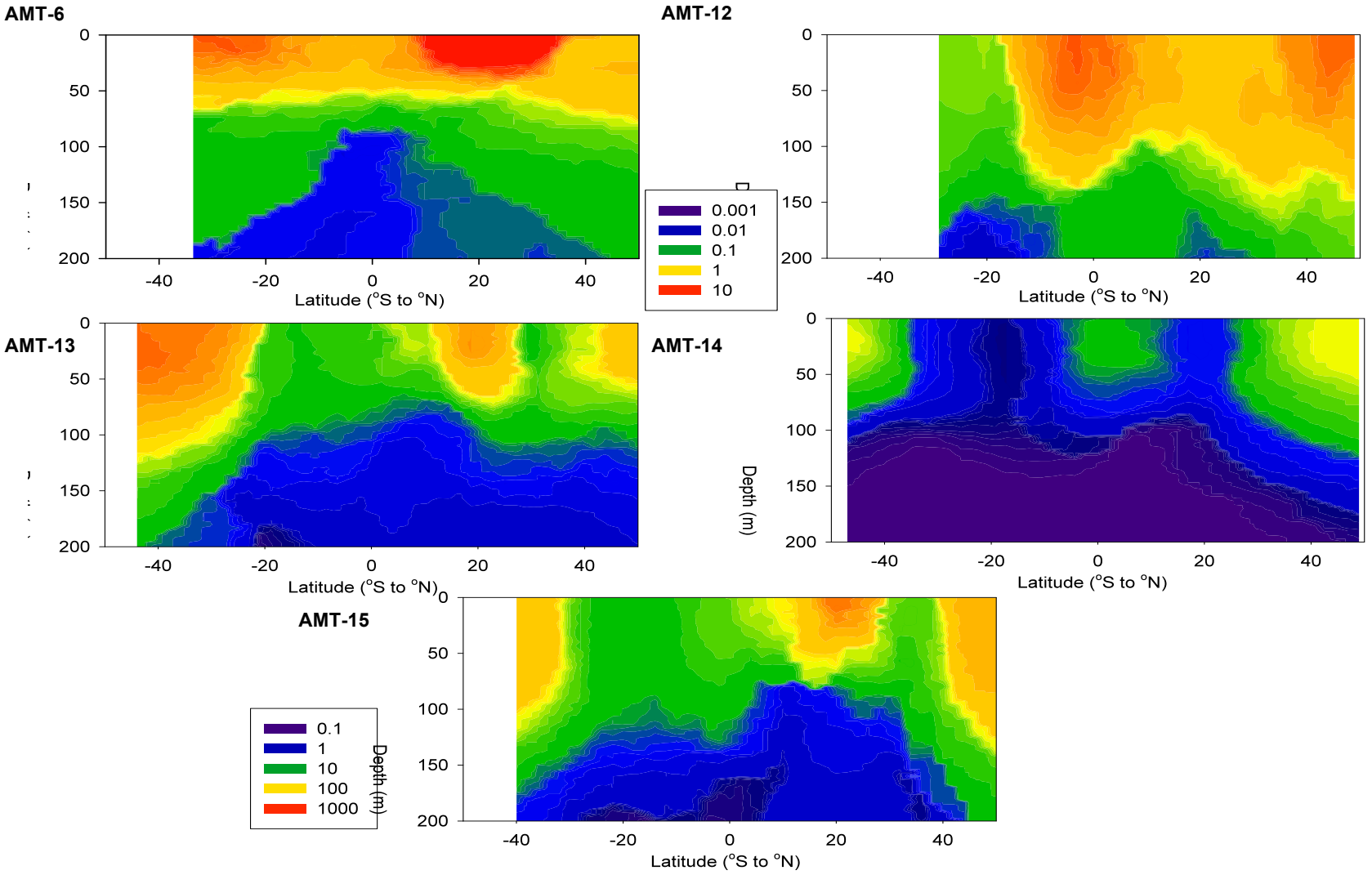

Synechococcus

Synechococcus (Syn) concentrations exceeded 10^4 cells mL^{-1} in the surface 50 m of the water column at low latitudes around the equator and again at high latitudes (> 20º) where high concentrations extended deeper in the water column. Low concentrations of Syn (< 2.0 x 10^3 cells mL^{-1}) were measured over the remainder of the transect on AMT-12 and 14. However, during AMT-6, 13 and 15 in the Mauritanian upwelling region, centred around 20º N, high abundance in surface waters was measured (> 1.2 x 10^5 cells mL^{-1} during AMT-6; > 2.0 x 10^4 cells mL^{-1} during AMT-13 and > 5.0 x 10^4 cells mL^{-1} during AMT-15), comparable to that measured in the high latitude temperate regions (Fig. 3.15).

3.3.5 Picoplankton abundance and distribution in the Scotia Sea

Heterotrophic bacteria

In the Scotia Sea, the concentration of heterotrophic bacteria (HB) decreased with increasing latitude. The vertical and horizontal distribution averaged along two transects, one to the south west (A) and one to the south east (B) of S. Georgia are shown in Figure 3.16. The location of the transects used to plot these data is shown in Figure 2.10. The highest concentration of HB (2 x 10^6 cells.mL^{-1}) was found in the surface 25 m at the northern end of both transects, close to S. Georgia. The distribution of HB along transect A followed the shape of the pycnocline with higher concentrations located north east of the SBACC around 59 ºS (Fig. 3.16a; see section 2.6.3).

The influence of the SBACC on heterotrophic bacteria along transect B was not as distinct as along transect A; however abundances were generally higher to the north west of the density front at 56 ºS (Fig. 3.16b and Fig. 2.12). At the southern end of transect B in the south west Scotia Sea, a vertical gradient in HB abundance was found ranging from 0.7 x 10^6 cells.mL^{-1} at 20 m to 0.1 x 10^6 cells.mL^{-1} at 150 m.

Figure 3.16: Concentration of heterotrophic bacteria (x 10^6 cells.mL^{-1}) in the Scotia Sea. Black dots indicate the location of samples analysed.

a. Transect A

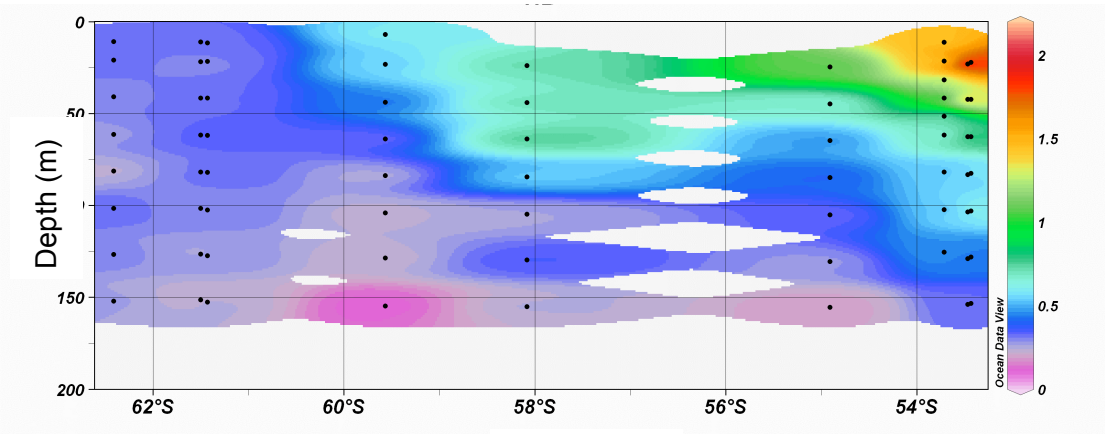

b. Transect B

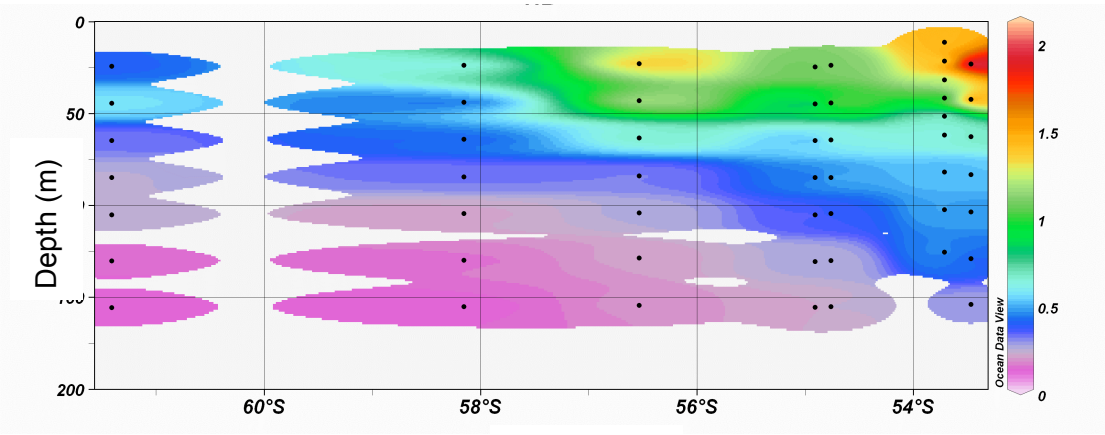

Picophytoplankton

Picophytoplankton were most abundant (in excess of 10 x 10^3 cells.mL-1) in surface waters of the northern Scotia Sea, close to S. Georgia (Fig. 3.17 a and b). This peak abundance is co-located with the peak abundance of heterotrophic bacteria for this cruise. The lowest inorganic nitrogen concentrations measured on this cruise were also found in this region (Fig. 2.13).

In both the south west (transect A; Fig. 3.17a) and the south east (transect B; Fig. 3.17b) Scotia Sea, picophytoplankton generally extended deeper in the water column than in the northern region (down to 100 m compared to 45 m).

Figure 3.17: Concentration of picophytoplankton (x 10^3 cells.mL^{-1}) in the Scotia Sea. Black dots indicate the location of samples analysed.

a. Transect A

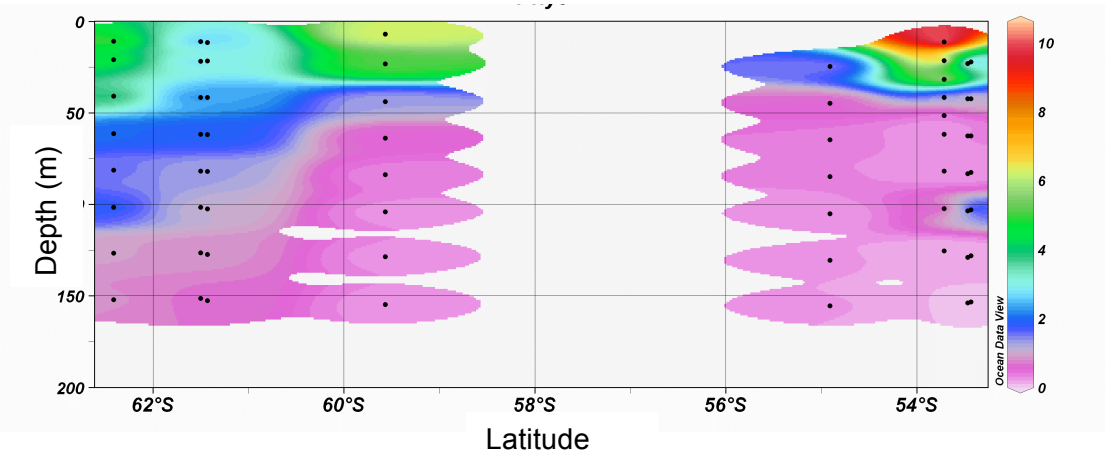

b. Transect B

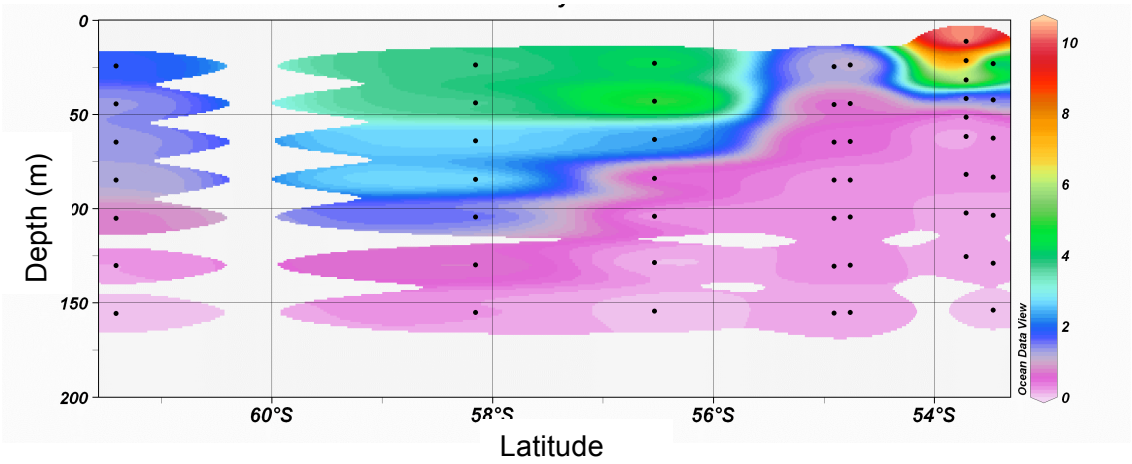

3.4. Discussion

The vertical and horizontal distribution of picoplankton has been shown to vary between different regions of the Atlantic Ocean and the Scotia Sea. Some regions or provinces, although geographically separated from each other, exhibit similar cellular abundances and vertical distributions associated with similar physical and chemical characteristics. Picoplankton group composition and distribution in the Atlantic Ocean was consistent with previous studies along the AMT transect (Zubkov et al., 1998, 2000). In general, the northern and southern oligotrophic gyres have more similar picoplankton abundances and vertical distribution than the more nutrient-rich upwelling regions near the coast of Africa and around the equator and in the northern and

southern temperate regions. The abundance of bacterioplankton in different provinces and between different cruises is analysed in more detail in chapter 4. The abundance of HB in the Scotia Sea was also the same order of magnitude as previously found in more westerly Antarctic waters, also close to the Antarctic peninsula (Pedros-Alio et al., 2002; Vaque et al., 2002).

The quantification of picoplankton cell losses due to freezing prior to flow cytometric analysis has, to the author's knowledge, only been published for prochlorophytes (Olsen et al., 1990). Flow cytometric analysis of picoplankton is often carried out post-cruise on previously frozen samples therefore; the group specific cell loss values presented here are important measurements that can be used to estimate *in situ* concentrations.

It would be expected that cell size varies with genome size and consequently DNA content (Velduis et al., 1997) (Veldhuis and Kraay, 2004) however, this was not the case for the heterotrophic bacteria. Several nucleic acid stains, including SYBR Green I, have been used previously to estimate cellular DNA content (Button and Robertson, 2001; Li et al., 1995; Marie et al., 1997). The difference in cell size distribution and DNA content may be due to a change in bacterioplankton community composition with a higher contribution of species with larger genome sizes in deeper waters. There may also be species specific staining, with some cells taking up SYBR Green I more than others, regardless of genome size. The stain may also bind to RNA and single stranded DNA, although it has lower binding affinities for these compared to double stranded DNA (Haugland, 1992).

Both *Prochlorococcus* and heterotrophic bacteria abundances increased with depth towards the nitracline in many vertical profiles from the gyres. This has been reported previously in the northern Atlantic gyre (Li, 1995; Olson et al., 1990), however this is the first report of a similar vertical distribution in the southern Atlantic gyre. It is unlikely that this is due to methodological differences such as the use of SYBR Green I stained samples to enumerate *Prochlorococcus* in surface waters. If not all the *Prochlorococcus* were stained, numbers in surface waters would be underestimated and as the abundance of heterotrophic bacteria is determined after subtraction of the phototrophic bacteria, an underestimation of *Prochlorococcus* abundance in surface waters would result in an overestimation of heterotrophic bacteria. However, as heterotrophic bacteria were also more abundant in deeper samples, it is unlikely that this is due to differences in methodology.

Prochlorococcus extended deeper in the water column than *Synechococcus* in the gyres, this has been widely reported, for example, in Atlantic Ocean oligotrophic waters in the Sargasso Sea (DuRand et al., 2001) and the Northeast Atlantic Ocean (Partensky et al., 1996). The abundance and appearance of the deep population of *Prochlorococcus* in deeper waters highlights the adaptation of these cyanobacteria to grow successfully at low-light levels (Moore et al., 1995, 1998; Moore and Chisholm, 1999). The increased red fluorescence of the deep *Prochlorococcus* observed by flow cytometry indicates a higher cellular chlorophyll content compared to the surface *Prochlorococcus*. Similar vertical profiles of *Prochlorococcus* chlorophyll content were obtained using HPLC pigment analysis in the Northern Atlantic gyre (Veldhuis and Kraay, 2004). The two populations are probably the previously identified high-light and low-light ecotypes (Moore et al., 1998) although as no molecular analysis was carried out in this study, this cannot be proven.

The concentration of total picophytoplankton in the Scotia Sea was several orders of magnitude lower in both identified regions during the JR82 cruise than in any province on the AMT cruises. This large concentration difference can be attributed to a difference in phytoplankton communities observed by flow cytometry. Picophytoplankton at low latitudes and in the subtropics along the AMT is dominated by small prokaryotic cells, mainly *Prochlorococcus* and *Synechococcus*, in contrast, in the Scotia Sea on JR82, no *Prochlorococcus* and very few *Synechococcus* were observed. Instead, the picophytoplankton community in the Scotia Sea consisted of groups of larger phytoplankton (as indicated by their larger side scatter), probably picoeukaryotes.

The data presented here have enabled further characterisation of the Atlantic Ocean and Scotia Sea picoplankton abundance and distribution over large spatial and temporal scales. The hypotheses proposed that the abundance and distribution of prokaryotes varies both horizontally and vertically has been proved enabling the characterisation of different regions of the Atlantic Ocean and the Scotia Sea.

Chapter 4

Bacterioplankton standing stocks in oligotrophic gyre and equatorial provinces of the Atlantic Ocean: Evaluation of inter-annual variability

4.1. Introduction

For many years, the oligotrophic ocean gyres were considered to be stable, steady-state environments (Karl, 1999). However, in recent years, temporal variability in physical and biological parameters including the picoplankton has been reported at fixed stations in the North Pacific and North Atlantic oligotrophic gyres (Karl et al., 2001; Karl and Lukas, 1996; DuRand et al., 2001; Carlson et al., 1996) and on across-gyre cruises (Maranon et al., 2003). Since the area and boundaries of the gyres change seasonally and inter-annually (McClain et al., 2004), geographically fixed time series stations in gyres will not remain fixed in their position within the gyre, i.e. they will be located closer or farther away from the gyre boundaries as these move in time. In order to resolve gyre boundaries and to gain average abundance and biomass values for these provinces, (i.e. more robust estimates of basin scale temporal changes) sampling across the gyres and at several points in time would be required. Due to the extensive area covered by oligotrophic gyres, few studies have examined spatial variability in bacterioplankton abundance across these regions (e.g. in the Atlantic, Li, 1995; Buck et al., 1996; Zubkov et al., 1998, 2000). Sampling along such transects is often only carried out once or over short time-scales, resulting in a lack of knowledge regarding inter-annual variability in oceanic provinces (Longhurst, 1995).

Typical physical properties of the water column in oligotrophic gyres include a deep surface mixed layer. These very low nutrient surface waters are prevented from mixing with deeper, more nutrient rich waters due to a clearly defined pycnocline. It would be expected that the physical separation of these waters with differing nutrient and light conditions would result in different biological communities. For the purpose of this study, the depth of the nitracline, defined as 50 nM, was therefore chosen as the depth for integration of data in order to study the community and abundance of bacterioplankton in the oligotrophic surface mixed layer. Comparison is also made between these surface mixed layer communities and the entire photic zone using data integrated to 200 m.

The aims of this study are to examine spatial and temporal (including inter-annual) variability of bacterioplankton in three oceanic provinces, the Northern Gyre (NAG), Southern Gyre (SAG) and Equatorial region (EQ). The hypothesis to be tested is that bacterioplankton standing stocks do not vary significantly inter-annually or seasonally in the NAG and the SAG. The minimum number and frequency of stations required to characterise the prokaryotic plankton standing stocks at the province scale was also investigated. Bacterioplankton standing stocks of the Atlantic oligotrophic gyres were the major focus of this work, however, the equatorial region separating the oligotrophic gyres in the northern and southern hemispheres was included as a comparison to more nutrient-rich waters containing similar communities. Average bacterioplankton abundances and biomass were also compared between northern and southern temperate waters and in the Scotia Sea.

4.2 Methods

4.2.1 Cell size and biomass calculations

The mean value of side scatter measured by flow cytometry for each identified group of picophytoplankton was converted into a ratio to the mean side scatter of fluorescent reference beads in each sample for calibration of the instrument. Cell size estimates for each bacterioplankton group determined previously using a size fractionation method (Zubkov et al., 1998) were used in conjunction with the side scatter values to estimate biomass. These mean diameters were 0.63 µm for all *Prochlorococcus*, 0.95 µm for *Synechococcus* and 0.46 µm for heterotrophic bacteria. The mean side scatter value (s) for each prokaryotic group was calculated using all samples from AMT-12, 13 and 14. The mean cell diameter (d) reported previously for each bacterioplankton group (Zubkov et al., 1998) was then related to this calculated mean side scatter using non-linear regression as illustrated in Figure 4.1. The relationship between cell diameter and side scatter is described by the equation; $d = 1.49.s^{0.41}$ ($r^2 = 0.99$; $p < 0.05$; $n = 4$).

Cell volumes, computed from diameters assuming spherical cell shape, were converted into biomass using a conversion factor of 220 fg C μm^{-3} (Christian and Karl, 1994). Different bead stocks were used for AMT-12, 13, 14 and 15 cruises. In order to account for any variability in bead size, the calculated mean diameter of each bacterioplankton group was corrected using the mean side scatter of bacterioplankton at 300 m for each cruise and for all four cruises as it was assumed that cell size at these depths would be more constant.

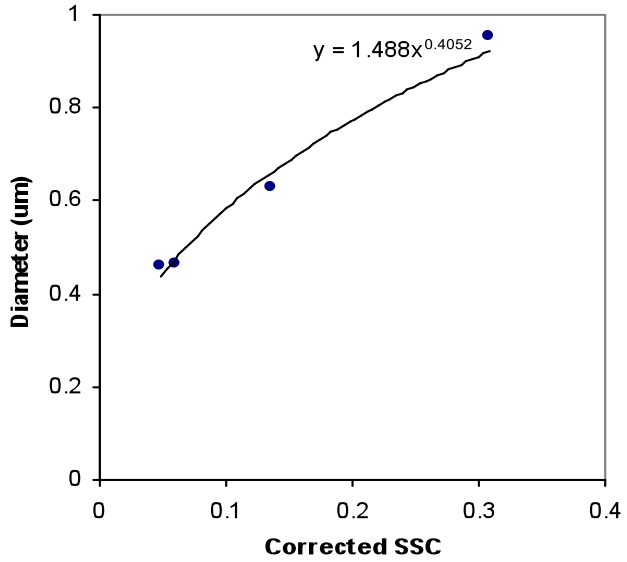

Figure 4.1: Non-linear regression between mean side scatter, SSC (*x*) and cell diameter (*y*). The equation relating the two factors is indicated.

4.2.2 Province analysis

The bacterioplankton abundance data, measured by flow cytometry and presented in chapter 3 was further analysed in this chapter to define provinces. Mean cell concentrations of *Prochlorococcus, Synechococcus*, total picophytoplankton and heterotrophic bacteria above the nitracline (or above 200 m for cruise JR82) were used to group the stations into oceanic provinces using Bray-Curtis similarity tests followed by hierarchical agglomerative cluster analysis (Clarke and Warwick, 2001) performed with PRIMER 5 software (PRIMER-E Ltd., Plymouth, U.K.). Stations with at least 90 % similarity were grouped together.

4.2.3 Data analysis

Data from cruises AMT-6, 12, 13, 14 and 15 were analysed along with data collected in previous years from cruises AMT-3 and 4 (Zubkov *et al.*, 1998; 2000). Cell concentrations and biomass values were depth-integrated from the surface to the start of the nitracline. Mean cell concentrations were calculated by dividing the depth-integrated cell abundance by the integration depth. As the majority of stations sampled were in oligotrophic waters, the start of the nitracline was defined as the depth where the concentration of inorganic nitrogen (nitrate plus nitrite), measured as described in chapter 2, increased above 50 nM. Cell concentrations and biomass values were also

depth-integrated to 200 m to encompass the entire photic zone and to compare with published values.

Mean integrated biomass and mean cell concentrations above the nitracline and above 200 m for each province were compared between cruises using ANOVA followed by multiple pairwise comparisons performed with Tukey tests (Sigmastat 2.03). To obtain mean cell concentrations and integrated biomass values for each province, the data from different cruises were combined omitting those that were significantly different ($p < 0.05$).

4.3 Results

4.3.1 Determination of provinces

For the AMT cruises a conservative level of at least 90 % similarity between mean cell concentrations above the nitracline was chosen to cluster stations into provinces as this produced between 5 and 8 groups or individual stations using cluster analysis. Stations around the tropics in both N and S parts of the transect clustered together and stations at the southern and northern ends of the transect also clustered together. These clusters were divided into northern and southern parts to define provinces. Figure 4.2 highlights the stations that were grouped together to form provinces on cruises AMT-6, 12, 13, 14 and 15. Five provinces were identified; Northern temperate (NT), NAG, EQ, SAG and Southern temperate (ST).

Stations sampled south of the EQ province during AMT-6 were located farther east towards the coast of Africa than on other cruises and water here was more influenced by coastal processes. Consequently, no data from the SAG was obtained from AMT-6. The southern and northern gyre provinces appear to be shifted slightly southwards during the boreal spring (AMT-12 and 14) compared to the boreal autumn (AMT-13 and 15; Figs. 3.12, 3.15 and 3.17). This is consistent with earlier seasonal comparisons between AMT-3 and 4 (Zubkov et al, 2000).

Figure 4.2: Location of depth profiles analysed for bacterioplankton abundance on cruises AMT-6 (a), AMT-12 (b), AMT-13 (c), AMT-14 (d) and AMT-15 (e). Open circles represent stations within the gyre provinces, solid circles indicate the equatorial province stations and solid squares represent the temperate provinces. Solid triangles highlight the stations that were omitted from the province analysis due to their high degree of dissimilarity to other surrounding stations.

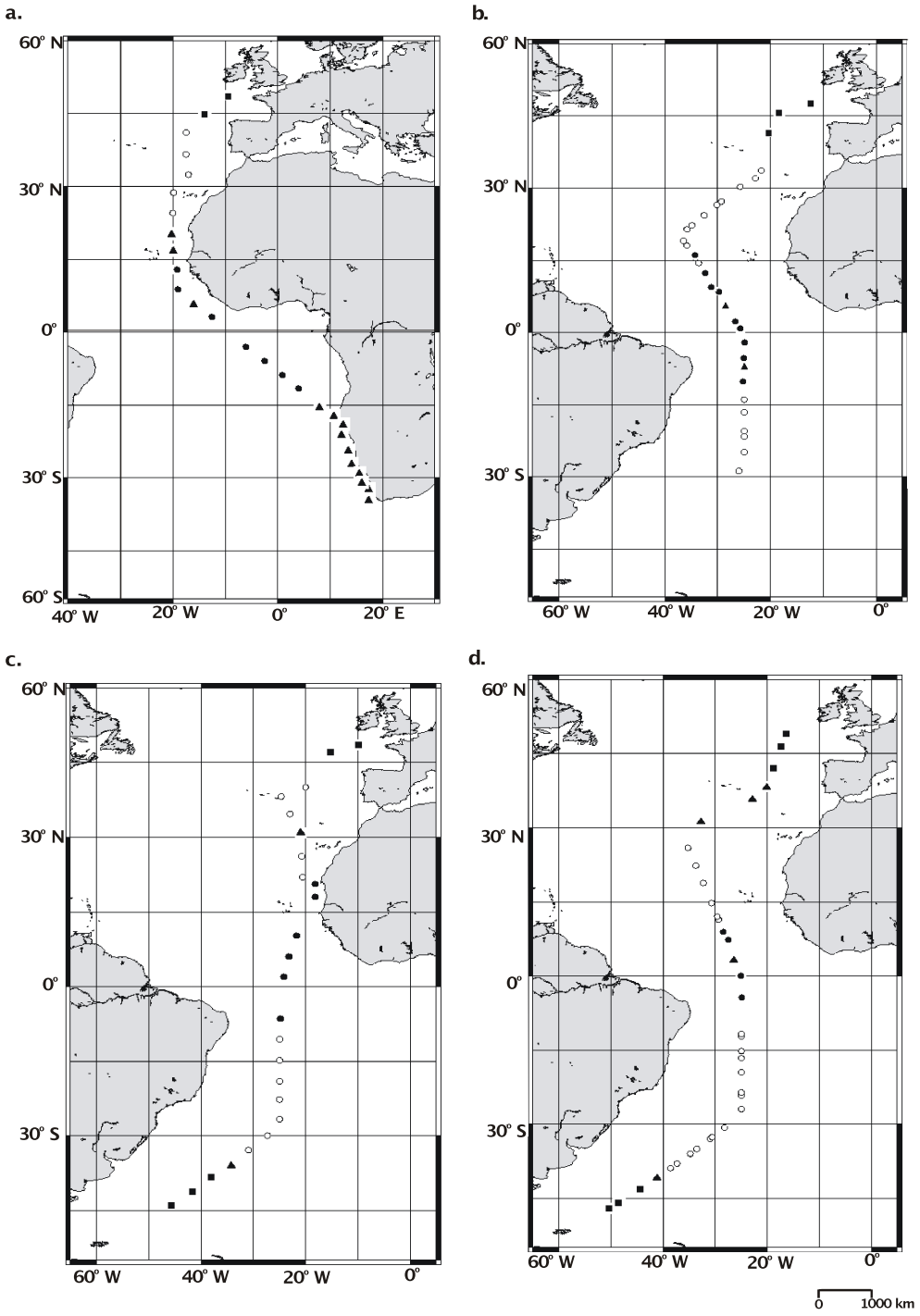

e.

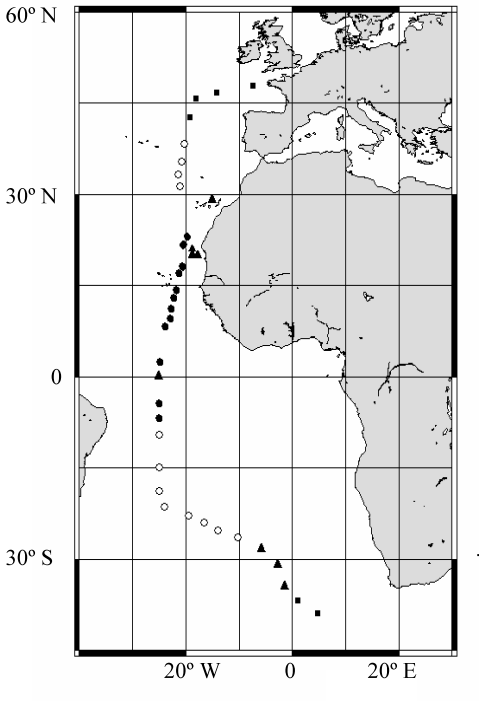

Stations in the Scotia Sea during the JR82 cruise clustered into two main groups, one group of stations was located mainly around S. Georgia, named the coastal region (JR82 C), whilst the majority of the remaining stations were located further away from land, named the off-shore region (JR82 O; Fig. 4.3).

Figure 4.3: Location of depth profiles analysed for bacterioplankton abundance on cruise JR82 in the Scotia Sea. Open circles represent stations within the coastal regions, solid circles indicate the offshore stations and the open triangle highlights the station that was omitted from the regional analysis due to its high degree of dissimilarity to other surrounding stations.

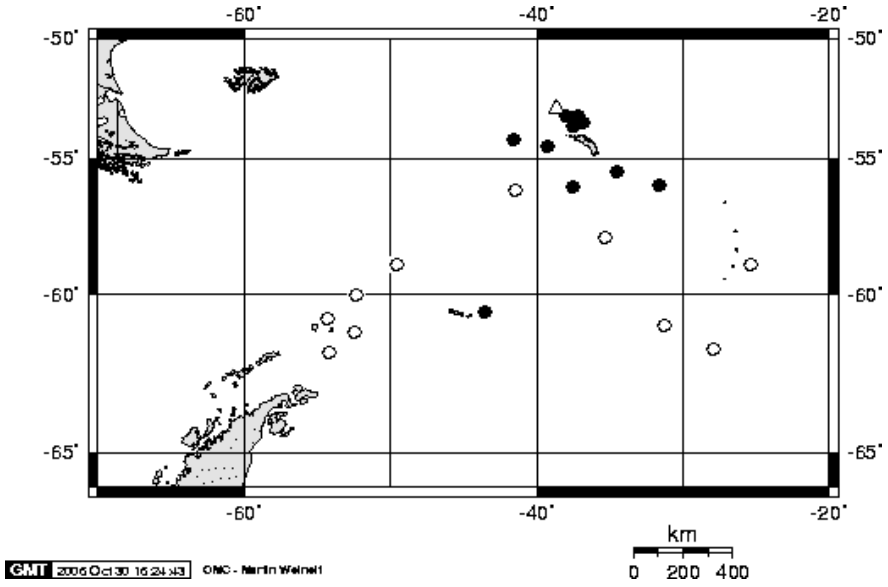

4.3.2 Comparison of surface and average cell concentrations above the nitracline

To examine the homogeneity of bacterioplankton distribution above the nitracline, surface abundances were compared with average values in the northern (NAG) and southern (SAG) Atlantic gyres and the equatorial region (EQ). Surface *Synechococcus* concentrations showed good agreement with average values above the nitracline in all provinces (r^2 = 0.96; Fig. 4.4 and Table 4.1). However, more variability was observed between the surface and average concentrations of *Prochlorococcus* (Pro) and heterotrophic bacteria (HB) in the NAG and SAG (r^2 values between 0.39 and 0.79). On closer inspection of the data from outlying stations, the majority exhibited an increase in Pro with an associated increase in HB in deeper waters of this surface layer, close to the start of the nitracline (up to 20 m above).

Figure 4.4: Comparisons between average cell concentrations above the nitracline and surface concentrations in the SAG, NAG and EQ. Depth-integrated cell numbers were divided by the depth of integration to obtain the average cell concentrations. The regression line (solid line) and the 95 % confidence intervals (dotted lines) are shown.

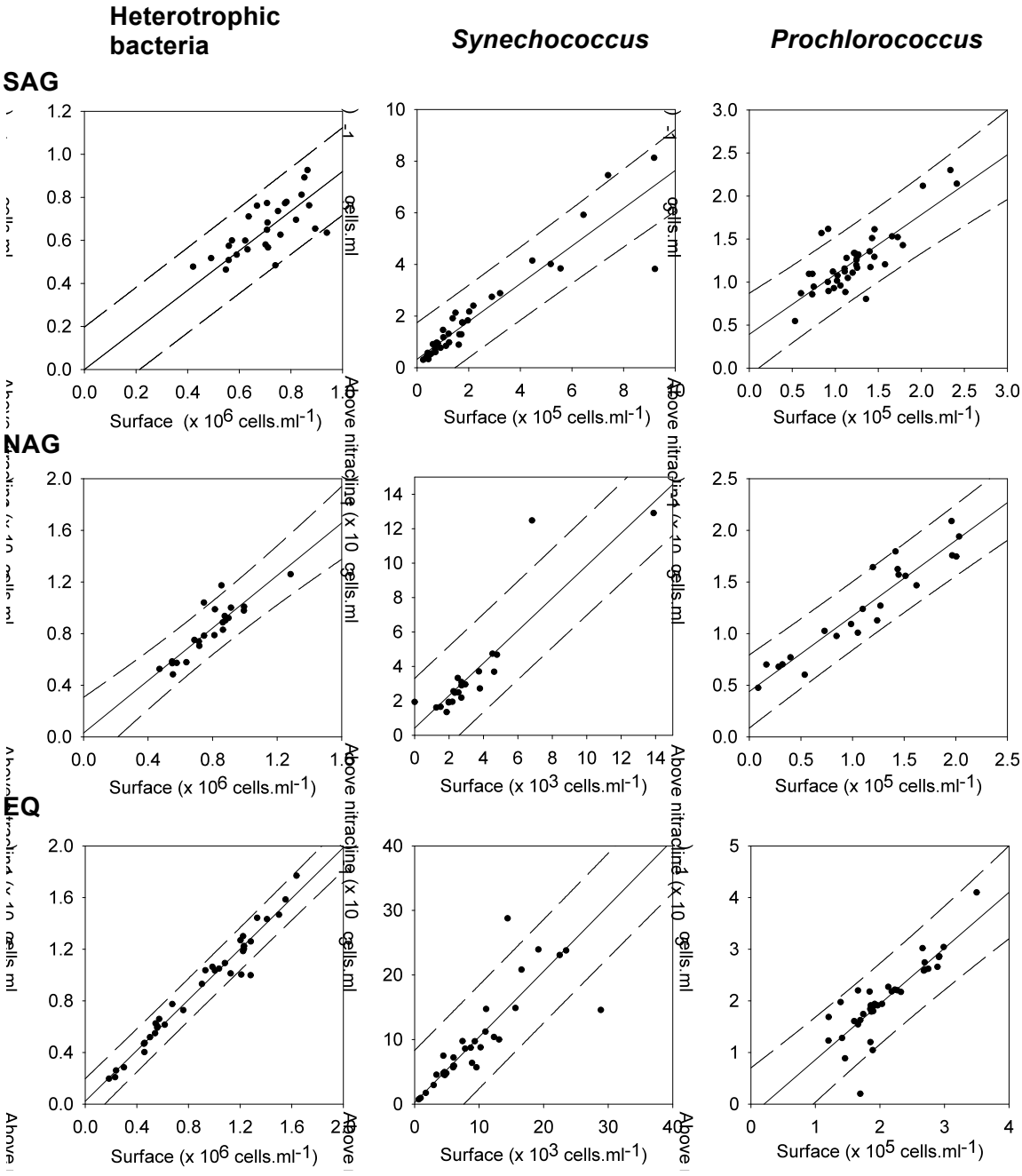

Table 4.1: Relationships (regression coefficients) between the surface and average concentrations above the nitracline. R^2 values are shown in brackets. The number of stations in each province is stated (n). P-values are also indicated. P < 0.05 (*); p < 0.01 (**); p < 0.001 (***).

Province	**Heterotrophic bacteria**	***Synechococcus***	***Prochlorococcus***
SAG (n = 18)	0.99 (0.39)* n = 28	0.90 (0.96)*** n = 41	0.98 (0.53)** n = 41
NAG (n = 19)	1.05 (0.79)*** n = 23	0.97 (0.96)*** n = 23	1.04 (0.69)*** n = 23
EQ (n = 16)	1.00 (0.96)*** n = 37	1.02 (0.96)*** n = 37	1.00 (0.79)*** n = 37

4.3.3 Cell size

The calculated mean diameters for each bacterioplankton group showed little variance between AMT cruises (Table 4.2). Mean diameters ranged from 0.91 to 0.97 μm for *Synechococcus* and 0.46 to 0.49 μm for heterotrophic bacteria. As previously reported (e.g. Partensky et al., 1996), two distinct populations of *Prochlorococcus* can be identified by flow cytometry, one abundant in surface waters and the other being more abundant in deeper waters of the photic zone. Surface *Prochlorococcus* have lower light side scatter values than the deeper population (Fig. 3.3), resulting in the calculated mean diameter of deep *Prochlorococcus* as almost double that of the surface population (approximately 1.0 μm compared to 0.5 μm for the surface population).

Table 4.2: Mean cell diameters with standard errors of the mean for each bacterioplankton group on each cruise. Surface and deep *Prochlorococcus* (Pro) populations were discriminated based on the different flow cytometry signatures of each group.

	Mean cell diameter, μm ± S.E.M.			
Cruise	Surface *Pro*	Deep *Pro*	*Synechococcus*	Heterotrophic bacteria
AMT12	0.546 ± 0.007	1.014 ± 0.016	0.939 ± 0.006	0.488 ± 0.002
AMT13	0.551 ± 0.007	0.942 ± 0.022	0.937 ± 0.006	0.481 ± 0.001
AMT14	0.531 ± 0.005	1.006 ± 0.019	0.905 ± 0.004	0.483 ± 0.001
AMT15	0.495 ± 0.004	1.066 ± 0.027	0.969 ± 0.005	0.484 ± 0.001

4.3.4 Average bacterioplankton abundances in different provinces

Average abundances above the nitracline

Average heterotrophic bacteria (HB), *Prochlorococcus* (Pro) and *Synechococcus* (Syn) concentrations above the nitracline in the northern (NAG) and southern (SAG) Atlantic gyres and the equatorial region (EQ) on each AMT cruise are shown in the bar charts in the left hand panels of Figure 4.5. The abundance of all three groups of bacterioplankton was similar in both the NAG and SAG provinces and was slightly higher in the EQ province. The concentration of HB in all provinces was consistently lower on AMT-3, 4 and 6 than on AMT-12, 13, 14 and 15 (with the exception of the EQ province during AMT-15). The data from later cruises only was used to calculate province average values for both abundance and integrated biomass due to differences in sample storage explained in more detail later. In addition, the average HB concentration above the nitracline during both AMT-14 and 15 was significantly lower ($p < 0.05$) in all provinces relative to AMT-12 and 13 with the exception of the EQ province where no significant difference was observed between AMT-13 and 14. The average concentration of HB was also significantly lower during AMT-15 than AMT-14 in both the SAG and the EQ ($p < 0.05$).

High variability in *Synechococcus* (Syn) concentration was observed both within cruises and between cruises in the NAG and EQ provinces, in particular for AMT-6 and

13. However, the only significant inter-cruise difference in Syn concentration above the nitracline was observed in the NAG province between AMT-12 and AMT-13 ($p = 0.02$), with a higher concentration observed during AMT-13. *Prochlorococcus* (Pro) concentrations were not significantly different between most cruises in the NAG and SAG, however, a significantly lower concentration ($p < 0.02$) was observed during AMT-15 in the SAG compared to AMT-4, 13 and 14 and was therefore not included in the subsequent average province estimates. There was also a significantly higher Pro concentration in the EQ on AMT-13 compared to AMT-4 ($p <0.01$).

Average abundances above 200 m

Cell concentrations averaged over the upper 200 m of the water column were lower for all bacterioplankton groups in all provinces relative to the average values above the nitracline (Fig. 4.6). Inter-cruise comparisons of average cell concentrations above 200 m were similar to those found above the nitracline, with the following exceptions. The concentration of heterotrophic bacteria (HB) was significantly higher ($p < 0.05$) during AMT-12 than AMT-13 in both the NAG and the EQ provinces. *Synechococcus* (Syn) concentration was also higher in the NAG during AMT-6 than AMT-12 and 14 ($p < 0.05$). The only inter-cruise difference in Syn concentration in the SAG was between AMT-12 and 13 ($p < 0.05$) and the only inter-cruise difference in the EQ province was a higher concentration during AMT-6 relative to AMT-12 ($p < 0.01$). In contrast to average concentrations above the nitracline, *Prochlorococcus* (Pro) concentrations were not significantly different during AMT-4 and 13 in the EQ province, however there was a significantly higher average concentration above 200 m in the EQ province during AMT-6 compared to AMT-4. All other average concentrations showed no significant differences between cruises (Fig. 4.6).

Province estimates of abundance

Estimates of average bacterioplankton concentrations both above the nitracline and above 200 m for each province are shown in Table 4.3. The average concentration of heterotrophic bacteria (HB) above 200 m during the JR82 cruise was similar to the estimated concentration in the NAG for the coastal stations (JR82 C) however, the average concentration in the offshore region (JR82 O) was significantly lower than in any other region ($p < 0.05$). In contrast, the average concentration of total picophytoplankton in the offshore region was higher than in the coastal region, however due to high variability between stations, this was not statistically significant. The

average concentration of picophytoplankton above 200 m in both regions identified during JR82 is several orders of magnitude lower than the average concentration of *Prochlorococcus* and *Synechococcus* combined in all provinces of the AMT cruises.

Average cell concentrations in the northern and southern temperate regions exhibited wide variation between cruises, mostly due to seasonal differences e.g. spring blooms of *Synechococcus* (Figs. 3.12, 3.15 and 3.17). Data from all AMT cruises in these regions were therefore combined despite significant inter-cruise differences in order to obtain an average combined value for autumn and spring for each region for comparison to other provinces. The nitracline depth was not chosen for the integration of data in these regions as nitrate concentrations were usually greater than 50 nM. The NT had a higher concentration of HB than any other province. A lower concentration of HB was found in the ST, more comparable to the closely located JR82C region and the northern and southern gyres (Table 4.3).

Figure 4.5: Mean cell concentrations and mean integrated biomass of heterotrophic bacteria (HB), *Synechococcus* (Syn) and *Prochlorococcus* (Pro) above the nitracline in each province during each AMT cruise. Bars indicate the standard error of the mean.

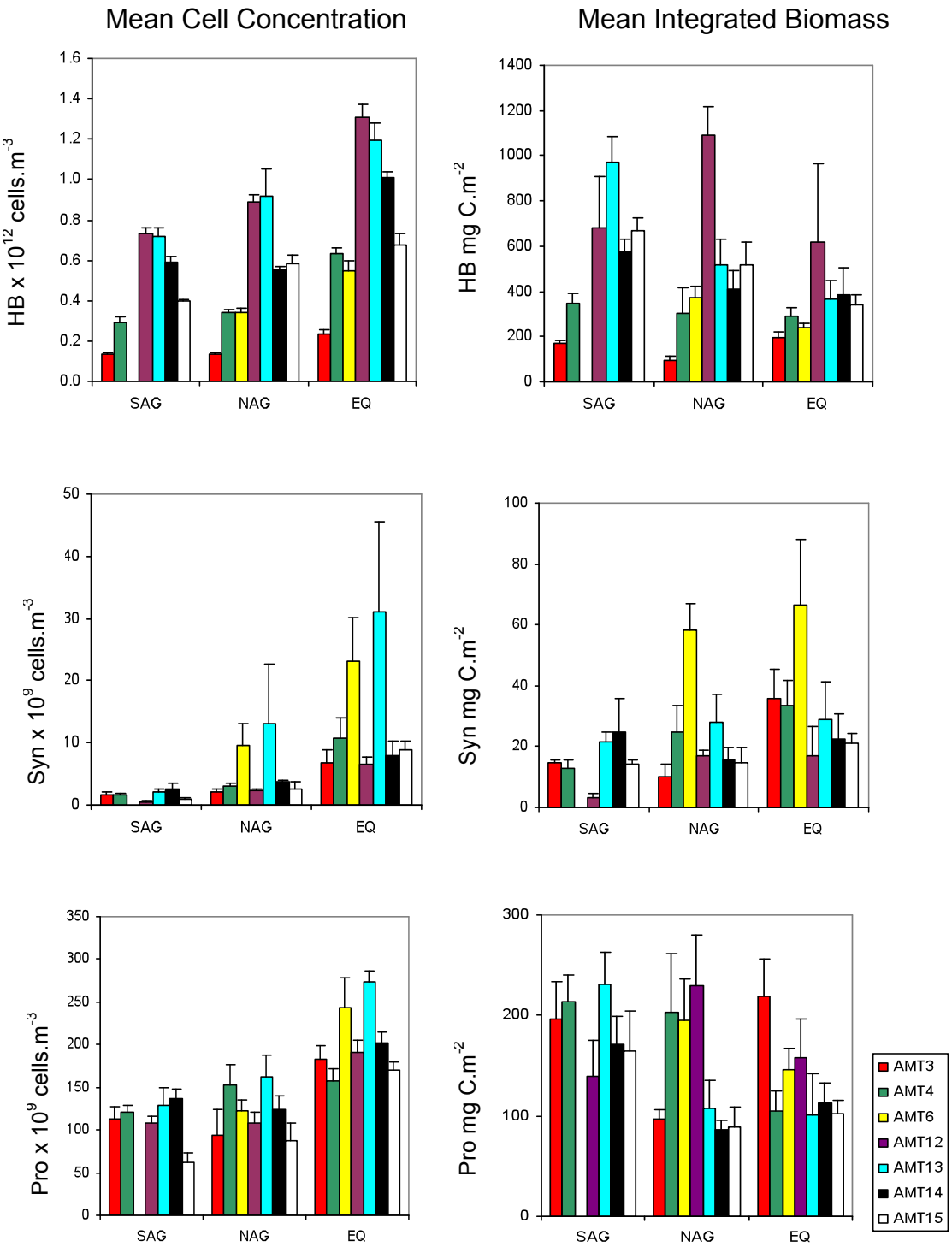

Figure 4.6: Mean cell concentrations and mean integrated biomass of heterotrophic bacteria (HB), *Synechococcus* (Syn) and *Prochlorococcus* (Pro) above 200 m in each province during each AMT cruise. Bars indicate the standard error of the mean.

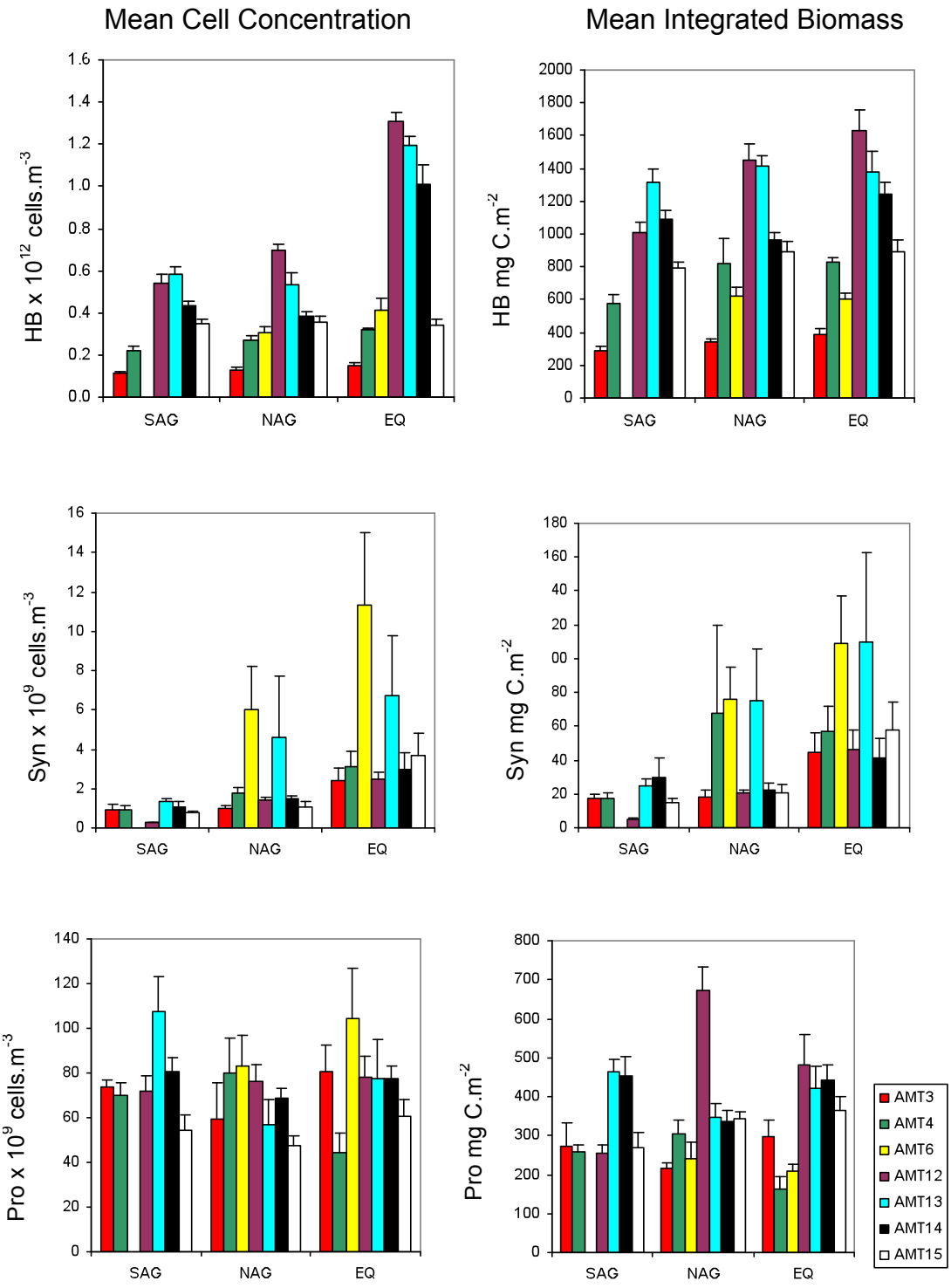

Table 4.3: Average *Prochlorococcus* (Pro), *Synechococcus* (Syn) and heterotrophic bacteria (HB) concentrations from all statistically similar cruises for the North (NAG) and South Atlantic gyres (SAG) and the Equatorial region (EQ). Average values from the NT and the ST were calculated using all AMT cruises despite large inter-cruise differences (see text). Data from the JR82 cruise are also included. Standard error of the mean is also shown (SEM).

	Concentration cells mL^{-1} ± SEM						
	Above the nitracline			**Above 200 m**			
Province	**HB x 10^6**	**Pro x 10^5**	**Syn x 10^3**	**HB x 10^6**	**Pro x 10^5**	**Syn x 10^3**	**Total Picophyt x10^3**
NAG	0.84 ± 0.04	1.19 ± 0.07	4.57 ± 1.02	0.58 ± 0.03	0.72 ± 0.04	2.55 ± 0.49	-
SAG	0.63 ± 0.04	1.14 ± 0.06	1.73 ± 0.25	0.49 ± 0.02	0.81 ± 0.04	0.94 ± 0.11	-
EQ	1.08 ± 0.07	1.88 ± 0.10	13.06 ± 2.33	0.65 ± 0.04	0.79 ± 0.06	4.97 ± 0.96	-
NT	-	-	-	0.71 ± 0.17	-	151.9 ± 90.7	-
ST	-	-	-	0.53 ± 0.14	-	18.84 ± 2.26	-
JR82 C	-	-	-	0.57 ± 0.14	-	-	0.84 ± 0.48
JR82 O	-	-	-	0.27 ± 0.05	-	-	1.22 ± 0.65

4.3.5 Integrated biomass in different provinces

Integrated biomass estimates above the nitracline for each province on each cruise are shown in the right hand panels of Figure 4.5. Due to variability in the depth of the nitracline between AMT cruises (Fig. 3.4), mean integrated biomass values for each province did not follow the same trends as the mean cell concentrations, this was true for all bacterioplankton groups. Data were integrated over greater depths during AMT-3, 4 and 6 resulting in integrated biomass values of NP that were more comparable than average concentrations on the three subsequent cruises.

Southern Atlantic gyre

In the southern Atlantic gyre (SAG), the greatest depth of the start of the nitracline used for integration was similar on all cruises (approximately 135 m) however, during AMT-3, 4 and 13 a higher proportion of stations had a deeper nitracline compared to AMT-12 and 14. Consequently, the integrated biomass of heterotrophic bacteria (HB) was significantly higher on AMT-13 than AMT-12 and 14 ($p \leq 0.01$). Despite integrating over a greater area during AMT-3 and 4, the considerably lower concentrations of HB measured in the SAG resulted in integrated biomass values also significantly lower ($p < 0.01$) than during AMT-12, 13 and 14. As expected, similar patterns of higher mean integrated *Prochlorococcus* (Pro) and *Synechococcus* (Syn) biomass on AMT-3, 4 and 13 were observed in the SAG, although there was no significant difference between all cruises (Fig. 4.5).

The biomass of HB integrated to 200 m resulted in similar inter-cruise differences compared to integration above the nitracline with AMT-13 significantly higher and AMT-3 and 4 significantly lower than all other cruises ($p < 0.05$; Fig. 4.6). In contrast to the integrated biomass above the nitracline, the integrated biomass of Pro above 200 m was greater in the SAG during AMT-13 and 14 than all other cruises ($p < 0.05$). Syn biomass above 200 m also differed significantly with lower values during AMT-12 than AMT-3, 4 and 13 ($p< 0.05$).

Northern Atlantic gyre

In the northern Atlantic gyre (NAG), the maximum depth of the nitracline was 150 m during AMT-12 compared with 100 m and 120 m on AMT-13 and 14 respectively. This was reflected in a significantly higher integrated biomass of heterotrophic bacteria (HB) on AMT-12 ($p < 0.05$) although both *Prochlorococcus* (Pro) and *Synechococcus* (Syn) biomass did not differ significantly. The deeper nitracline in the NAG on AMT-6 resulted in significantly higher integrated Syn biomass relative to all other cruises ($p \leq 0.01$; Fig. 4.5).

The integrated biomass of HB above 200 m in the NAG differed more between cruises than the integrated biomass above the nitracline with AMT-12 and 13 significantly greater than all other cruises ($p < 0.01$; Fig. 4.5). Pro biomass above 200 m was significantly greater during AMT-12 than all other cruises ($p < 0.05$). Differences between integrated Syn biomass above the nitracline and above 200 m were also

observed in the NAG with a significantly lower biomass above 200 m during AMT-12 than AMT-4, 6 and 13 ($p < 0.05$; Figs. 4.5 and 4.6).

Equatorial province

The only significant difference in prokaryotic plankton biomass above the nitracline in the equatorial province (EQ) was a higher integrated *Synechococcus* (Syn) biomass during AMT-6 compared to AMT-12 ($p = 0.02$). Due to a shallower nitracline in this province relative to the gyres, higher bacterioplankton concentrations did not necessarily relate to a greater integrated biomass. For example, the integrated biomass of heterotrophic bacteria (HB) was lower and mean concentration was higher in the EQ than the SAG or the NAG for all cruises (Fig. 4.4).

Biomass values integrated to 200 m in the EQ also did not exhibit any inter-cruise differences for HB and the only difference in Syn biomass was between AMT-6 and AMT-12 ($p = 0.03$) as before. Despite no differences in *Prochlorococcus* (Pro) biomass above the nitracline, when integrated to 200 m, a greater biomass was observed during AMT-12 compared to AMT-4 and 6 ($p < 0.05$; Fig. 4.6).

Province estimates of integrated biomass

Combining data from all cruises produced estimates of integrated biomass for each province (Table 4.4). Integrated biomass of heterotrophic bacteria (HB) and *Prochlorococcus* (Pro) above the nitracline was greater in the Southern Atlantic gyre (SAG) than in the northern Atlantic gyre (NAG) and in the equatorial region (EQ). When integrated above 200 m, the biomass of HB was greatest in the EQ and lowest in the SAG whereas Pro biomass was greatest in the EQ and lowest in the NAG. *Synechococcus* (Syn) biomass above the nitracline was similar in both gyres and almost double in the EQ. Higher integrated biomass values were obtained for the upper 200 m of the water column with a higher value in the NAG than the SAG and over double this in the EQ. The combined biomass of Pro and Syn above the nitracline was equivalent to 42 % of HB biomass in the NAG, 33 % in the SAG and 36 % in the EQ compared to 25 % in the NAG, 32 % in the SAG and 28 % in the EQ when data was integrated to 200 m.

Table 4.4: Integrated biomass of *Prochlorococcus* (Pro), *Synechococcus* (Syn) and heterotrophic bacteria (HB) from all statistically similar cruises for the North (NAG) and South Atlantic gyres (SAG) and the Equatorial region (EQ). Average values from the northern (NT) and southern (ST) temperate regions were calculated using all AMT cruises despite large inter-cruise differences (see text). Standard error of the mean is also shown (S.E.M).

	Integrated biomass mg C m^{-2} ± S.E.M					
	Above the nitracline			**Above 200 m**		
Province	**HB**	**Pro**	**Syn**	**HB**	**Pro**	**Syn**
NAG	460 ± 66	173 ± 21	18 ± 2	1314 ± 142	293 ± 17	30 ± 3
SAG	618 ± 40	190 ± 14	17 ± 4	1105 ± 41	338 ± 27	20 ± 4
EQ	480 ± 63	141 ± 15	32 ± 5	1485 ± 80	353 ± 33	69 ± 11
NT	-	-	-	1261 ± 215	-	194 ± 70
ST	-	-	-	1282 ± 378	-	308 ± 29

4.3.6 Comparison of different sample sizes to characterise a province

The extent of horizontal variance and at the province-scale was investigated in the southern Atlantic gyre (SAG) to determine whether twice daily sampling provided any further information than sampling only once a day. Samples were collected and analysed from pre-dawn stations and late morning stations during AMT-14. The mean integrated biomass of heterotrophic bacteria, *Prochlorococcus* and *Synechococcus* from the 7 pre-dawn stations were 600, 150 and 30 mg C m^{-2} respectively. These values did not differ significantly from the mean integrated biomass calculated using the total 15 stations (t-test, $p < 0.05$).

4.4 Discussion

Do bacterioplankton standing stocks vary temporally?

Heterotrophic bacteria

A clear inter-cruise variance was observed in the concentration of heterotrophic bacteria (HB) with the earlier three AMT cruises between 1996 and 1998 having

considerably lower values than the four latter AMT cruises between 2003 and 2004. As no similar pattern was observed in the concentration of either *Prochlorococcus* (Pro) or *Synechococcus* (Syn), this difference was probably not attributable to methodological differences for example in the flow rates used and calculation of sample analysed by flow cytometry. Samples from AMT-3, 4 and 6 were stored at -20ºC prior to flow cytometric analysis in contrast to samples from AMT-12, 13 and 14 that were stored at -80ºC. It is possible that bacterioplankton populations were differentially affected by the different storage temperatures, i.e. Pro and Syn were more robust and suffered less cell loss than the HB cells of which a higher proportion may have been damaged or destroyed by storage at -20ºC than -80ºC. However, despite a higher concentration of HB during AMT-15 relative to AMT-3, 4 and 6 in the southern and northern gyres, no difference was observed in the equatorial region on AMT-15 compared to AMT-4 and 6. This suggests that the variability may not be due to methodological differences in samples storage.

During the earlier cruises, fewer depths were sampled at each station than on AMT-12, 13, 14 and 15. The distribution of HB above the nitracline is not constant in the gyres and the lower average concentrations measured on the earlier cruises may be due to under-sampling, missing the sub-surface peak abundance (see chapter 3). However, the peak abundance of HB was co-located with the sub-surface Pro maximum abundance in all seven cruises. The deeper nitracline between 1996 and 1998 indicates a deeper surface mixed layer and the lower abundance of bacterioplankton could be due to nutrient limitation. Differences observed in integrated biomass above the nitracline between cruises are therefore a consequence of differences in the nitracline depth used for integration. Variability in the depth of the nitracline across the transect was caused by variability in physical properties influencing mixing in the water column. Internal waves (McGowan and Hayward, 1978), mesoscale eddies (Mahaffey et al., 2004), wind-driven Ekman pumping and storm events (McGillicuddy et al., 1998) result in the mixing of deeper nutrient-rich water with nutrient-depleted water, thus making the nitracline shallower.

Prochlorococcus and Synechococcus

Prochlorococccus (Pro) and *Synechococcus* (Syn) standing stocks were found to show no significant temporal variation above the nitracline in the northern (NAG) and southern (SAG) Atlantic gyres. This appears to support the original view that the gyres are stable environments and less variable than has been reported previously (Karl et

al., 2001; Karl and Lukas, 1996; DuRand et al., 2001; Carlson et al, 1996). There were only three significant inter-cruise differences in Pro and Syn concentrations above the nitracline (i.e. Pro in the EQ between AMT-4 and 13; in the SAG between AMT-15 and 4, 13 and 14 and Syn in the NAG between AMT-12 and 13). However, these were only found between the highest and lowest values. In both cases where only two cruises differed, the standard error of the mean was high for one of the cruises and neither cruises differed significantly from any of the other cruises. Many stations sampled in the SAG during AMT-15 were located farther east than during the other AMT cruises and this is probably the cause of the lower average Pro concentrations above the nitracline compared to the other cruises. Although there was little difference in temperature and salinity in the eastern side of the SAG compared to the western side sampled during the other cruises (Chapter 2, Figs. 2.3 and 2.4) other factors such as decreased light levels due to increased cloud cover, increased grazing or increased viral lysis could have contributed to the lower cell concentrations during AMT-15.

The higher variability in Syn biomass observed above 200 m compared to above the nitracline in the NAG and the SAG indicates a higher variability in the lower photic zone below the nitracline. However, again these differences no not reflect variability in temperature or salinity or seasonal differences. The higher integrated biomass of Pro above 200 m in the NAG on AMT-12 than all other cruises indicates a proportionately higher contribution of deeper Pro from below the nitracline to the overall biomass during this cruise. The opposite was true for Syn biomass integrated over the whole photic zone that was significantly lower during AMT-12 compared to AMT-4, 6 and 13.

Although some inter-cruise differences in integrated biomass over 200 m can be explained by corresponding differences in cell concentrations, some differences cannot and must be attributable to variability in cell size. For example, integrated *Prochlorococcus* biomass to 200 m was significantly higher in the SAG during AMT-13 and 14 compared to all other cruises whereas the concentration above 200 m did not vary significantly. Picophytoplankton have been shown to undergo cell division approximately once a day and the diel cycle of cell growth and division has been well studied, especially for *Prochlorococcus* (e.g. Vaulot and Marie, 1999; Vaulot et al., 1995 and Shalapyonok et al., 1998). The cellular carbon content of *Prochlorococcus* can vary by up to 50 % per day with the lowest carbon content at dawn (Shalapyonok et al., 2001). During AMT-14 and 15 some samples were collected at 11.00 local time whereas during the other cruises all samples were collected pre-dawn. It would be expected that differences in cell size due to cells being in different stages of the cell

cycle should occur between these two cruises and the other AMT cruises however this was not the case.

Standing stocks are not necessarily a good indicator of variability within oligotrophic regions as shown by Marañón et al. (2000) who reported that algal biomass remained relatively constant over three cruises in the oligotrophic Atlantic Ocean, whereas productivity and growth varied eight-fold. However, the higher integrated *Prochlorococcus* biomass during AMT-13 and 14 corresponds to a higher rate of primary production during AMT-13 and a higher chlorophyll-*a* concentration during AMT-14 at the chlorophyll-*a* maximum (Poulton et al., 2006). The activity and production of bacterioplankton is addressed in chapters 5 and 6. These results indicate that although *Prochlorococcus* and *Synechococcus* concentrations and biomass vary little above the nitracline, the populations located in deeper waters are more temporally variable.

Are surface abundances representative of waters above the nitracline?

Due to mixing processes in surface waters, it was expected that the surface abundance of bacterioplankton groups would exhibit strong correlation with average concentrations above the nitracline, indicating a homogenous community throughout this part of the water column. Although this was true for *Synechococcus*, variance between the surface and average concentrations of *Prochlorococcus* and heterotrophic bacteria in the oligotrophic gyres demonstrated an uneven vertical distribution above the nitracline. This is consistent with the vertical profiles presented in chapter 3. Previous comparisons between surface and integrated cell abundances at oligotrophic sites in the Arabian Sea were highly correlated especially for *Prochlorococcus* and *Synechococcus* (Shalapyonok et al., 2001). An integration depth of 100 m was used for all stations unlike the varying nitracline depth used here. Many of the stations sampled in the Arabian Sea had stratified conditions and shallow mixed layers due to inter-monsoon conditions and as such, many stations did not exhibit a sub-surface peak *Prochlorococcus* abundance as found in this study.

In the EQ province, greater mixing in surface waters and concentrations averaged over fewer depths (due to a shallower nitracline) resulted in surface concentrations that were more indicative of average concentrations. Therefore, surface *Prochlorococcus* and *Synechococcus* concentrations can be used to estimate abundances of these two groups in the upper water column, above the nitracline in the EQ province. In contrast,

several depths depending on the complexity of vertical distribution need to be sampled to gain an accurate representation of the abundance of *Prochlorococcus* and NP in the NAG and the SAG. Data from up to 8 depths were integrated in this study, and for future work a higher vertical sampling resolution in the 20 m above the nitracline (e.g. every 2 to 5 m), where the largest variance from surface values was observed, combined with a surface sample may provide more information than equally spaced depths throughout the surface layer.

How many stations are necessary to characterise a gyre province?

The calculation of similar average integrated biomass values for the southern Atlantic gyre (SAG) when 7 stations were used instead of the total 15 (AMT-14) indicates that variance across the gyre is constant and therefore, for community analyses in this province, 7 stations could be sufficient. Approximately 7 stations from each gyre province were sampled on each of the other cruises, therefore, it was assumed that this number of stations would be sufficient to generate an accurate province estimate of the bacterioplankton community structure.

Province estimates of concentration and biomass

Average concentrations of all bacterioplankton groups in the northern and southern Atlantic gyres are in the same order of magnitude as previously published values from the northern Atlantic and the northern Pacific gyres (Partensky et al., 1996; Li and Harrison, 2001; Campbell and Vaulot, 1993; Andrade et al., 2004). Integrated biomass values vary considerably both within published data and with our estimates. This is partly attributable to differences in the depths chosen for integration but also due to the large variation in C conversion factors used to calculate biomass. Many published estimates of biomass have integrated data to either fixed depths, e.g. 100 or 200 m or integrate data over the whole of the photic zone. Therefore, data integrated to 200 m have also been presented to examine inter-annual variability over the whole photic zone and to compare values from the AMT cruises with values from the JR82 cruise and with other published data.

The separation of stations on JR82 into the coastal and off-shore regions is consistent with other biological, physical and chemical studies during this cruise (Topping et al., 2006; Ward et al., 2005). Korb et al. (2005) reported very high chlorophyll a concentrations close to S. Georgia attributed to diatom blooms. The slightly lower total

picophytoplankton concentration we observed in this region relative to the HNLC offshore region (Korb et al., 2005) is therefore likely to be due to iron or other micronutrient limitation of these smaller phytoplankton as they are out competed by the larger diatoms during the bloom conditions. As there were diatom blooms in the coastal region, it would be expected that heterotrophic bacteria would also be abundant in this region due to the plentiful supply of organic matter, however this was not the case. Instead there may be another factor limiting the heterotrophic bacteria community in this region, for example increased grazing rates or the sinking of particulate organic matter from the surface waters, thus making it unavailable for heterotrophic prokaryotes in the surface (Vaque et al., 2002).

Partensky et al. (1996) reported considerably larger integrated *Prochlorococcus* and *Synechococcus* biomass values for the NAG (800 to 1330 mg C m^{-2} and 52 to 95 mg C m^{-2} respectively) this is mainly attributable to higher C conversion factors of 53 and 250 fg C $cell^{-1}$ compared to the average values of 29 and 99 fg C $cell^{-1}$ used in this study. Li and Harrison (2001) used an even higher C conversion factor for *Prochlorococcus* (59 fg C $cell^{-1}$) although the conversion factor for *Synechococcus* was closer to the one used here (115 fg C $cell^{-1}$). Their estimates of total picophytoplankton integrated biomass in the NAG (361 to 753 mg C m^{-2}) were lower than Partensky et al. (1996), and their lowest values were more comparable to the estimates of *Prochlorococcus* and *Synechococcus* biomass integrated to 200 m in the SAG in this study. However, it is important to note, that their estimates of total picophytoplankton concentration and biomass also include picoeukaryotes.

Overall, the data showed little variability in *Prochlorococcus* or *Synechococcus* concentration above the nitracline either seasonally or inter-annually in the NAG, SAG or EQ between 1996 and 2004. The overall lack of temporal variability of bacterioplankton above the nitracline in the oligotrophic gyres reported here is based on repeated sampling at different sites across the gyres. Due to the dynamic nature of gyre boundaries, overall size, and variability resulting from small-scale physical processes, repeated transect studies such as the AMT programme are necessary to examine biological parameters at the province-scale compared to fixed station time-series studies.

Chapter 5

Bacterial production in different provinces of the Atlantic Ocean

5.1 Introduction

As primary production (PP) measures the amount of carbon fixed into new phytoplankton biomass, bacterial production (BP) measures the amount of carbon assimilated into new heterotrophic bacterioplankton cells (Ducklow, 2000; Kirchman et al., 1982). BP is often expressed as a percentage of PP and used as an indicator of the importance of the microbial loop in oceanic food webs (Ducklow, 1999; Hoppe et al., 2002; Perez et al., 2005).

Several studies have shown that certain parts of the Atlantic oligotrophic gyres along with the equatorial region are net heterotrophic. Hoppe et al. (2002) calculated a higher bacterial carbon demand (BCD) for production and respiration than the rate of carbon fixed by phytoplankton between 8 ºN and 20 ºS in the Atlantic Ocean at approximately 30 ºW. These calculated values do not include the respiratory carbon demand of larger organisms such as zooplankton and therefore underestimate the heterotrophic state of these waters. The rate of respiration (determined by dark community oxygen consumption rates) alone has also been shown to exceed that of primary production in oligotrophic waters (Del Giorgio et al., 1997; Duarte and Agusti, 1998). For net heterotrophy to exist, external inputs of carbon via upwelling, terrestrial sources or by slow-degrading phytoplankton must fulfil the remaining heterotrophic carbon demand not sustained by primary production. Due to variability in the magnitude and frequency of external carbon inputs, it is unlikely that net heterotrophy can be sustained over long time periods. Other studies have reported a more balanced relationship between primary production and respiration with the carbon demand for respiration fulfilled entirely by carbon fixation (Williams, 1998).

The majority of dissolved organic carbon consumed by heterotrophic bacterioplankton is in the form of dissolved free amino acids (DFAA) (Cherrier and Bauer, 2004). For the purpose of estimating bacterial production along the AMT, the uptake and incorporation of two amino acids was used; leucine and methionine. Unlike leucine, the methionine

molecule contains a sulphur group enabling the use of the ^{35}S radioisotope along with ^{3}H to differentially label each amino acid. These amino acids belong to different families, which involve different intracellular biosynthesis pathways (leucine via the glycolysis pathway and methionine via the citric acid cycle) (Madigan and Martinko, 2006) when not obtained directly from the environment. Due to these differences, it is possible that the cellular uptake and requirement for each amino acid differs depending on the availability of different nutrients, community composition and cellular growth rate.

Calculations of bacterial production rates are dependent on the use of a conversion factor usually to convert the uptake of a measured substrate such as leucine into the rate of new carbon biomass production (Kirchman and Ducklow, 1993). Previous research has produced widely varying conversion factors and consequently the choice of conversion factor heavily influences the resulting bacterial production values. In order to reduce inaccuracies of using published conversion factors derived from different water masses or at different time points, experiments were conducted to derive conversion factors from each province of the Atlantic sampled for bacterial production. This was carried out by relating the uptake of amino acids to the increase in cell numbers and subsequently new bacterial biomass in dilution culture experiments.

The aims of this study are to examine the rates of bacterial production along the AMT transect and relate these to the rates of primary production. The hypotheses to be tested are (1) that the ratio of bacterial production to primary production is greater in the oligotrophic gyres than in more nutrient-rich waters and (2) that environmentally influenced change in the metabolism of heterotrophic bacterioplankton occurs.

5.2 Methods

5.2.1 Bacterial production

Bacterial production during AMT-14 was measured by incubating samples with radiolabelled ^{35}S-methionine diluted with unlabelled methionine at saturating concentrations. A dual labelling method was used to measure bacterial production on AMT-15 samples with both ^{35}S-methionine and ^{3}H-labelled leucine added to the incubations. Saturating concentrations of amino acids were used in order to suppress

intracellular amino acid synthesis so that the uptake of amino acids was directly related to the amount of protein synthesis. Saturating concentrations of methionine and leucine were determined by incubating water samples with 5 different concentrations of either amino acid, using the same method as for determining *in situ* uptake and concentration (see chapter 6) but with higher concentrations. From a graph of the uptake rate verses concentration, the concentration above which uptake rate remained constant was taken as the saturating concentration (Fig. 5.1). The saturating amino acid concentrations determined at several stations along the AMT-14 and 15 transects are shown in Table 5.1.

Seawater samples (1.6 ml) were incubated with radiolabelled amino acids and incubations were stopped by the addition of paraformaldehyde (PFA). All incubations were carried out in 2 ml screw-top polypropylene vials in the dark at ambient water temperature as measured by the temperature probe fitted to the CTD frame (chapter 2). For each sample, three replicates were incubated for 30, 60 or 90 minutes at ambient water temperature. Longer incubations (90, 180 and 270 mins) were used for deep water samples due to low uptake rates. Regression analyses of D.P.M. and incubation time were used to determine the rates of precursor uptake as described in chapter 6.

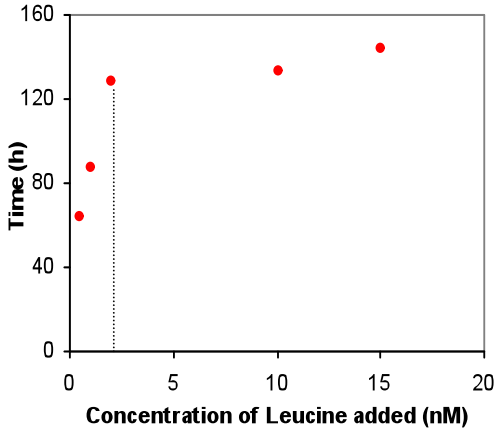

Figure 5.1: The time taken to turnover different concentrations of leucine. The dotted line was fitted by eye and indicates the saturating concentration, used for bacterial production incubations.

Table 5.1: Saturating amino acid concentrations determined in different provinces along the AMT-14 and 15 transects.

Cruise	Province	Methionine (nM)	Leucine (nM)
AMT-14	ST	0.9	-
	SAG	0.7	-
AMT-15	NT	2.1	2.1
	EQ	1.1	2.1
	EQ	1.1	-
	SAG	0.9	0.9

Killed controls are often used in uptake experiments; however, PFA fixes cells by cross-linking proteins on the cell surface thus altering the chemical structure that may in turn affect the extent of radiochemical adsorption onto the cells. In place of killed controls, a fourth time point of 2 minutes was included for some AMT-15 samples as it is assumed that the incubation is too short to permit the uptake of radiolabel into cells.

At four stations on AMT-15 a duplicate set of samples were incubated and fixed with trichloroacetic acid (TCA). This precipitates organic molecules rather than fixes whole cells hence only the radiotracer that has been assimilated into proteins will be measured when hot TCA is used. This is in contrast to PFA fixation when any amino acid that has been taken up into the cell but not metabolised is also measured.

5.2.2: Dilution culture experiments

During AMT-15, dilution culture experiments were performed on surface waters in order to obtain a conversion factor to relate the rate of amino acid uptake to the rate of new biomass production (i.e. bacterial production). Water samples were diluted 50 % with 0.2 µm filtered seawater from the surface and incubated in darkness at ambient sea temperature for at least 28 hours. Sub-samples were removed from each bottle approximately every 4 hours and bacterial production incubations were carried out as previously described. Samples were also collected for flow cytometry to measure cell abundance as described in chapter 3. The increase in cell concentration during the

growth phase was converted to bacterial biomass using the method described in chapter 4. The total increase in biomass was divided by the total amino acid uptake during the growth phase to produce conversion factors.

The rates of bacterial production were compared with primary production rates where data were available. Pearson's correlation was used to examine the relationship between these two variables in the photic zone.

For the purpose of comparing BP between different provinces, only data from AMT-15 were used as BP was measured over a wider range of latitudes and provinces. Bray-Curtis similarity matrices followed by hierarchal cluster analysis using Primer software was used to divide the stations into the provinces as described previously (chapter 4) using data integrated from the surface to the depth of the chlorophyll maximum (determined by the fluorescence maximum, f_{max}) and over the entire photic zone, i.e. from the surface to the 0.1 % light level. Integrated BP values in each province during AMT-15 were compared using ANOVA followed by multiple pairwise comparisons using Tukey tests (Minitab).

5.3 Results

5.3.1 Determination of conversion factors

During AMT-15, dilution culture experiments were carried out in the North West African upwelling (UP), the northern (NAG) and southern (SAG) gyres and the equatorial upwelling (EQ). Amino acid uptake rates in the dilution cultures were very low in the northern and southern gyres (< 0.02 nM h^{-1}). In surface waters from the NAG, both methionine and leucine uptake rates decreased over the initial 12 hours of incubation with a subsequent increase to a slightly higher uptake rate than at the start of the incubation (Appendix A). The initial decrease in cell activity following dilution in the NAG could be attributable to cells being 'over-saturated' with nutrients as the competition for dissolved organic nutrients was reduced 50 % by dilution. In surface waters from the SAG, uptake rates of both amino acids were low and variable for the first 20 hours of incubation (Appendix A).

Prokaryotes in the gyres are adapted to oligotrophic conditions and the change in environment caused by dilution and incubation could have caused a decrease in cellular activity and / or an increased mortality rate (the bottle effect). Cell concentrations in dilution cultures from both gyres also fluctuated with no clear increase in abundance over the duration of the incubations. Consequently, no clear growth phase could be identified over the period of the incubations in either of the gyre samples. In contrast, amino acid uptake rates were much higher in the UP and the start of the growth phase could be identified. However, the incubations were stopped whilst uptake rates were still increasing, therefore, a conversion factor could not be determined (Appendix A).

In the EQ, the graph of uptake rates against time is sigmoidal allowing the total amount of amino acid uptake during the peak growth phase to be determined (Fig. 5.2). The uptake rates of both leucine and methionine increased during the first 4 hours, whereas an increase in cell concentration didn't occur until after 4 hours. During the overall growth phase, 2.15 nM of leucine and 1.61 nM of methionine were taken up to produce an increase in cell numbers of 2.24×10^8 cells L^{-1}. The resulting biomass conversion factors calculated from this experiment were 1.31 kg C mol^{-1} leucine and 1.76 kg C mol^{-1} methionine and were used to calculate bacterial production (BP) for all samples from both cruises. By applying this conversion factor to the whole dataset, a constant rate of conversion of amino acids to carbon biomass is assumed, therefore not accounting for differences in respiration rates and growth efficiencies. Although, this is not ideal, a lack of comparable published conversion factors for oligotrophic gyres and the lack of obtaining any from this study limit the study of true bacterial production rates. However, using a single conversion factor for the whole dataset does have the advantage of eliminating an additional potential source of error of using different conversion factors and therefore differences in bacterial production rates reported here are directly related to differences in the rates of amino acid uptake.

Figure 5.2: Rate of methionine (met) and leucine (leu) uptake and concentration of heterotrophic bacteria in a 50 % dilution incubation in the equatorial province during AMT-15. Arrows indicate the maximum values of amino acid uptake rates and cell concentration taken at the end of the peak growth phase, used for calculation of the bacterial production conversion factors.

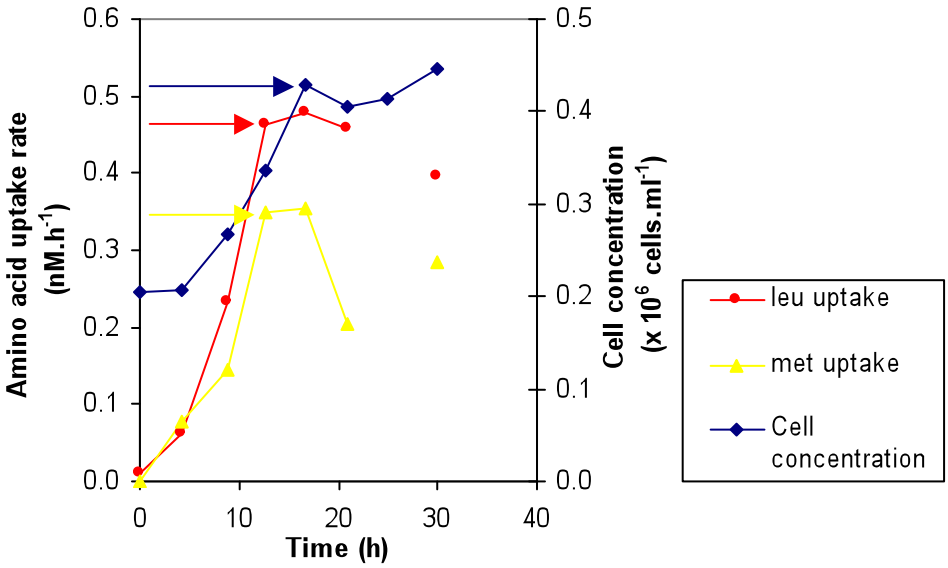

5.3.2: Comparison of fixation methods

Paired t-tests and Pearson's correlation were used to compare the rates of bacterial production (BP) measured when cells were fixed with either paraformaldehyde (PFA) or trichloroacetic acid (TCA). Data from below the photic zone were not included in these tests due to the low and variable values obtained using the TCA fixation method at depth. In the photic zone (above the 0.1 % light level), the rates of BP obtained from both fixation methods and both amino acids were significantly correlated ($p < 0.001$; $n = 13$; Fig. 6.3). However, bacterial production was significantly lower when TCA was used rather than PFA ($p = 0.02$ for leucine and 0.03 for methionine; $n= 15$). Correlation between the two fixation methods produced ratios of BP calculated from leucine uptake and fixation with TCA compared to PFA fixation of 0.78 for leucine and 0.64 for methionine (Fig. 5.3). Hence, approximately 22 to 36 % of the amino acids measured by the PFA fixation method are either inside the cells but have not yet been incorporated into proteins or have been adsorbed onto the surface of the cells and have not been actively taken up into the cells. Another explanation is that a fraction of the amino acids taken up have been

metabolised into other compounds, involving cleavage of the compound and removal of the radiolabelled molecule from the cell. However, this would be energetically more expensive than assimilating the amino acids directly and therefore it is not expected to be a major factor.

Figure 5.3: Relationship between bacterial production (mg C m^{-3} d^{-1}) determined after fixation with PFA and TCA using either (a) the uptake of leucine or (b) methionine. The correlation between both factors is indicated by the solid line and the dotted line indicates a 1 to 1 relationship for reference. Number of samples (n) = 17.

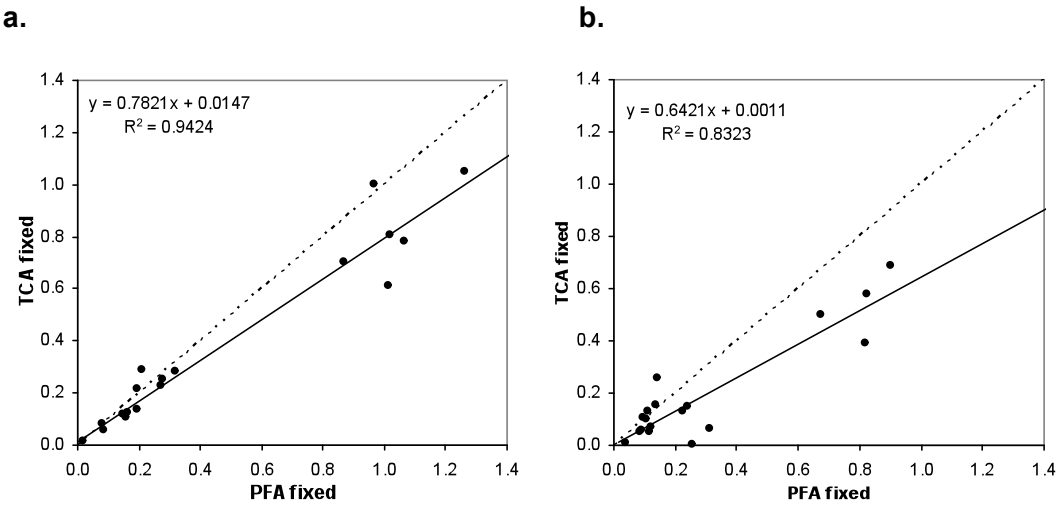

5.3.3: Bacterial production

During AMT-14 bacterial production (BP) measurements were only made between 16 ºS and 42 ºN due to time restrictions (the main focus during this cruise was estimating the *in situ* amino acid uptake rates, rather than BP; chapter 6). The peak rate of bacterial production (3.5 mg $C.m^{-3}.d^{-1}$) was located in the upper 50 m of the water column in the EQ, between 7 ºS and 13 ºN with considerably lower rates at higher latitudes and in deeper waters (Fig. 5.4). In the northern temperate region, BP increased steadily in surface waters with increasing latitude with values increasing from 0.20 mg $C.m^{-3}.d^{-1}$ at 31 ºN to 1.3 mg $C.m^{-3}.d^{-1}$ at 42 ºN.

Figure 5.4: Bacterial production (BP) in the northern hemisphere on AMT-14 (mg $C.m^{-3}.d^{-1}$). BP measurements were only made at a depth of 6.5 m at 16 ºS and 4 ºS, therefore these data are omitted from the contour plot, however, these BP values were also at the peak rate of approximately 3.5 mg $C.m^{-3}.d^{-1}$. Sample locations are indicated by black dots.

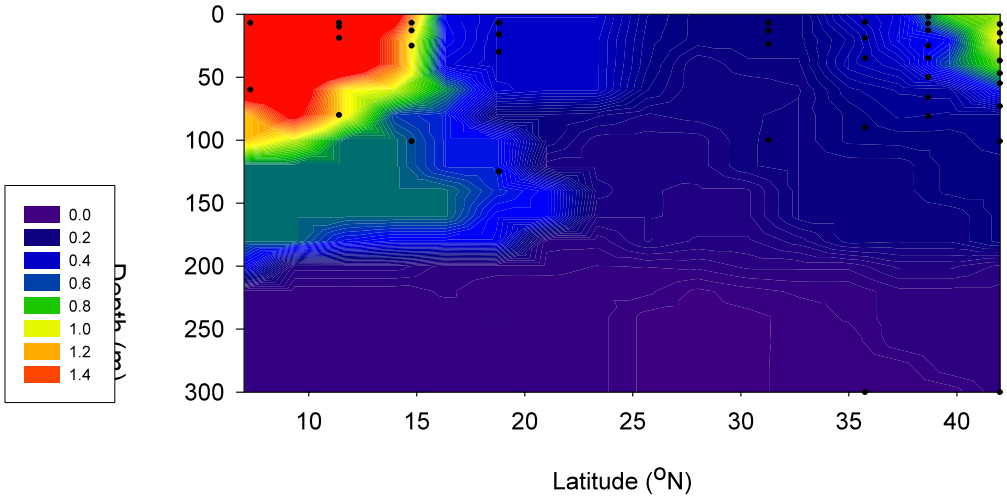

Bacterial production as determined by methionine and leucine uptake experiments during AMT-15 was highest in the upper 50 m of the water column between 15 and 25 ºN (> 1.0 mg $C.m^{-3}.d^{-1}$; Figs. 5.5 and 5.6). BP was slightly higher when calculated using leucine uptake than methionine uptake in surface waters along the entire transect. Uptake rates in surface waters at one station in the North West African upwelling (21 ºN) were approximately 15-fold higher than at adjacent sample sites, associated with high numbers of heterotrophic bacteria in this nutrient-rich region (chapter 3). At this station, BP determined by leucine uptake was 24 mg $C.m^{-3}.d^{-1}$ and by methionine uptake was 21 mg $C.m^{-3}.d^{-1}$ (these anomalous high values are omitted from the contour plots).

Figure 5.5: Bacterial production (mg $C.m^{-3}.d^{-1}$) determined using the methionine uptake method on AMT-15. Data from 21 ºN is omitted (see text). Sample locations are indicated by black dots.

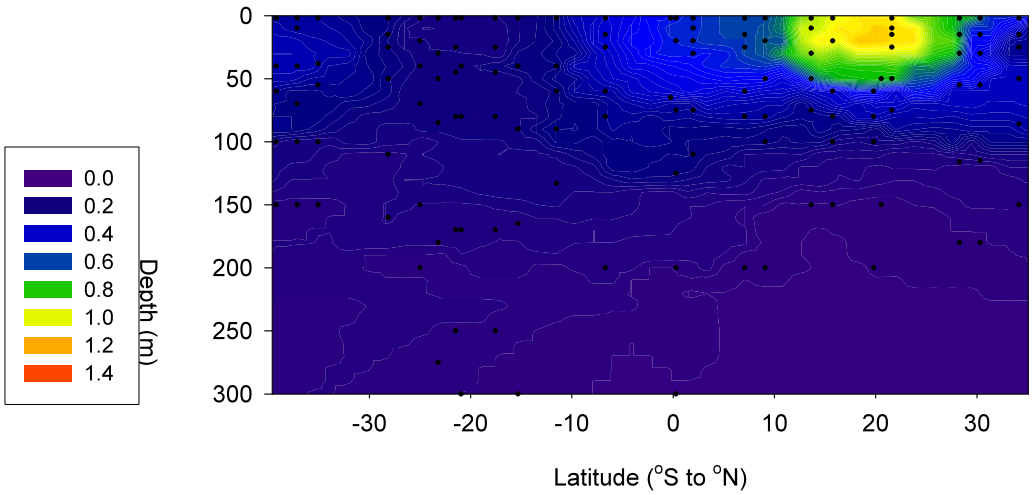

Figure 5.6: Bacterial production (mg $C.m^{-3}.d^{-1}$) determined using the leucine uptake method on AMT-15. Data from 21 ºN is omitted (see text). Sample locations are indicated by black dots.

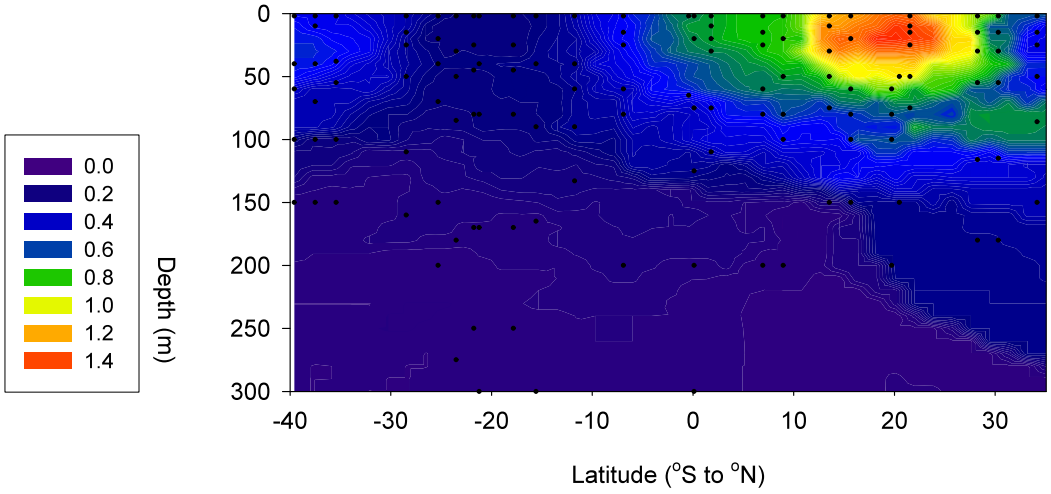

Linear regressions of uptake rates for both the photic and aphotic zone in each province during AMT-15 indicated a fairly constant methionine to leucine uptake ratio. The ratios in the photic zone ranged from 0.43 in the southern temperate region (ST) to 0.67 in the southern gyre (SAG). Uptake ratios in the aphotic zone ranged from 0.55 in the ST to 0.96 in the equatorial upwelling (EQ). The greatest difference in BP with depth occurred in the EQ with a ratio in the aphotic zone almost double the ratio in the photic zone (Table 5.2).

Table 5.2: Ratios of methionine (met) to leucine (leu) uptake in the photic (P) and aphotic (A) zones in the North West African upwelling (UP), the northern (NAG) and southern (SAG) gyres, the equatorial upwelling (EQ) and the southern temperate (ST) provinces as determined by linear regression analysis. The goodness of fit of each slope is indicated by the r^2 value and the p values are indicated: * < 0.05; ** < 0.01; *** <0.001. n is the number of samples.

Province	P or A zone	met uptake / leu uptake	n	r^2
UP	A	0.60 ***	8	0.98
	P	0.63 ***	16	1.00
NAG	A	0.58 ***	9	0.96
	P	0.56 ***	14	0.88
EQ	A	0.96 ***	6	0.98
	P	0.49 **	14	0.61
SAG	A	0.64 **	6	0.93
	P	0.67 ***	22	0.73
ST	A	0.55 *	7	0.61
	P	0.43 ***	13	0.89

Over the whole AMT-15 transect, there was a significant correlation between the uptake of methionine and leucine ($p < 0.05$). Cells took up less methionine than leucine with the rate of methionine uptake 58 % of the rate of leucine uptake (Fig. 5.7).

Figure 5.7: Linear regression of leucine and methionine uptake rates during AMT-15. Note the logarithmic scale used. n = 146.

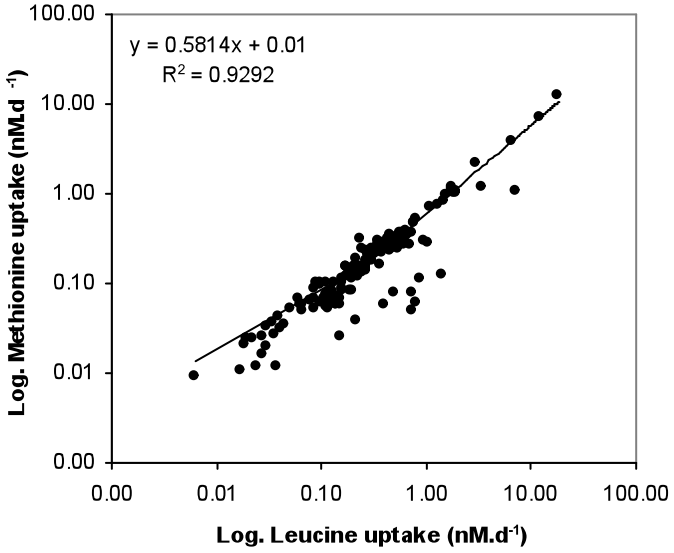

5.3.4: Does bacterial production vary between different oceanic provinces?

In order to compare bacterial production rates between provinces, data were depth-integrated and divided into provinces using hierarchical cluster analyses as described previously in chapter 4. Only the depth-integrated bacterial production values were used in the cluster analysis to group stations into provinces. The depth chosen for integration was either the fluorescence maximum (f_{max}; AMT-14 and 15 samples) or the 0.1 % light level (AMT-15 samples only). These light levels were chosen for subsequent comparison with depth-integrated primary production values.

For AMT-14, three clusters at the 90 % similarity level were produced, these were designated the northern gyre (NAG, n = 3), the equatorial upwelling (EQ, n = 1) and the northern temperate (NT, n = 4) provinces. Depth-integrated bacterial production was higher in the NAG (82 ± 44 mg $C.m^{-2}.d^{-1}$) than both the EQ (57 mg $C.m^{-2}.d^{-1}$) and the NT (28 ± 7 mg $C.m^{-2}.d^{-1}$; Table 5.3).

Table 5.3: Province estimates (± standard error of the mean) of bacterial production (BP) integrated from the surface to the depth of the chlorophyll maximum (f_{max}) on AMT-14. The number of stations in each province is indicated (n).

Province	BP (mg $C.m^{-2}.d^{-1}$)
NAG (n = 3)	82 ± 44
EQ (n = 1)	57
NT (n = 4)	28 ± 7

Bacterial production rates from AMT-15 were depth-integrated to either the depth of the chlorophyll maximum (f_{max}) or over the entire photic zone (to the 0.1 % light level) and separated into 8 clusters at the 90 % similarity level (Fig. 5.8). The rates of bacterial production in the upwelling region were much higher and therefore showed only 60 % similarity to the remaining provinces. Samples from both the northern (NAG) and southern (SAG) gyres fell into the same cluster and were split into two groups based on the latitude, i.e. northern or southern hemisphere. Samples around the equator (EQ) clustered together, whereas samples in the North West African upwelling (UP) were more variable and fell into 3 clusters. Due to the highly variable waters in the UP, these 3 clusters were grouped together to gain a more accurate average estimate for BP in this region. A sample from the UP region at 22 ºN clustered with the samples from the EQ region, again indicating the high variation in bacterial production rates in the upwelling region. One sample from 39.6 ºS fell into a separate cluster and was designated the southern temperate region (ST) (Fig. 5.8).

Three stations were excluded from the province group averages due to their high dissimilarity to samples from similar latitudes (Fig. 5.8). On closer inspection of the data from these outlying stations, the differences were due to either a proportionately higher value when integrated to the 0.1 % light level compared to the f_{max} integrated value (15 ºS) or proportionately lower values obtained using the methionine uptake method compared to the leucine uptake method (18 ºS and 25 ºS). Bacterial production at these three stations was very low, especially at depth; therefore, these discrepancies are likely to be errors arising from a reduced accuracy of the method at these low rates of amino

acid incorporation. The clusters obtained using depth-integrated BP data from both cruises are similar to those obtained using cell abundances in chapter 4.

Figure 5.8: Cluster analysis of depth-integrated bacterial production during AMT-15. Samples are labelled by latitude and negative values indicate ºS. The dashed line indicates the 90 % similarity level chosen for the grouping of samples into provinces. Red boxes indicate the samples grouped together for each province and samples highlighted in blue are the ones excluded from the subsequent province analysis (see text for further explanation).

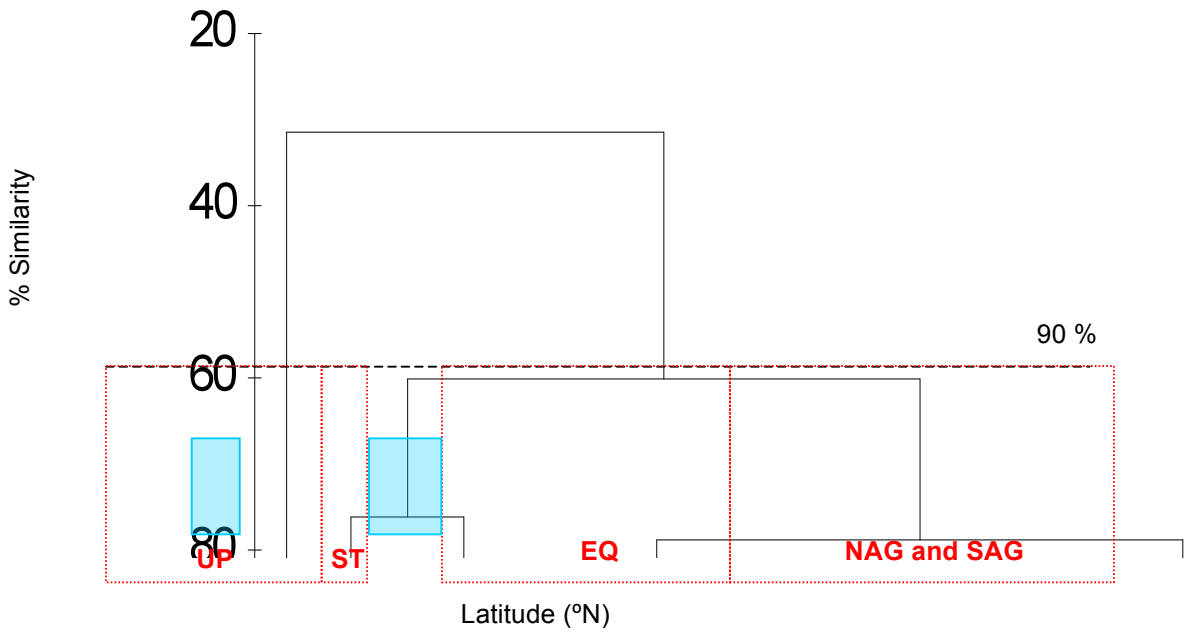

Table 5.4: Province estimates (± standard error of the mean) of bacterial production (BP) integrated either from the surface to the depth of the f_{max} or over the whole photic zone (to the 0.1 % light level) on AMT-15. BP determined from both the methionine (met) and leucine (leu) uptake methods are shown and the number of stations in each province is indicated (n).

Province	BP f_{max} (mg $C.m^{-2}.d^{-1}$)		BP Photic zone (mg $C.m^{-2}.d^{-1}$)	
	leu	met	leu	met
NAG (n = 4)	58 ± 10	28 ± 2	87 ± 21	34 ± 1
SAG (n = 5)	30 ± 3	26 ± 2	37 ± 3	33 ± 3
EQ (n = 7)	43 ± 1	34 ± 2	57 ± 4	44 ± 3
UP (n = 4)	139 ± 37	98 ± 35	159 ± 37	112 ± 36
ST (n = 1)	29	12	45	20

Despite the mean depth-integrated bacterial production (BP) values being higher when calculated using leucine uptake than methionine uptake for all provinces (Table 5.4), this difference was only significant in the EQ province for data integrated to both the f_{max} ($p = 0.003$) and the photic zone ($p = 0.021$). Hence for subsequent analyses, the mean integrated BP determined by leucine and methionine uptake was used.

Figure 5.9: Depth-integrated rates of bacterial production (BP) in each province during AMT-15. Bars represent the mean BP (from methionine and leucine uptake experiments) integrated to either the depth of the f_{max} or the 0.1 % light level. Error bars indicate the standard error of the mean (S.E.M.) calculated from all integrated values in each province. Numbers above the bars indicate the number of stations in each province.

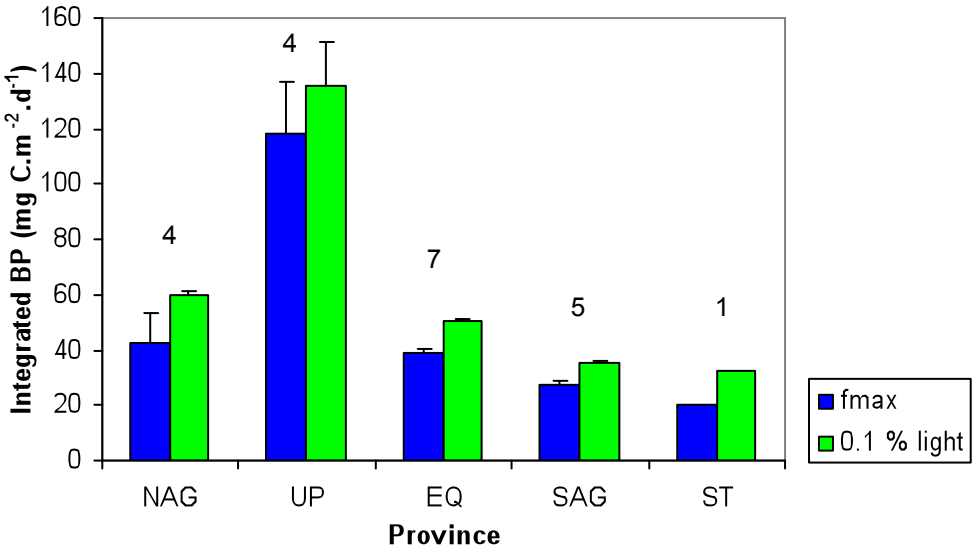

There was no significant difference in mean depth-integrated bacterial production rates in the northern gyre (NAG) during AMT-15 and AMT-14 (t-test; $p > 0.05$; Tables 5.3 and 5.4). During AMT-15, mean depth-integrated bacterial production was significantly higher in the North West African upwelling (UP) than in all other provinces (Fig. 5.9; $p < 0.05$). Low variability in the southern gyre (SAG) and the equatorial upwelling (EQ) resulted in significant differences between these provinces, with the EQ province having a higher mean integrated BP than the SAG (Table 5.4). This was the case for data integrated to the depth of the f_{max} and the whole photic zone as well as when calculated from methionine and leucine uptake values. Depth-integrated BP rates were also significantly higher for the NAG than the SAG when integrated over the whole photic zone only.

5.3.5 What factors control bacterial production?

To examine further, the differences in bacterial production along the transect and with depth, the relationships if any, between bacterial production and various biological and

physical parameters were tested. There was no significant relationship between heterotrophic bacterial biomass (calculated as described previously in chapter 4) and mean bacterial production ($p > 0.05$; Fig. 5.10). The abundance of heterotrophic bacteria (HB) also showed no significant correlation with the mean bacterial production (BP; $p > 0.05$).

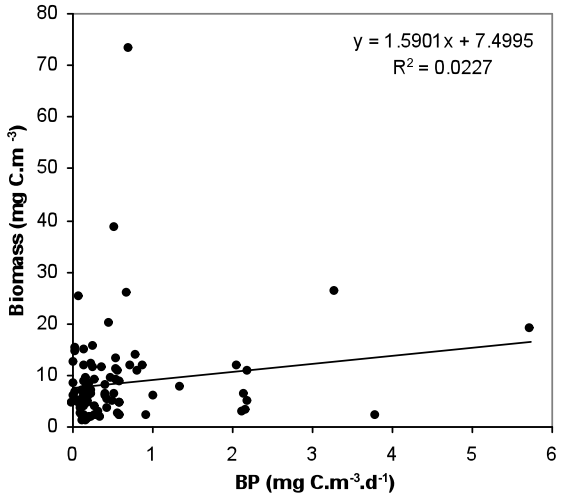

Figure 5.10: Comparison of bacterial production (averaged from methionine and leucine measurements) and heterotrophic bacterial biomass. The solid line is the line of regression and the equation and r^2 value are also shown. n = 94.

The lack of correlation between either HB abundance or biomass and bacterial production indicates variability in the cellular and biomass-specific rates of bacterial production. It was expected that cellular activity would decrease with depth as the availability of dissolved organic matter decreases below the photic zone. However, depth was also not found to have a significant influence on the cellular rates of bacterial production. This can be observed in depth profiles of the uptake of either leucine or methionine during AMT-15 (Fig. 5.11). Despite an apparent decrease in cellular amino acid uptake rates with depth below 150 metres, this was not a significant relationship ($p > 0.05$).

Figure 5.11: Relationship between cellular uptake rates of methionine (met) and leucine (leu) and depth for all samples during AMT-15. n = 86. Note the logarithmic scale used.

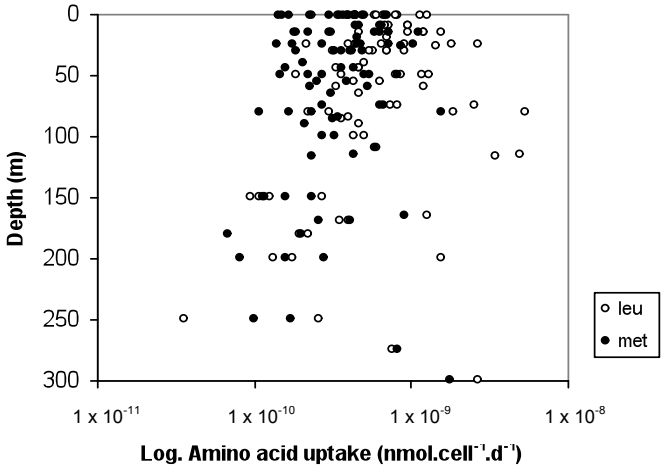

The relationship between biomass-normalised bacterial production (BP) and latitude was also examined however, no clear trend in any province was observed at either the surface, the depth of the chlorophyll maximum (f_{max}) or the 0.1 % light level (Appendix B). Bacterial production rates were also not significantly correlated with temperature ($p > 0.05$).

5.3.5: Proportion of photosynthetically fixed C taken up by bacterioplankton

Similarly to the rates of bacterial production, primary production was lower in the equatorial upwelling (EQ) and the northern gyre (NAG) during AMT-15 than AMT-14 (Tables 5.4 and 5.5). During AMT-14, bacterial production (BP) was lower than primary production (PP) in all samples except one from the depth of the chlorophyll maximum in the northern gyre (NAG). BP was highest relative to PP in surface waters between 10 and 15 ºN, at the northern boundary of the EQ province (Appendix C). However, when the data were integrated to the depth of the f_{max}, the highest ratio of BP to PP was found in the NAG (Table 5.5).

BP was higher relative to PP on AMT-15 when calculated from both methionine and leucine uptake. The shoaling of the photic zone and nitracline in the upwelling region

centred around 21 ºN during AMT-15 are evident in the contour plots by the increased percentage of BP relative to PP below a depth of 50 m (Appendix C).

Table 5.5: Province estimates (± standard error of the mean) of primary production (PP) rates integrated from the surface to the depth of the f_{max} during AMT-14. The number of stations in each province is stated (n). The primary production data were provided by A. Poulton using the method described in chapter 2.

Province	**PP (mg C.m^{-2}.d^{-1})**
NAG (n = 3)	400 ± 34
EQ (n = 1)	401
NT (n = 4)	324 ± 75

Table 5.5: Province estimates (± standard error of the mean) of primary production (PP) rates integrated from the surface to either the depth of the f_{max} or the 0.1 % light level (photic zone) during AMT-15. SAG – represents the SAG province excluding the southernmost station (see text). The number of stations in each province is stated (n). The primary production data were provided by A. Poulton and T. Adey using the method described in chapter 2.

	PP (mg C.m^{-2}.d^{-1})	
Province	**f_{max}**	**Photic zone**
NAG	156 (n = 1)	173 (n = 1)
SAG	354 ± 146 (n = 3)	520 ± 279 (n = 3)
EQ	307 ± 43 (n = 4)	342 ± 48 (n = 4)
UP	827 (n = 1)	-

There was no significant relationship between bacterial production (the mean BP values calculated from methionine and leucine uptake) and primary production over the whole of the AMT-15 transect as shown by regression analysis (Fig. 5.12a). Even within the different provinces, no significant relationship was found between BP and PP (Fig. 5.12b). However, when surface samples from all provinces except the upwelling region were compared, bacterial production significantly correlated with primary production ($p = 0.02$;

Fig. 5.12b) indicating that variability in the ratio of BP to PP is greater with depth rather than latitude. Samples from the upwelling region were omitted from this analysis as before, due to the considerably higher bacterial and primary production values measured in this region.

Figure 5.12: Relationships between bacterial production (BP) and primary production (PP) during AMT-15 in (a) all samples (n = 50) and (b) all surface samples except from the upwelling region (n = 9). Note the logarithmic scale used on graph a due to the wide range of values across the transect. Solid lines are the lines of correlation and the equations and r^2 values are also shown.

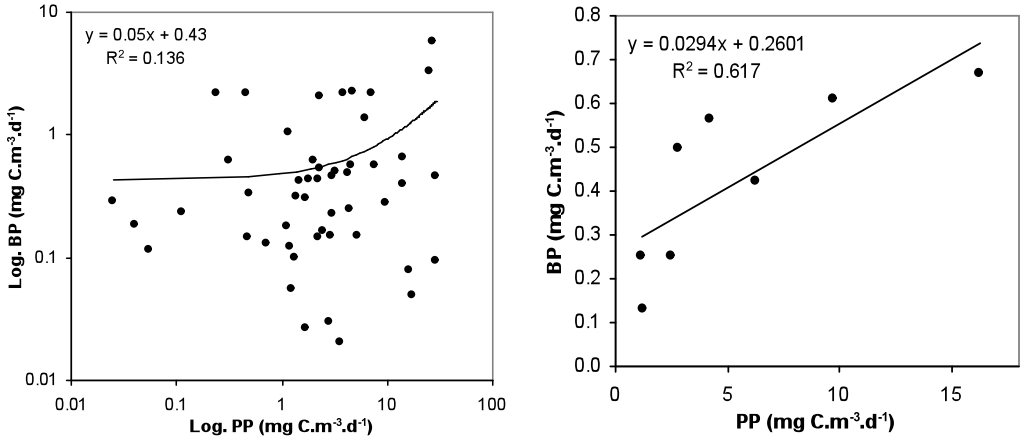

The proportion of photosynthetically fixed carbon taken up by bacterioplankton in each province was compared by calculating bacterial production as a percentage of primary production (BP/PP * 100; Table 5.6). The lowest percentages of BP/PP were found in the north-west African upwelling (8 %) and the northern temperate regions (9 ± 1 %) whereas the highest percentages were found in the northern gyre (NAG; 22 to 52 %). In the southern gyre (SAG), the ratio of BP/PP was considerably lower than in the NAG with bacterial production rates between 11 and 12 % of primary production rates.

Table 5.6: Depth-integrated bacterial production to either the chlorophyll maximum (f_{max}) or the whole photic zone as a percentage of the depth-integrated primary production in each province. The number of stations used in each province is stated (n). Where there were both primary production and bacterial production data for more than one station in the province, the standard error of the mean (S.E.M.) is shown. Bacterial production was determined from methionine uptake experiments only during AMT-14 and from the mean values obtained from methionine and leucine uptake experiments during AMT-15.

	AMT-14	AMT-15	
Province	**f_{max} (% ± S.E.M.)**	**f_{max} (% ± S.E.M.)**	**Photic (% ± S.E.M.)**
NAG	22 ± 13 (n = 3)	36 (n = 1)	52 (n = 1)
SAG	-	11 ± 3.6 (n = 3)	12 ± 4.1 (n = 3)
EQ	14 (n = 1)	16 ± 1.9 (n = 3)	17 ± 4.2 (n = 3)
UP	-	8 (n = 1)	8 (n = 1)
NT	9 ± 1 (n = 4)	-	-

5.4: Discussion

5.4.1: Biomass conversion factors

The biomass conversion factors calculated during AMT-15 are in the same range as previously published values. Conversion factors calculated in the northern Atlantic Ocean vary between 0.4 kg C.mol^{-1} leucine (Zubkov, 2000) and 3.1 kg C.mol^{-1} leucine (Kirchman, 1993). Perez et al. in 2005 determined conversion factors using similar dilution culture experiments, measuring bacterial production by ^{3}H-Leucine incorporation and cell abundance by microscopy, at two oligotrophic stations along the AMT transect. Their mean value was lower than the ones calculated in this study; 0.73 compared to 1.31 kg C.mol^{-1} leucine.

Due to low cellular amino acid uptake in the oligotrophic gyres, conversion factors could not be calculated and as such it is likely that the conversion factors used in this study

result in an overestimation of bacterial production rates in these regions. The widely ranging conversion factors available in the literature indicate that variability in bacterial production estimates can be largely due to the differences in conversion factors used. Despite the limitations of using only one biomass conversion factor for the whole transect, this removes subjective estimations of growth rates and efficiencies that would arise by using multiple conversion factors. The differences in bacterial production rates reported here are therefore direct effects of variability in amino acid uptake rates.

5.4.2: Comparison between cruises

During AMT-14, the highest rates bacterial production (BP) rates of 3.5 mg $C.m^{-3}.d^{-1}$ were located in the surface 50 m in the equatorial region with lower rates of approximately 0.5 mg $C.m^{-3}.d^{-1}$ in deeper waters (> 200 m) across the entire transect and also above 200 m in the northern gyre. A similar pattern was observed during AMT-15 with high BP in the photic zone around the equator, however, the highest values were measured in surface waters of the North West African upwelling, not sampled during AMT-14. During both cruises, high BP values were also located in the upper 50 m of the water column in the high latitude, temperate waters.

The lower BP values obtained during AMT-14 compared to AMT-15 are probably due to the incubation of many of the samples with sub-saturating concentrations of methionine. The saturating concentration of methionine during this cruise was determined initially in the southern temperate region and then the southern gyre and this latter concentration was used for the remainder of the cruise. Cellular turnover rates and ambient concentrations of amino acids vary in different regions (chapter 6) and therefore it is possible that the pre-determined concentration of saturation of methionine was too low for saturation at some stations. If some samples were incubated with under-saturating methionine concentrations, lower BP rates could be attributed to either substrate limitation or to intra-cellular production of methionine resulting in a reduced uptake of radiolabelled methionine from the water. To account for variations in the saturating concentrations of amino acids, this was determined (for both methionine and leucine) at several points along the transect in different provinces during AMT-15 to ensure that samples were saturated with amino acids during the bacterial production incubations.

5.4.3: Distribution of bacterial production along the AMT

The highest rates of bacterial production were co-located with the highest abundance of heterotrophic bacteria in the upper 50 m of the water column in the equatorial upwelling, the North West African upwelling and the temperate regions (chapter 3). A similar peak in bacterial production was found around the equator during AMT-11, although the estimated values were an order of magnitude lower (Perez et al., 2005). The lower values obtained by Perez et al. (2005) can be partly attributed to the lower conversion factors they used compared to this study, but also to methodological differences, as they used TCA to precipitate organic molecules rather than fixing whole cells using PFA. The data presented here showed that on average, bacterial production rates as measured by leucine incorporation were 78 % lower when TCA was used compared to PFA.

The greater abundance of either prokaryotic or eukaryotic phytoplankton in the equatorial upwelling, the North West African upwelling and the temperate regions (chapter 3; (Tarran et al., 2006) provides a potentially large source of DOM for heterotrophy, thus capable of supporting a greater abundance of heterotrophic bacteria and a higher rate of bacterial production (Bell and Sakshaug, 1980; Cherrier and Bauer, 2004). Despite these apparent trends, there were no significant relationships between either heterotrophic bacterial abundance or biomass and bacterial production.

Bacterioplankton activity, in terms of the uptake of DOM, can vary greatly. This may be due to inter-specific variation in DOM uptake affinity (Alonso and Pernthaler, 2006) or intra-specific variation forced by nutrient concentrations (Carrero-Colon et al., 2006). Previous research in surface waters along the AMT transect found variability in cellular activity in different provinces although this was generally higher in the southern gyre and the North West African upwelling than at the equator or in the temperate regions (Mary et al. 2006).

Province estimates of depth-integrated bacterial production for the northern gyre and equatorial regions are in the same order of magnitude as previously published values (Ducklow, 1999). Although the rates for the NAG were considerably higher during both AMT-14 and 15 (82-171 mg $C.m^{-2}.d^{-1}$) than those found by Carlson et al. (1996) in the Sargasso Sea (11-36 mg $C.m^{-2}.d^{-1}$). Bacterial production rates measured previously in

temperate waters of the North Atlantic were in the range of values produced in this study (Zubkov et al., 2001b).

It has been suggested that the uptake of amino acids by bacterioplankton is enhanced by the use of several uptake systems with different kinetic parameters, therefore facilitating amino acid uptake at a wide range of concentrations (Schut, 1993; Unanue et al., 1999). The positive correlation between biomass specific bacterial production and uptake affinity for methionine compared to leucine suggests that as the concentration of DOC decreases with depth (Thurman, 1985), methionine is energetically favoured over leucine as a C source in nutrient limiting conditions. The differences in amino acid uptake affinities may be attributable to changes in the community composition and this is discussed in more detail in chapter 6.

Previous research has shown that despite differences in cell specific amino acid uptake rates, a relatively constant biomass specific uptake rate between different groups of flow sorted bacterioplankton and with depth was found in the Celtic Sea (Zubkov et al., 2001a). The differences in biomass specific bacterial production may not be entirely due to changes in the activity of heterotrophic bacteria as depth related variability has been observed in methionine uptake rates of *Prochlorococcus*. The low light (high chlorophyll fluorescence) population is responsible for up to 50 % of the total bacterioplankton amino acid uptake below 100 m in the southern Atlantic gyre. The lower biomass specific bacterial production observed in surface waters may be attributable to the lower amino acid uptake rates of high light (low chlorophyll fluorescence) *Prochlorococcus* in the surface waters and the higher biomass specific uptake of the low light ecotype in deeper waters of the photic zone (Zubkov et al., 2004) as these cells dominate the bacterioplankton community over a large part of the transect.

The ratios of DNA to protein synthesis vary temporally and spatially (Gasol et al., 1998; Pomroy and Joint, 1999) indicating that the growth state of bacterioplankton is controlled by a complex interaction of factors including temperature (Longnecker et al., 2006) and chlorophyll (Longnecker et al., 2005). The negative correlation between temperature and biomass specific bacterial production found in this study indicates that the metabolic state of heterotrophic bacterioplankton is controlled to a certain degree by temperature.

5.4.4: Ratios of BP to PP

The uncoupling of bacterial and primary production highlighted by the lack of correlation between these two parameters contradicts previous research (Coffin et al., 1993; Cole et al., 1988). Despite a lack of difference in integrated rates of bacterial production between both the northern and southern gyres during AMT-15, there was a large difference in the relationship between primary production and bacterial production in these provinces. This difference is attributed to a difference in rates of primary production between these two regions, with the southern gyre having a higher integrated primary production than the northern gyre. During AMT-15 the NAG was sampled during the boreal autumn and the SAG during the boreal spring. Despite seasonal changes in PP in the gyres, BP does not appear to differ.

The ratios of bacterial production to primary production reported here were comparable with many previously published values (Carlson et al., 1996; Ducklow, 1999). Hoppe et al. (2002) reported ratios of between 2-10 % in the cooler temperate regions to 40 % in the tropics. The same pattern was observed along the AMT transect with the low ratios located in the northern temperate region during AMT-14 (9 %), comparable to those reported by Hoppe et al. and the highest rates located in the northern oligotrophic gyre during AMT-15. Although the ratio calculated for the northern gyre (52 %) is slightly higher than the average ratio for the northern Atlantic presented by Hoppe et al. (2002), similarly high ratios were also found during their study at several stations in the northern and southern gyres and the equatorial region.

The first hypothesis that a higher ratio of bacterial production to primary production exists in the oligotrophic gyres has been proven for the northern Atlantic gyre however the lowest ratios were found in the southern Atlantic gyre. This difference may reflect seasonal differences although the abundance and biomass of heterotrophic bacterioplankton did not differ accordingly (chapter 4). The second hypothesis that metabolic changes in heterotrophic bacterioplankton occur in response to environmental conditions has been shown to be true for the differential uptake of leucine and methionine in response to temperature and depth. These results provide further insight into ecosystem functioning at the microbial level and are important in understanding importance of the microbial loop in the oceanic carbon cycle.

Chapter 6

Bacterioplankton metabolic activity and community composition in different Atlantic oceanic provinces

6.1 Introduction

Bacterioplankton dominate the uptake of dissolved organic matter (DOM; (Azam, 1998; Azam et al., 1983; Ducklow, 2000), yet the contribution of different bacterial clades to the turnover of DOM in the oceans remains poorly understood. Several recent studies have examined the activity of defined bacterioplankton groups in incorporating metabolic precursors using culture-dependent and independent techniques (for example, (Alonso and Pernthaler, 2005; Malmstrom et al., 2005; Malmstrom et al., 2004; Pernthaler et al., 2001; Zubkov et al., 2001b). Bacteria from the SAR 11 clade are the most abundant bacterioplankton in the ocean (Morris et al., 2002). Studies using a combination of microautoradiography and fluorescent *in situ* hybridisation (FISH) have linked the SAR 11 clade to between 30 and 50 % of the total community uptake of leucine (Malmstrom et al., 2005). However, this technique is only semi-quantitive and exact rates of substrate incorporation cannot be obtained using this method (Sintes and Herndl, 2006; Vila et al., 2004).

For the purpose of this study, flow cytometric sorting was used to divide the bacterioplankton community in order to examine the methionine uptake rates of each sorted cell group. Cells were sorted into groups based upon nucleic acid content and cell size (side scatter). Previous studies using this approach have reported higher leucine incorporation rates for cells with high nucleic acid content compared to cells with low nucleic acid content (Lebaron et al., 2001; Longnecker et al., 2006; Servais et al., 2003). Whereas other studies have shown little or no difference in the cell-specific and biomass-specific leucine or methionine uptake rates of cells with high or low nucleic acid content (Longnecker et al., 2005; Zubkov et al., 2001b).

In order to link the methionine uptake rates of flow cytometrically defined groups to phylogenetic clades, fluorescent *in situ* hybridisation (FISH) was also carried out on flow cytometrically sorted cells. A signal amplification step was incorporated into the FISH procedure in order to visualise the small less active cells in the oligotrophic gyres (catalysed reporter deposition fluorescence *in situ* hybridisation; CARD-FISH). In the Celtic Sea, Zubkov et al. (2001) found that cells with high nucleic acid content were

dominated by bacteria from the *Roseobacter* spp. and *Cytophaga-Flavobacterium-Bacteroides* clades and cells with low nucleic acid content contained bacteria from the SAR 86 clade.

The availability of organic substrates has been reported to significantly restrict the growth of heterotrophic micro-organisms (Konopka, 2000). More specifically, the uptake of leucine by bacterioplankton has been shown to be dependent on concentration. The existence of inter-species variations in the response of leucine uptake rates to leucine concentration support the idea of differing ecological roles and the adaptation of certain clades to environmental conditions (Alonso and Pernthaler, 2006). Bioassays using radiolabelled substrates were used in this study to estimate the *in situ* methionine and leucine uptake rates and concentrations in order to examine any interdependence and to estimate the methionine uptake rates of flow sorted cell groups.

The aims of this study were to examine the methionine uptake rates and community composition of bacterioplankton cells along with the *in situ* leucine and methionine uptake rates and concentrations in different provinces of the Atlantic Ocean. The hypotheses to be tested were that the uptake rates of methionine and leucine uptake were related to the ambient concentrations and these were higher in the temperate regions and in upwelling regions than in the oligotrophic gyres. Also, cells from different bacterioplankton clades have different methionine uptake rates, therefore both the community composition and uptake rates are determined by the ambient concentration.

6.2. Methods

6.2.1 Sample collection

Samples for flow sorting were collected during three cruises (AMT-13, 14 and 15) as described in chapter 2 from a near-surface depth of between 2 and 7 metres at 24 stations on AMT-13; 9 stations on AMT-14 and 12 stations on AMT-15. Samples for the determination of substrate turnover and concentrations were collected from near-surface waters and also from waters at the fluorescence maximum (f_{max}) at some stations. Data from AMT-13 were provided by M. Zubkov. Sub-samples for flow sorting and CARD-FISH were fixed using paraformaldehyde (PFA; 1 % final concentration) within an hour of collection and stored at 4 ºC overnight before freezing at -80 ºC until analysed post-cruise. Details of sampling procedures are described in chapter 2.

6.2.2 Concentration and turnover of metabolic substrates

The concentration and turnover of the amino acids methionine and leucine in the water were measured by incubating samples with 5 different concentrations of radiolabelled substrate using a concentration series bioassay (Wright and Hobbie, 1966),. Water samples (1.6 mls each) from AMT-14 were incubated with small volumes (≥ 16 µl) either ^{3}H-Leucine (final concentrations of 0.1, 0.2, 0.4, 0.6 and 0.8 nM) or ^{35}S-Methionine (final concentrations of 0.2, 0.3, 0.5, 0.7 and 0.9 nM) for either 10, 20 or 30 minutes.

The same experiments were carried out during AMT-15 to measure the concentration and uptake of methionine and leucine only. Due to the high specific activity of ^{35}S-Methionine, only 0.1 nM of the radiolabelled substrate was added to each incubation and unlabelled methionine was also added to make up the desired final concentrations. The radiolabelled substrates were added at sub-saturating concentrations as indicated by the linear relationship between uptake and concentration (Fig. 6.1). Incubations were carried out in autoclaved 2 ml polypropylene screw-top vials and stopped by the addition of PFA (1 % final concentration). Samples were filtered through 0.2 µm nylon filters and the amount of radioisotope remaining on the filters (i.e. incorporated into cells or particulate material) was counted using a scintillation counter (Tricarb 3100, Perkin-Elmer).

The amount of radioactivity incorporated per minute of incubation was estimated for each different concentration by taking the gradient of a slope produced by regression analysis of the disintegrations per minute (D.P.M.) for each of the three time points. The inverse of these values (number of hours taken to uptake all the substrate) were subsequently analysed by regression analysis (Fig. 6.1) with the total concentrations of metabolic precursors to produce estimates of the ambient concentration (the intercept of the y-axis multiplied by the gradient, i.e. the intercept of the x-axis) and the fraction of substrate taken up per day (24/intercept). Only data that produced significant regressions were used ($p < 0.05$). Multiplication of the fraction of substrate taken up per day by the ambient concentration in the water produced the turnover rate for each sample.

Figure 6.1: Regression analysis used to calculate the ambient concentration and turnover of leucine (leu). The regression coefficient (r^2) is indicated on the graph.

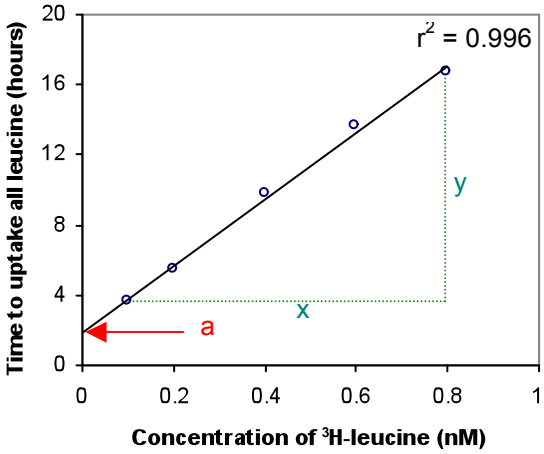

No. hours to uptake 1 nM leu = y/x

No. hours to uptake ambient leu = a

Ambient leu concentration (nM), C = a/(y/x)

Fraction amino acid taken up d^{-1}, F = 24/a

Uptake rate ($nM.d^{-1}$) = C x F

6.2.3 Flow Cytometry

Bacterioplankton including phototrophic cyanobacteria were enumerated and sorted using flow cytometry (FACSort, Beckton Dickinson, Oxford, U.K.) on samples radiolabelled previously with ^{35}S-Methionine, fixed and stored at -80 ºC. For CARD-FISH, non-radiolabelled samples were used for flow sorting of the same prokaryote groups with similar flow cytometry signatures. The flow sorting for CARD-FISH was carried out on either a FACScalibur (Beckton Dickinson, Oxford, U.K.) or MoFlo (Dako Cytomation) instrument. Cells sorted using the MoFlo instrument were reanalysed using the FACScalibur instrument to ensure the same flow cytometry signature was obtained to allow cross comparison of sorted cell groups from both instruments.

Three groups of heterotrophic bacteria were identified by their characteristic light side scatter and nucleic acid content indicated by SYBR Green I fluorescence. One group of cells had a low fluorescence, named the low nucleic acid group (LNA) and the other two cell groups had high fluorescence (high nucleic acid, HNA), with the cells from one group having a lower side scatter (HNAI) than the other group (HNAII) as illustrated in Fig. 3.2. In samples where the concentration of either *Synechococcus* or *Prochlorococcus* cells exceeded 2 x 10^3 $cells.mL^{-1}$, these cells were also sorted using unstained samples. For some of these samples, where *Prochlorococcus* could be

clearly separated from the heterotrophic bacteria, i.e. in deeper samples were cellular autofluorescence was higher (see chapter 3), cells were sorted from both unstained and SYBR Green I stained samples. Flow cytometry data was processed using either CellQuest (Beckton Dickinson, Oxford, U.K) or WinMDI 2.8 software.

6.2.4 Methionine uptake by defined cell groups

The relative contribution of distinct bacterioplankton groups to the total community uptake of methionine was determined using a combination of radiochemical incubations and flow cytometric sorting (Zubkov et al., 2001a). Water samples were incubated with ^{35}S-methionine (0.5 nM final concentration) at ambient water temperature for 3 hours (AMT-13) or 2 hours (AMT-14 and 15) before fixation with PFA and freezing as described previously. The concentration of methionine used is at sub-saturating concentrations (Table 5.1). Incubations were carried out in the dark in 2 ml polypropylene vials.

Samples were prepared for flow cytometry as previously described and cells from the representative cell groups (chapter 3, Fig. 3.2) and all prokaryotes were sorted and collected directly onto 25 mm 0.2 µm nylon membrane filters. The amount of ^{35}S retained on the filters was measured using an ultra-low level liquid scintillation counter (1220 Quantulus, Wallac, Finland). The measured counts per minute (CPM_{meas}) were corrected for radionuclide decay (CPM_{corr}) using the following equation:

$$\mathbf{CPM_{corr} = CPM_{meas} / e^{(-\lambda t)}}$$

Where t = number of elapsed days since ^{35}S-methionine manufacture
and λ (the decay constant) = $\ln 2 / t_{0.5}$
$t_{0.5}$ (the half life of the radioisotope) = 87.5 days

Three different numbers of cells between 500 and 50000 cells were sorted from each group and a regression line between the three results provided a mean CPM per cell with a mean standard error of counting of 5.3 %. Cellular methionine uptake for each sorted group was calculated as a proportion of the uptake by an average cell, determined from sorting the total stained cells. The abundance of cells in each cell group sorted was used to calculate the proportional contribution of each cell group to the total methionine uptake by all prokaryotes. In many surface samples it was not possible to separate *Prochlorococcus* from both the HNA groups as discussed in

chapter 3. Therefore the data from these two groups were combined after multiplying the activity per cell by the abundance of cells in each group. Rate measurements from HNAI and HNAII cell groups were not combined for the comparison with community composition data from flow sorted groups. The total methionine uptake in the water was determined by collecting three different volumes (50, 100 and 150 µl) of incubated sample onto filters and measuring the amount of ^{35}S-methionine incorporated into particulate matter using the same method as for the sorted cell groups.

In samples where the *in situ* methionine turnover was also measured using the bioassay described in section 6.2.2, this value was multiplied by the fractions of methionine uptake of each sorted cell group to determine the rate of methionine turnover for each cell group. During AMT-15, bacterial production measurements were the main focus of the work (chapter 5) hence the *in situ* methionine turnover was only determined at one station where cell sorting was conducted. Therefore for AMT-15, instead of using *in situ* methionine turnover rates, the rate of methionine uptake at saturating concentrations (see chapter 5) was used to calculate the theoretical maximum methionine uptake of each cell group.

6.2.5 CARD-FISH

Samples were either fixed as described previously, filtered through 47 mm 0.2 µm polycarbonate filters and stored at -80 ºC before analysis (AMT-12) or water samples were fixed and frozen for flow sorting prior to CARD-FISH. Water samples for flow cytometric sorting were sorted into the groups described previously and either collected directly onto 13 mm 0.2 µm polycarbonate filters (when using the FACScalibur instrument) or collected into autoclaved 1.5 ml tubes and subsequently pipetted onto small areas of 25 mm 0.2 µm polycarbonate filters to concentrate the cells (when using the MoFlo instrument). Oligonucleotide 16S rRNA probes labelled with horseradish peroxidase were hybridised with cells using a modified version of the CARD-FISH technique (Pernthaler et al., 2002). After removing any unbound probe by washing, tyramide molecules conjugated to fluorescein are attached to each probe through reaction with the horseradish peroxidase.

Table 6.1: 16S rRNA oligonucleotide probes used to analyse community composition and their target bacterial or archaeal groups. The formamide concentrations (FA conc.) used for each probe are also shown.

Probe	Target group	Sequence	FA conc. (%)	Source
EUB338	Bacteria	GCTGCCTCCCGTAGGAGT	55	Amann et al., 1990
NONEUB	Sense compliment to EUB338	ACTCCTACGGGAGGCAGC	55	Wallner et al., 1993
EURY806	Euryarchaea	CACAGCGTTTACACCTAG	20	B. Fuchs, pers. comm.
CREN554	Crenarchaea	TTAGGCCCAATAATCMTCCT	20	Massana et al., 1997
CF319a	Cytophaga-Flavobacterium-Bacteroides	TGGTCCGTGTCTCAGTAC	55	Snaidr et al., 1997
Pla886	Planctomycetes	GCCTTGCGACCATACTCCC	55	B. Fuchs, pers. comm.
Alf968	Alpha Proteobacteria	GGTAAGGTTCTGCGCGTT	55	Snaidr et al., 1997
Gam42a	Gamma Proteobacteria	GCCTTCCCACATCGTTT	55	Snaidr et al., 1997
SAR86	Core cluster of SAR86	TTAGCGTCCGTCTGTAT	55	Zubkov et al., 2001
Ros537	Roseobacter and SAR86	CAACGCTAACCCCCTCC	55	Eilers et al. 2001
Cya664	Cyanobacteria	GGAATTCCCTCTGCCCC	55	Schonhuber et al., 1999
405Pro	Prochlorococcus	AGAGGCCTTCGTCCCTCA	60	West et al., 2001
SAR406	Most of SAR406	CACCCGTTCGCCAGTTTA	45	B. Fuchs, pers. comm.
SAR116-1	Top half SAR116 cluster	GCTACCGTCATCATCTTC	45	B. Fuchs, pers. comm.
SAR116-2	Bottom half SAR116 cluster	CATCTTCACCAGTGAAAG	45	B. Fuchs, pers. comm.

The probes used and their respective target prokaryote groups are listed in table 6.1. Whole community samples, collected on filters from 25 m at 6 different stations along AMT-12 were screened with probes targeting general bacterioplankton groups. The results from these preliminary tests were then used to select more specific probes to target cells that were initially flow cytometrically sorted as described in 2.4. As a control, in addition to the group-specific probes, samples were also hybridised with the NON-EUB probe which is a complimentary sequence to the general bacterial probe EUB338. This probe was developed as a negative control to test for unspecific binding (Wallner et al., 1993).

A section of filter was cut and labelled for each probe and following the hybridisation, these were counterstained with the DNA stain, DAPI and mounted on glass slides. Fluorescent cells, both DAPI and probe labelled, were counted by epifluorescence microscopy (Fig. 6.2). A minimum of 300 DAPI cells were counted for each hybridisation. Duplicate counts were performed to obtain the standard error of the mean (SEM) of counting.

Figure 6.2: (a) DAPI stained cells and (b) cells hybridised with the EUBI-III probe. Arrows indicate example cells with both a positive probe and DAPI signal.

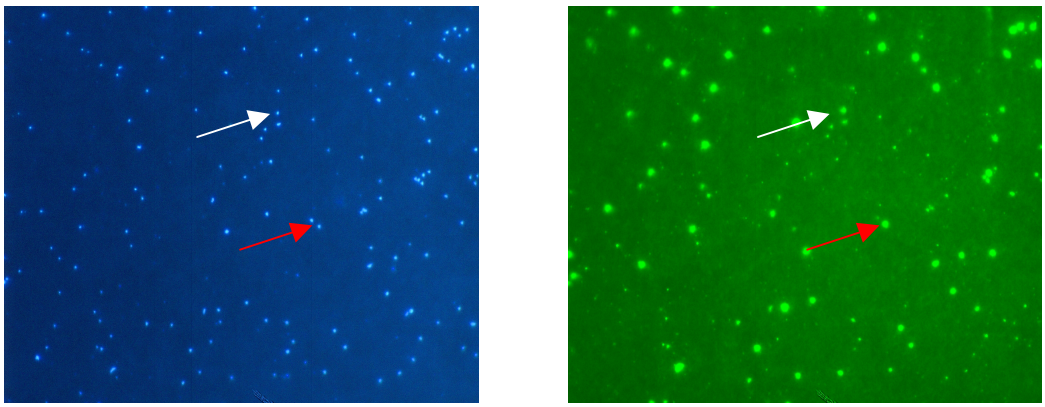

6.2.6 Permeabilisation experiment

For hybridisation to occur, the probes must be able to penetrate the cell wall. When using probes directly conjugated to a fluorochrome, probe penetration is not normally a problem, however probes conjugated to horseradish peroxidase are considerably larger and are not able to pass through many bacterial walls freely. To increase the permeability of cell walls, incubation with lysozyme is frequently used to hydrolyse polysaccharides in the cell wall. Other methods used to permeabilise gram positive bacteria include an additional incubation with achromopeptidase and incubation in 0.1 M HCl.

In order to obtain the optimum permeabilisation method for maximum probe penetration without causing cell lysis for the AMT samples, three different regimes using recommended concentrations and incubation times (A. Pernthaler, personal communication) were tested as follows:

1. 60 minute incubation in 10 $mg.ml^{-1}$ lysozyme solution
2. 60 minute incubation in 10 $mg.ml^{-1}$ lysozyme solution followed by a 30 minute incubation in 60 $U.ml^{-1}$ achromopeptidase solution
3. 30 second incubation in 0.1 M HCl

After permeabilisation, all filters were incubated with the general Eubacteria probe mixture, EUBI-III and counterstained with DAPI. Paired t-tests were used to compare the percentage of probe positive to DAPI positive cells between permeabilisation treatments.

6.3 Results

6.3.1 Amino acid concentration and uptake

On both cruises, methionine concentrations and uptake rates were generally lower in the northern (NAG) and southern gyres (SAG) than the temperate and equatorial regions (Fig. 6.3). The highest uptake rate (0.97 $nM.d^{-1}$) was located in surface waters of the northern temperate (NT) region during AMT-15 although the only other measurement in this region, also made during AMT-15, was considerably lower (0.25 $nM.d^{-1}$; Fig. 6.3). Linear regression analyses of concentration and uptake rates showed that methionine uptake was positively correlated with concentration only for AMT-14 samples (Fig. 6.4; $p = 0.021$, $n = 26$).

Figure 6.3: Methionine uptake rates and ambient concentrations in surface waters along the AMT transect (data from AMT-14 and 15 are shown). Dotted lines indicate the approximate location of the boundaries of each province.

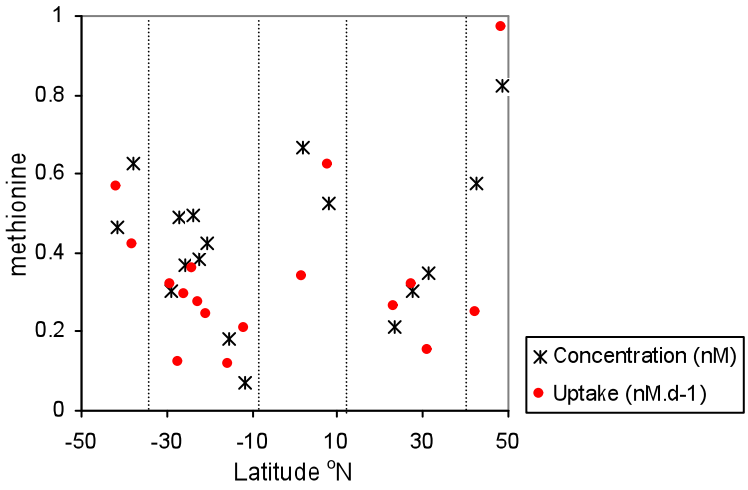

Figure 6.4: Linear regression analysis between the ambient concentrations and uptake rates of methionine during AMT-14. The solid line is the line of regression and the equation and r^2 values are shown. The dotted line represents a 1:1 relationship for reference.

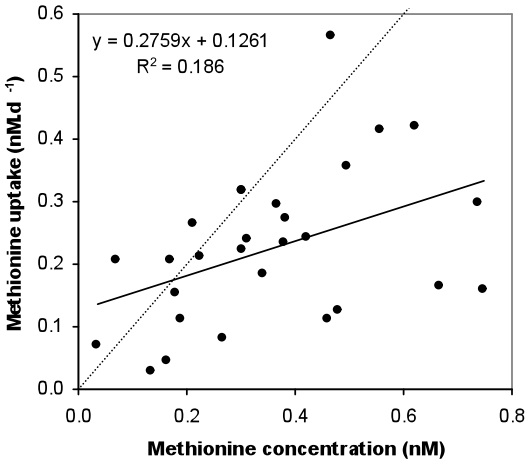

Despite similar methionine concentrations in surface waters in the southern gyre (SAG) during AMT-14 and 15, a considerably lower uptake rate was measured during AMT-15 than AMT-14 (0.118 and 0.281 $nM.d^{-1}$ respectively; Table 6.2). The methionine uptake rates were also lower during AMT-15 than during AMT-14 in the northern gyre despite a higher methionine concentration (Table 6.2), therefore indicating that the ambient methionine concentration did not limit uptake rates in this region during AMT-15.

Methionine concentrations were higher at the chlorophyll maximum (f_{max}) than in surface waters in all provinces and both cruises with the exception of the northern temperate region (NT) during AMT-15. In contrast, these higher methionine concentrations were associated with lower methionine uptake rates at the f_{max} than the surface. The NT province again differed from the remaining provinces, with a higher rate of methionine uptake at the f_{max} than in surface waters (Table 6.2).

The ambient concentrations of leucine were slightly lower but in the same order of magnitude as the ambient methionine concentrations (Tables 6.2 and 6.3). In general, the turnover rates in surface waters of this smaller pool of leucine were greater than for the larger pool of methionine. In fact, the pool of leucine molecules was turned over more than once a day at all stations except one in the southern temperate region (ST), indicated by uptake rates greater than the concentration (Fig. 6.5). As was found for methionine, the rate of turnover of leucine was lower in the two gyres than in the temperate or equatorial regions. In contrast to methionine concentration, the concentration of leucine in the surface waters was higher in the northern gyre (NAG) than the southern gyre (SAG) during AMT-14 and vice versa on AMT-15 (Table 6.3, Fig. 6.5). Linear regression analyses showed that the rate of leucine turnover was not significantly correlated with the *in situ* concentration during either AMT-14 or 15 ($p > 0.05$).

Table 6.2: Mean methionine concentrations and uptake rates at the depth of the chlorophyll maximum (f_{max}) and in surface waters (Surf) in each province during AMT-14 and 15. Where the number of samples (n) > 1, mean values with standard errors (SEM) are shown.

		AMT-14		AMT-15	
Province	Depth	Concentration (nM) ± SEM	Uptake rate ($nM.d^{-1}$) ± SEM	Concentration (nM) ± SEM	Uptake rate ($nM.d^{-1}$) ± SEM
NT	Surf	-	-	0.698 ± 0.123 **n = 2**	0.609 ± 0.361 **n = 2**
	F_{max}	-	-	0.451 **n = 1**	0.963 **n = 1**
NAG	Surf	0.258 ± 0.044 **n = 2**	0.291 ± 0.026 **n = 2**	0.351 **n = 1**	0.152 **n = 1**
	F_{max}	-	-	0.900 **n = 1**	0.133 **n = 1**
SAG	Surf	0.341 ± 0.060 **n = 6**	0.281 ± 0.022 **n = 6**	0.337 ± 0.154 **n = 2**	0.118 ± 0.004 **n = 2**
	F_{max}	0.379 ± 0.073 **n = 7**	0.191 ± 0.015 **n = 7**	0.629 **n = 1**	0.082 **n = 1**
EQ	Surf	-	-	0.596 ± 0.071 **n = 2**	0.481 ± 0.141 **n = 2**
	F_{max}	-	-	0.682 **n = 1**	0.365 **n = 1**
ST	Surf	0.545 ± 0.079 **n = 2**	0.492 ± 0.072 **n = 2**	-	-

Figure 6.5: Leucine uptake rates and ambient concentrations in surface waters along the AMT transect (data from AMT-14 and 15 are shown). Dotted lines indicate the approximate location of the boundaries of each province. Note the logarithmic scale.

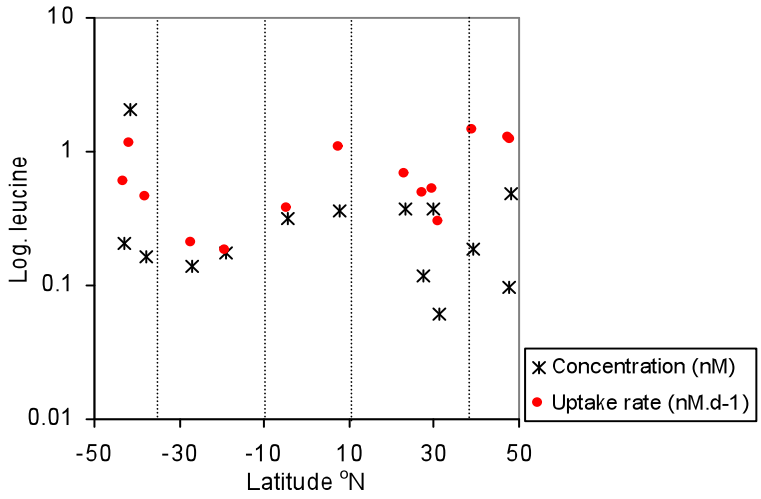

Table 6.3: Leucine concentrations and uptake rates at the depth of the chlorophyll maximum (f_{max}) and in surface waters (Surf) during AMT-14 and 15. Where the number of samples (n) > 1, mean values with standard errors (SEM) are shown.

		AMT-14		AMT-15	
Province	Depth	Concentration (nM) ± SEM	Turnover rate ($nM.d^{-1}$) ± SEM	Concentration (nM) ± SEM	Turnover rate ($nM.d^{-1}$) ± SEM
NT	Surf	0.141 ± 0.062 **n = 2**	1.344 ± 0.116 **n = 2**	0.486 **n = 1**	1.120 **n = 1**
NAG	Surf	0.286 ± 0.144 **n = 3**	0.557 ± 0.105 **n = 3**	0.062 **n = 1**	0.300 **n = 1**
	F_{max}	-	-	0.091 **n = 1**	0.089 **n = 1**
SAG	Surf	-	-	0.158 ± 0.017 **n = 2**	0.193 ± 0.010 **n = 2**
EQ	Surf	-	-	0.223 ± 0.126 **n = 2**	0.724 ± 0.488 **n = 2**
ST	Surf	1.105 ± 0.920 **n = 3**	0.837 ± 0.281 **n = 3**	-	-

Significant correlations between both the methionine and leucine uptake rates and the abundance of heterotrophic bacteria demonstrate that the variability in amino acid uptake rates is due to variability in the abundance of heterotrophic bacteria ($p < 0.05$; Fig. 6.6). This is in contrast to the uptake of amino acids at saturating concentrations (chapter 5). When the abundance of heterotrophic bacteria and *in situ* amino acid uptake rates are examined for each cruise, the correlation between both factors is significant for methionine and leucine during AMT-14 ($p < 0.001$ and 0.32 respectively). During AMT-15, the leucine uptake rates significantly correlated with the abundance of heterotrophic bacteria ($p < 0.001$), however this was not the case for methionine uptake rates ($p = 0.057$).

Figure 6.6: Regression analyses of either methionine uptake rates (a) or leucine uptake rates (b) and the abundance of heterotrophic bacteria (HB) during both AMT-14 and 15 cruises. The solid lines are the line of regression and the equations, r^2 values and p values are shown. The dashed lines indicate a 1:1 ratio for reference.

a. b.

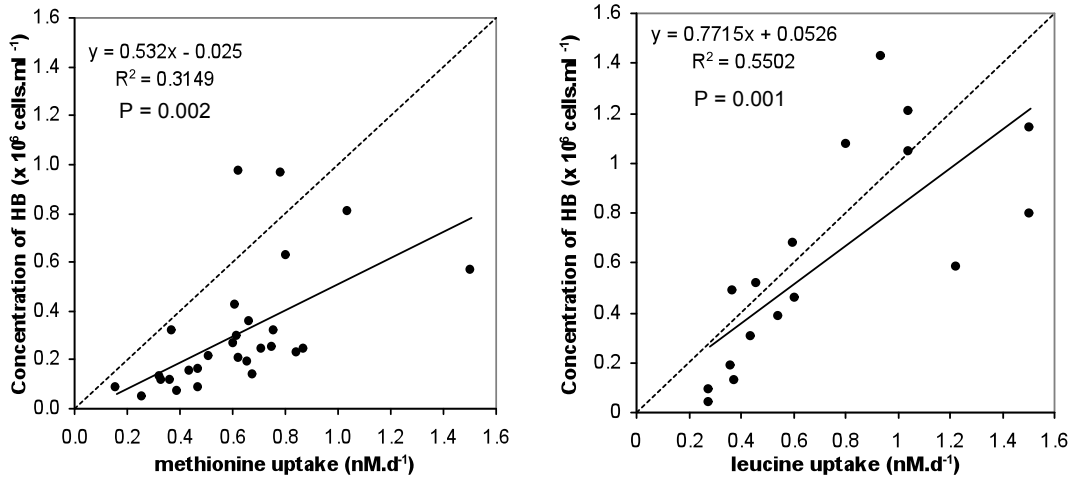

6.3.2 Contribution of cell groups to methionine uptake in surface waters

Bacterioplankton were responsible for almost the entire methionine uptake in the water. The sum of the methionine uptake of each sorted cell group accounted for 91 ± 4.5 % (n = 22) of the total methionine uptake into particulate matter.

Cells with low nucleic acid content

The contribution of cells with low nucleic acid content (LNA) to the total methionine uptake in surface waters varied across the AMT-13, 14 and 15 transects with fractions between 0.2 and 0.5. Similar variability was found in the contribution of the LNA group to the total abundance of bacterioplankton with fractions ranging from 0.3 to 0.5 (Fig. 6.7). There was no clear trend in the proportional contribution of the LNA cells to either methionine uptake or abundance in different provinces and between cruises.

The variability in methionine uptake of the LNA group was not significantly correlated with the fractional abundance in surface waters during AMT-14 and 15 ($p > 0.05$, $n = 9$ and 12). In contrast, a significant relationship was found between the fractional methionine uptake and fractional abundance of the LNA group during AMT-13 (linear

regression, $p = 0.0114$, $n = 17$). This indicates that the variability in methionine uptake rates is due to variance in the abundance of the LNA cells rather than differences in the methionine uptake per cell along the AMT-13 transect, however the uptake per cell was not constant.

The cellular methionine uptake of the LNA group as a proportion of the average cellular uptake varied between 0.59 and 1.35 along both AMT-13 and AMT-14 with no distinct differences between oceanic provinces (Fig. 6.8). Although similar proportions of the average cellular uptake were obtained in the northern temperate, southern temperate and equatorial regions along AMT-15 as during AMT-13 and 14, more variability in the LNA cellular uptake was observed in other regions. At approximately 21 ºN on AMT-15, the average LNA cell took up methionine at almost double the rate of an average bacterioplankton cell. This station was located close to the NW African coast in the centre of the upwelling region (Fig. 3.1), although the same region sampled on AMT-13 did not produce a similar peak in LNA cellular activity. Other differences in the LNA cellular activity during AMT-15 compared to the previous cruises were observed in the SAG: a high proportional uptake (1.8 times the uptake rate of an average cell) at 25 ºS and the lowest LNA proportional activity of 0.25 at 18 ºS (Fig. 6.8).

Neither the fractional methionine uptake of the total community uptake nor the proportional cellular uptake of the LNA cell group were related to changes in temperature along the AMT transects (linear regressions, $p > 0.05$).

Figure 6.7: Contribution of cells with low nucleic acid (LNA) content to the total community methionine uptake (a, c and e) and the total abundance of bacterioplankton (b, d and f) in surface waters during AMT-13, 14 and 15.

a. Fraction of methionine uptake (AMT-13)

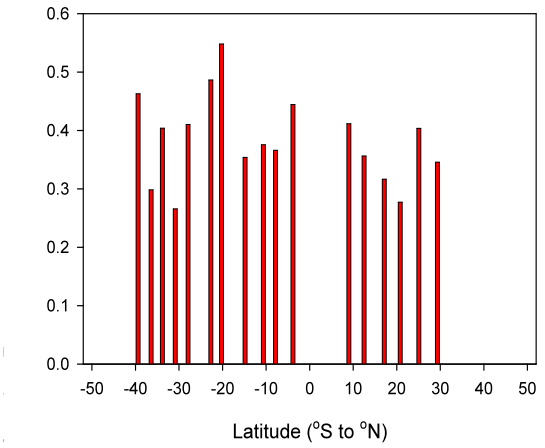

b. Fraction of abundance (AMT-13)

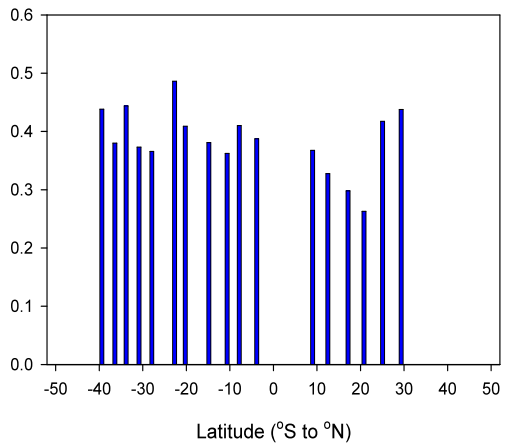

c. Fraction of methionine uptake (AMT-14)

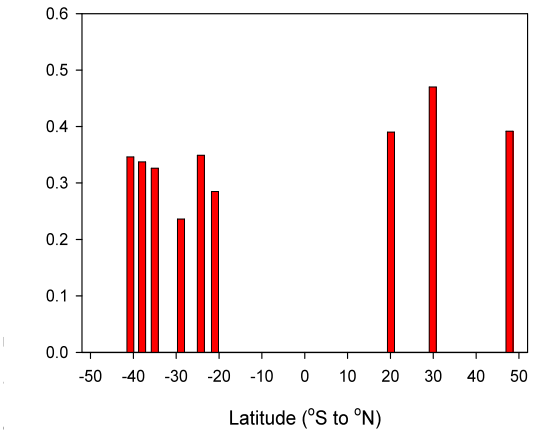

d. Fraction of abundance (AMT-14)

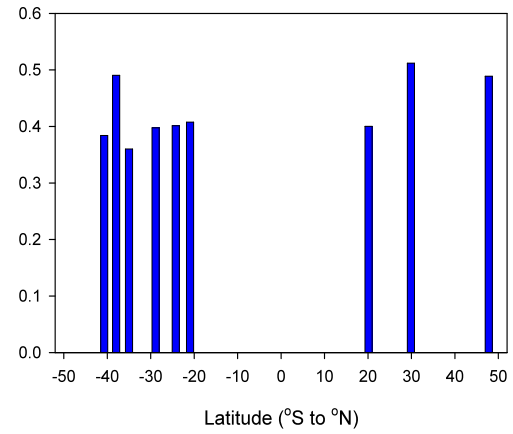

e. Fraction of methionine uptake (AMT-15)

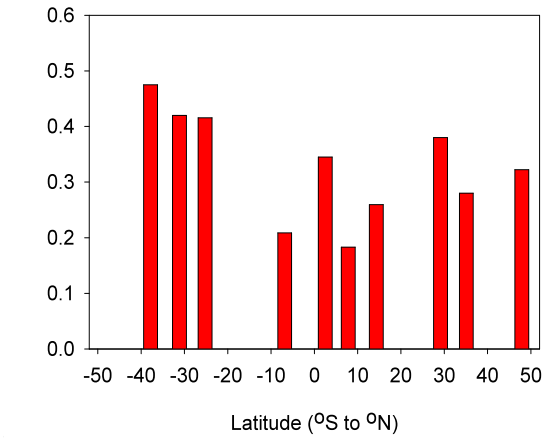

f. Fraction of abundance (AMT-15)

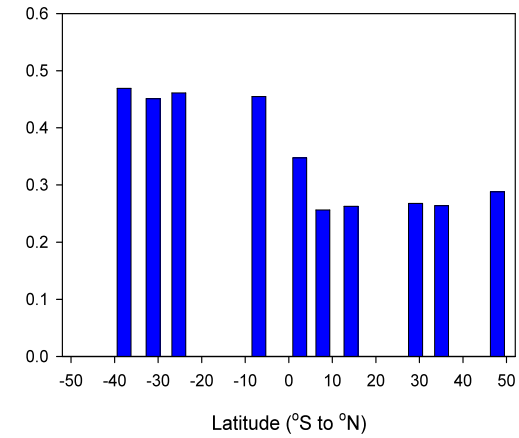

Figure 6.8: Cellular methionine uptake of cells with low nucleic acid (LNA) content as a proportion of the average bacterioplankton cellular uptake in surface waters along AMT-13 (a), AMT-14 (b) and AMT-15 (c). Dotted lines indicate the approximate position of province boundaries.

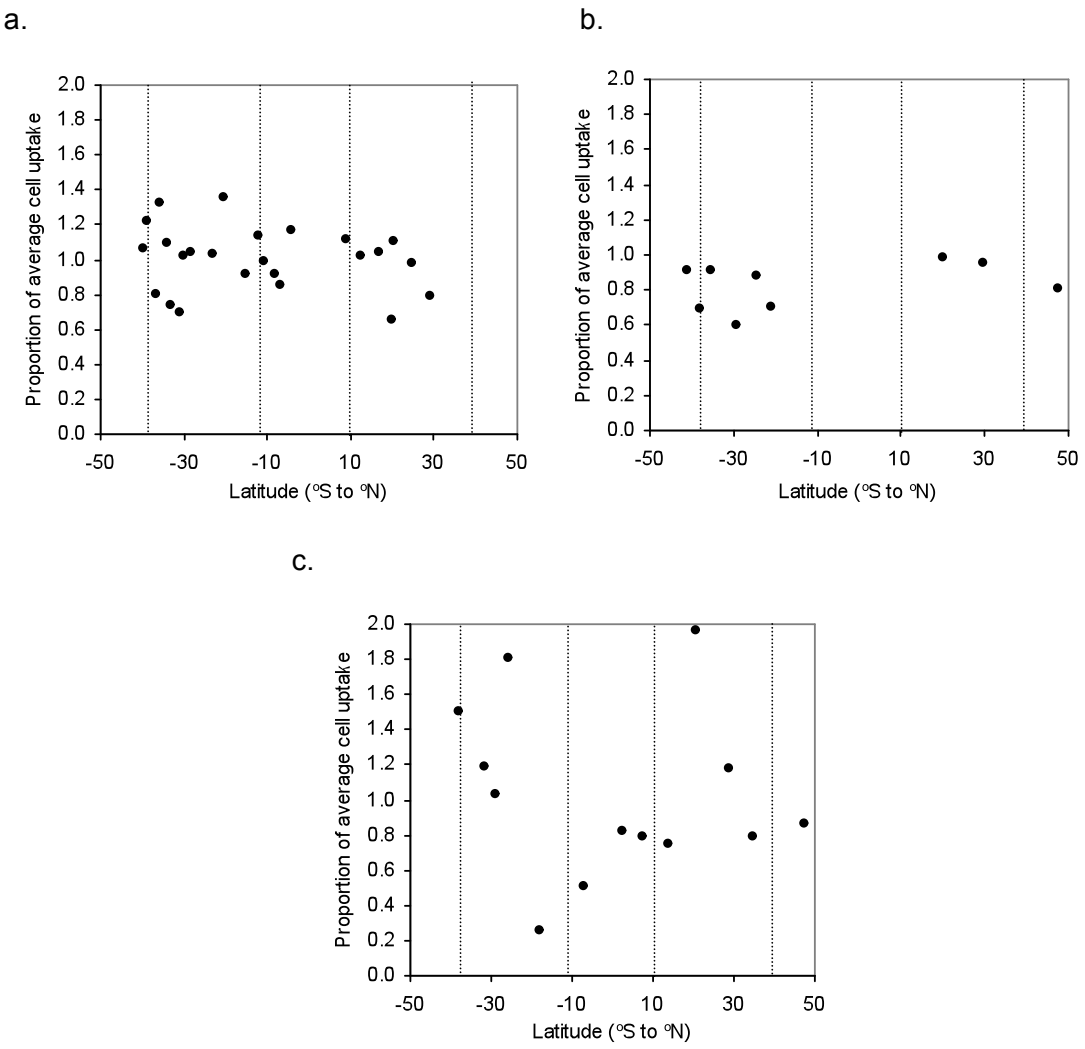

Cells with high nucleic acid content

Due to the difficulties in separating *Prochlorococcus* from heterotrophic bacteria in some surface samples, data for the high nucleic acid cell group include *Prochlorococcus*. The fractional contribution of cells with high nucleic acid (HNA) content to methionine uptake varied between approximately 0.4 and 0.8 with no clear trend along any of the three transects (Fig. 6.9). As was found for the LNA group, the fractional methionine uptake of the HNA cell group significantly correlated with the fractional abundance during AMT-13 (linear regression, $p = 0.01$, $n = 17$) but not during AMT-14 ($p = 0.43$, $n = 9$) or AMT-15 ($p = 0.27$, $n = 12$).

Figure 6.9: Contribution of cells with high nucleic acid (HNA) content to the total community methionine uptake (a, c and e) and the total abundance of bacterioplankton (b, d and f) in surface waters during AMT-13, 14 and 15.

a. Fraction of methionine uptake (AMT-13)

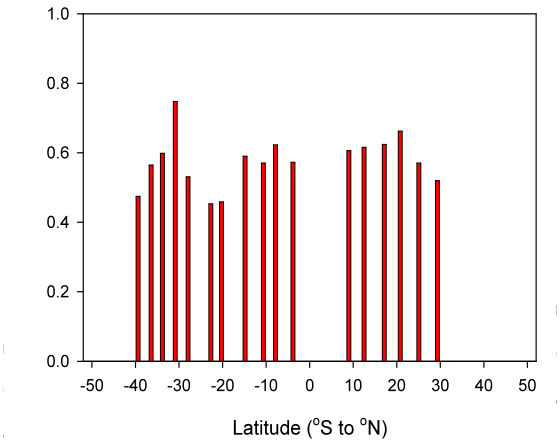

b. Fraction of abundance (AMT-13)

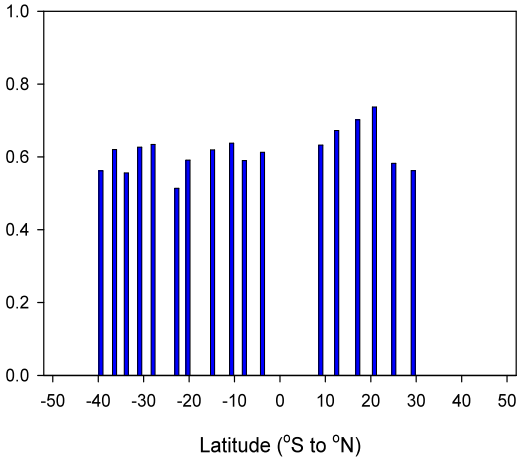

c. Fraction of methionine uptake (AMT-14)

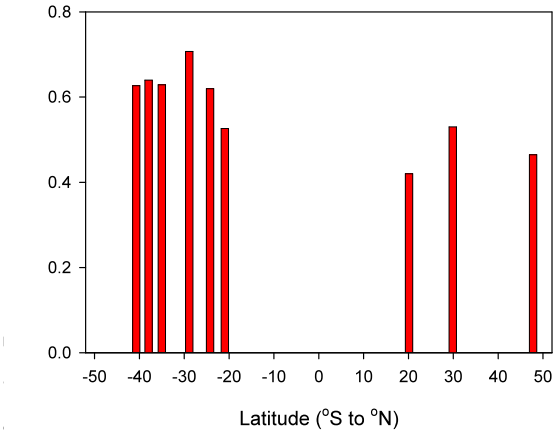

d. Fraction of abundance (AMT-14)

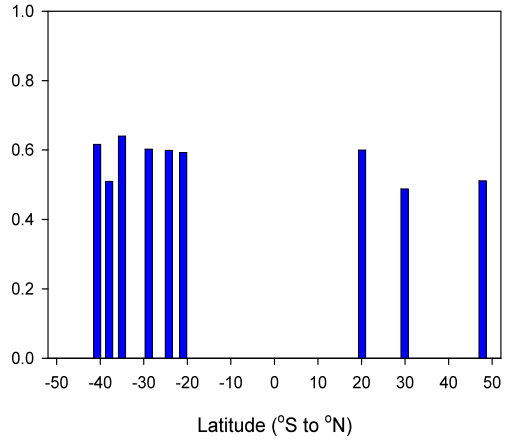

e. Fraction of methionine uptake (AMT-15)

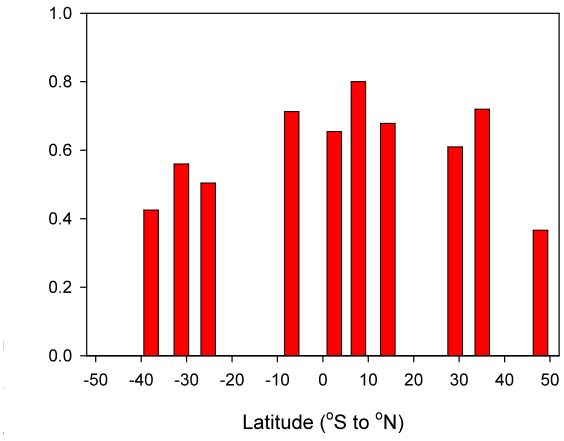

f. Fraction of abundance (AMT-15)

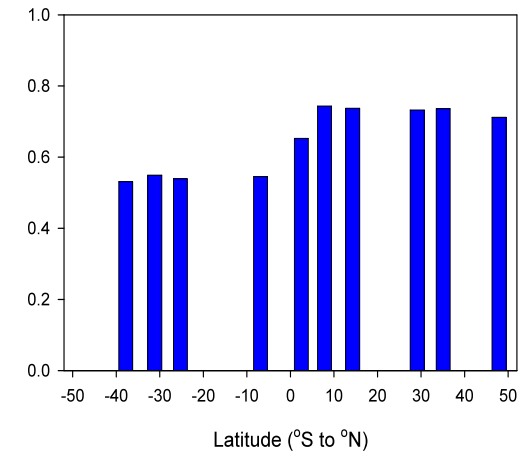

Methionine uptake rates per cell for the HNA group varied between 71 % and 223 % of the uptake of an average bacterioplankton cell over all three cruises. During AMT-13, cellular methionine uptake rates of the HNA group were generally more stable along the transect than during AMT-14 and 15 with the exception of four stations in the southern temperate and southern gyre provinces where the uptake rates were considerably higher than an average bacterioplankton cell (Fig. 6.10). Variability in proportional uptake rates of the HNA cell group did not follow any pattern between different cruises or provinces.

Cellular uptake rates were generally higher for the HNA group than the LNA group in all provinces although the differences were not statistically significant (t-test, $p > 0.05$). The lowest cellular methionine uptake rates for the HNA group were found in the southern gyre along with the lowest rates of methionine uptake for the LNA group (Table 6.4).

As to be expected from the large scatter of data along the transects, there were no relationships between the fractional methionine uptake of the total community uptake or the proportional cellular uptake of the HNA cell group and temperature (linear regressions, $p > 0.05$).

Figure 6.10: Cellular methionine uptake of cells with high nucleic acid (HNA) content as a proportion of the average bacterioplankton cellular uptake in surface waters along AMT-13 (a), AMT-14 (b) and AMT-15 (c). Dotted lines indicate the approximate position of province boundaries.

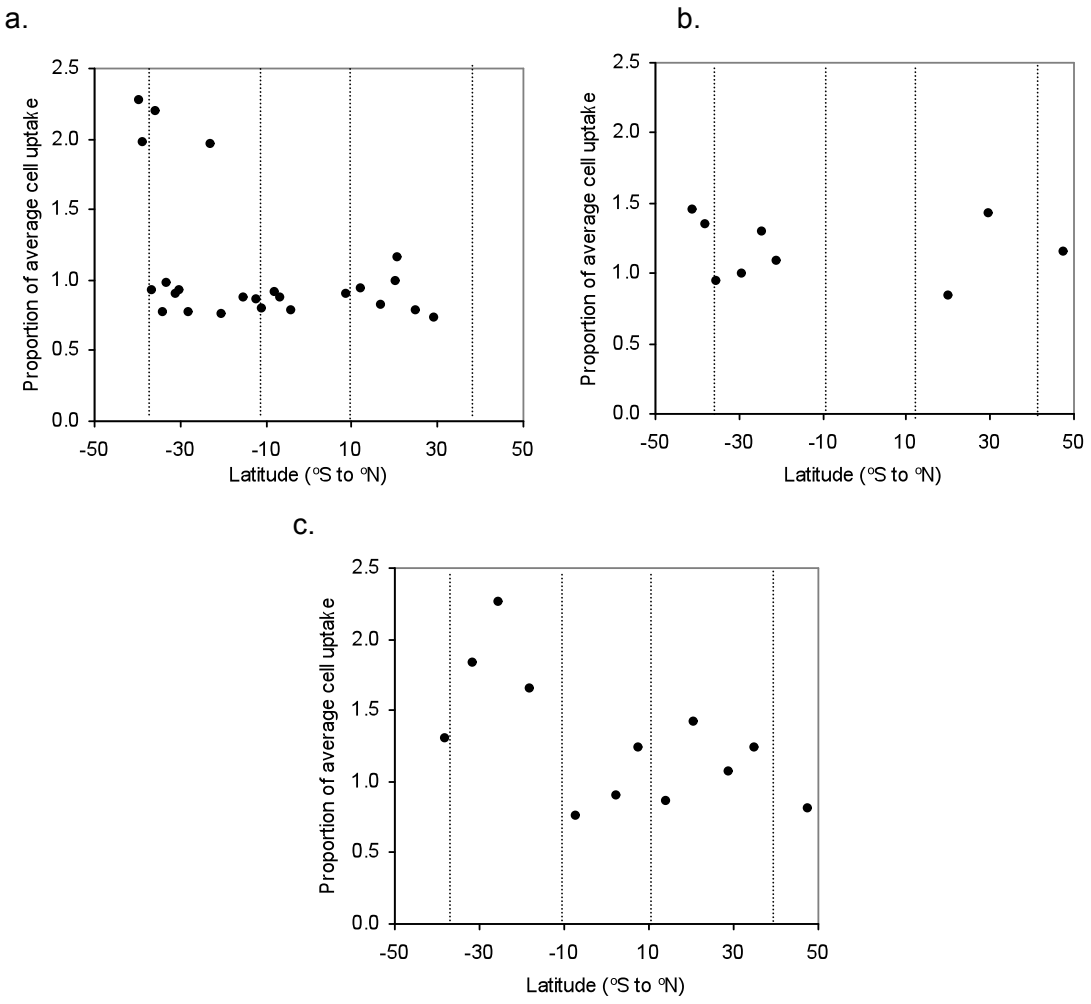

Table 6.4: Average cellular uptake rates of methionine in surface waters of each province for cells with low (LNA) and high (HNA) nucleic acid content. Values were calculated by multiplying the fractional contribution of each sorted group to the total community uptake by the total methionine uptake at saturating concentrations (AMT-15). Where the number of samples (n) > 1 the standard error of the mean (S.E.M.) is also shown.

	Mean uptake ± S.E.M. (amol.cell^{-1}.d^{-1})	
Province	LNA	HNA
NT	0.79 ± 0.56 n = 2	0.98 ± 0.56 n = 2
NAG	1.34 ± 0.70 n = 3	1.21 ± 0.66 n = 3
EQ	1.00 ± 0.63 n = 2	1.64 ± 0.23 n = 2
SAG	0.36 n = 1	0.53 n = 1
ST	1.22 n = 1	1.81 n = 1

6.3.4 The effect of depth on methionine uptake

The uptake of methionine by different cell groups was determined at the depth of the chlorophyll maximum (f_{max}) at nine stations during AMT-15. There was no trend in the fractional contribution of either cells with low (LNA) or high (HNA) nucleic acid content to the total methionine uptake between the surface and the f_{max} across the whole transect (Fig. 6.11). However when the actual uptake values of each cell group are compared at specific stations, differences are observed between the surface and the f_{max} (Fig. 6.12).

Figure 6.11: Contribution of cells with low nucleic acid (LNA) and high nucleic acid (HNA) content to the total community methionine uptake (a) and the total abundance of bacterioplankton (b) at the chlorophyll maximum (f_{max}) during AMT-15.

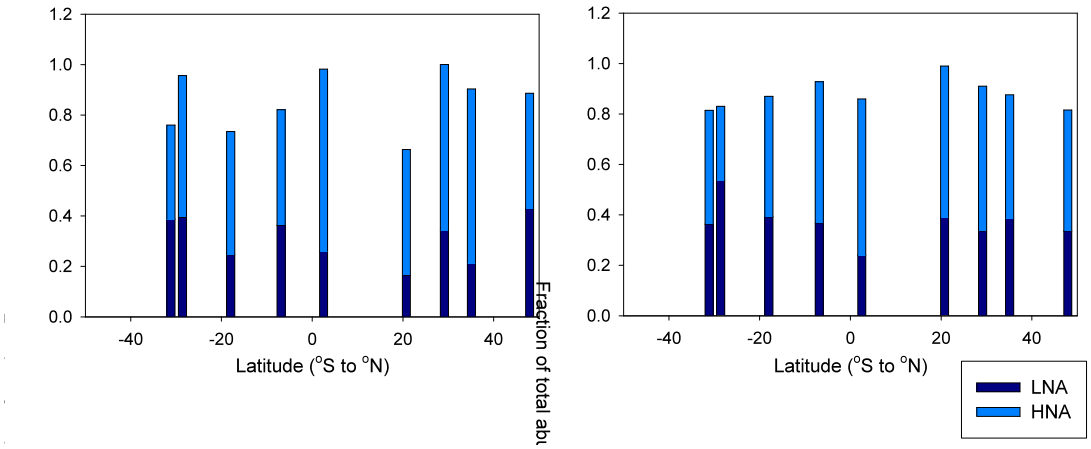

Figure 6.12: Methionine uptake by cells with low (LNA) and high (HNA) nucleic acid content at the surface and the f_{max} at six stations during AMT-15.

a. LNA

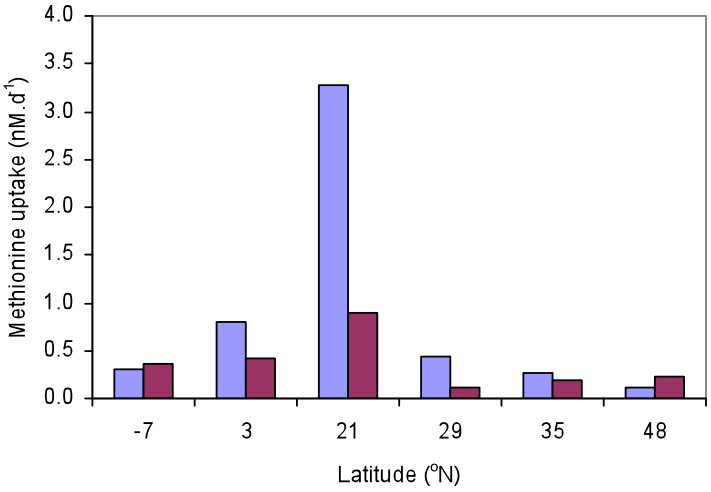

b. HNA

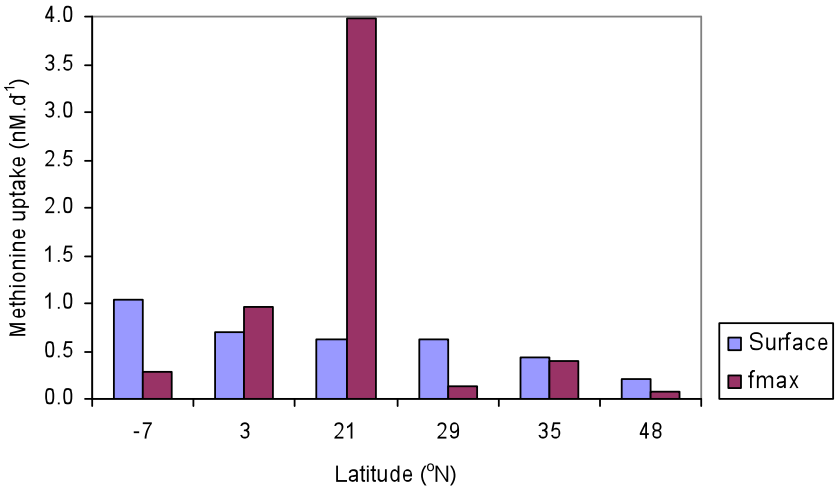

At At 21 ºN in the North West African upwelling region, the LNA group take up most of the methionine in surface waters and the HNA group take up most of the methionine at the f_{max} (Fig. 6.12). At the f_{max}, the HNA group constitute a greater proportion of the total cell abundance than in surface waters in the North West African upwelling (0.7 compared to 0.5) thus explaining their higher total uptake of methionine. However, the higher methionine uptake in the LNA group at the surface cannot be explained by a higher abundance, with the fractional abundance of this group remaining at 0.3 of the total community. Therefore the higher methionine uptake of the LNA group in surface waters in this region indicates a higher cellular activity than the HNA group.

6.3.4 Comparison between in situ and maximum methionine turnover rates

During AMT-13 and 14, *in situ* total methionine uptake rates were used in conjunction with the fraction of methionine uptake for each cell group to determine the amount of methionine taken up by each cell group per day. In both the northern (NAG) and southern (SAG) gyres, these rates did not differ greatly from the maximum methionine uptake rates determined by incubating samples at saturating methionine concentrations during AMT-15 (Fig. 6.13). In the equatorial province (EQ) at saturating methionine concentrations, all cell groups took up more methionine resulting in a total methionine turnover rate over double that at *in situ* methionine concentrations.

The only province where the total methionine uptake rates decreased at saturating concentrations relative to the *in situ* concentrations was in the North West African upwelling province (UP). There is a large difference in the methionine uptake rates of both the LNA and HNA cell groups in this province with HNA having a higher turnover rate at *in situ* concentrations and LNA having a higher turnover rate at saturating methionine concentrations (Fig. 6.13). A similar pattern is also observed in the southern temperate region (ST) where the methionine turnover rates are higher in the LNA group at saturating concentrations (Fig. 6.13).

Figure 6.13: Mean methionine uptake rates for each sorted cell group in each province in surface waters at *in situ* concentrations during AMT-13 and 14 (a) and at saturating concentrations during AMT-15 (b). Error bars represent the standard error of the mean (SEM). Note the logarithmic scale used.

a.

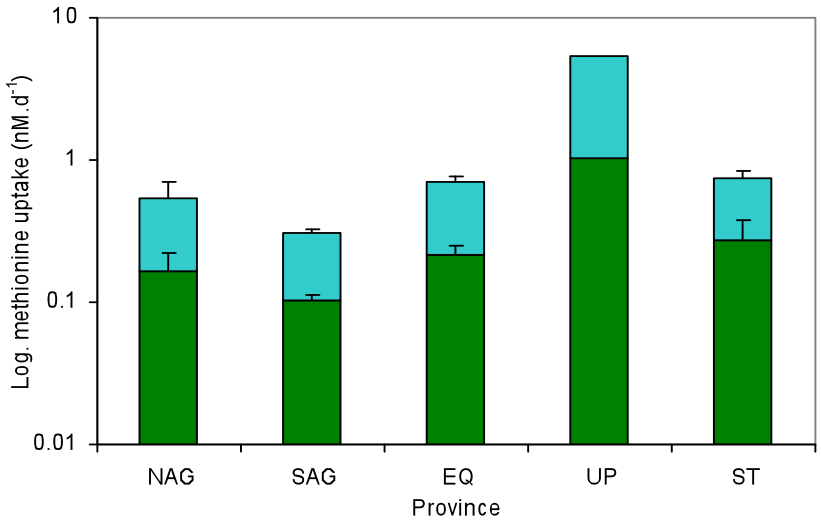

b.

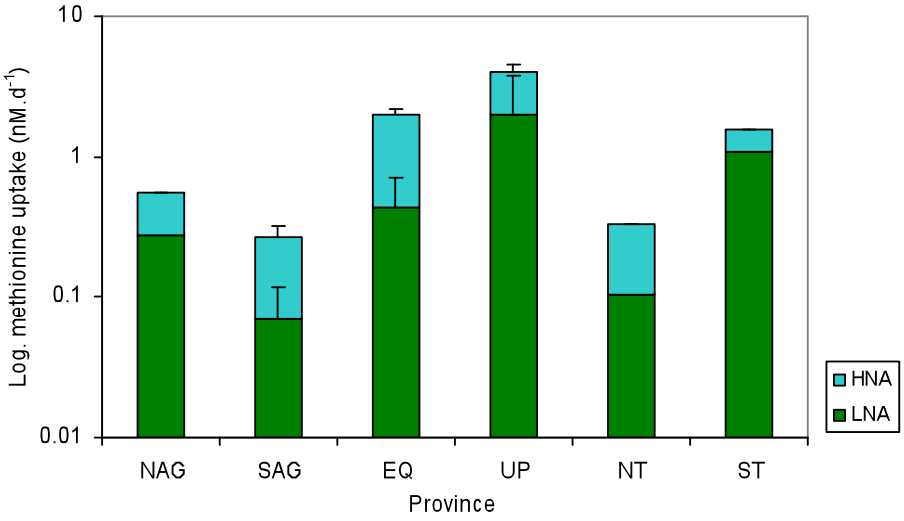

6.3.5 CARD-FISH

Permeabilisation experiment

Samples treated with lysozyme only, produced between 48.5 and 62.5 % (mean 54.5 ± 1.9 %) probe positive cells out of the total number of DAPI positive signals. When an incubation with achromopeptidase was added, significantly higher percentages (between 72.6 and 92.1 %; mean 83.9 ± 3.9; paired t-test, $p < 0.001$, $n = 7$) of probe positive cells were obtained from the same samples. For both techniques, a greater percentage of hybridised cells were observed in the higher latitude regions compared to lower latitudes. The percentages of cells hybridised with the EUBI-III probe following permeabilisation with 0.1 M HCl were 62.4 and 68.9 % ($n = 2$), this was lower than that obtained using the lysozyme and achromopeptidase treatment (73.2 and 86.9 %; $n = 2$). Therefore the optimum permeabilisation method for these samples was the combination of lysozyme and achromopeptidase incubations and this was used for all the hybridisations used to examine community composition.

Community composition

In unsorted samples from AMT-12, high percentages of DAPI stained cells hybridised with the general bacterial probe (EUBI-III) with values ranging from 71 % in the equatorial region (EQ) to 92 % in the northern (NAG) and the southern (SAG) gyres (Fig. 6.14). However, less than 60 % of the DAPI stained cells were hybridised with the group specific probes tested. Cyanobacteria (Cya 664) comprised most of the hybridised cells in all samples apart from one in the NAG at 24 ºN. The largest proportion of cells apart from the cyanobacteria hybridised with the Cytophagales-Flavobateria (CF319a), Alpha (ALF968) and Gamma-Proteobacteria (GAM42a) specific probes. Crenarchaea (CREN554) were present at less than 1 % and Euryarchaea (EURY806) and Planctomycetes (PLA886) were present at less than 3 % of DAPI positive cells in all samples (Fig. 6.14). In all samples, cells hybridised with the NON-EUB probe were less than 1 % of the total DAPI stained cells.

Figure 6.14: Community composition of whole water samples from 25 metres at six stations determined by CARD-FISH. % of DAPI stained cells hybridised with EUBI-III (a) and with group specific probes (b). Error bars represent the standard error of counting.

a.

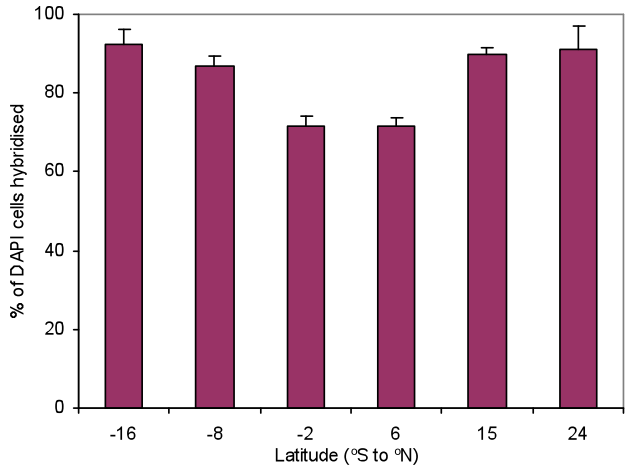

b.

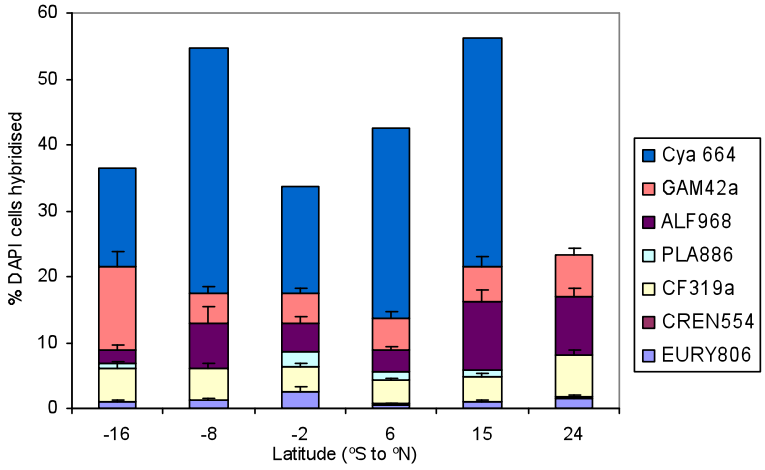

Community composition of flow sorted cell groups

To further define the community composition and to compare this to methionine uptake rates, water samples were flow sorted into the same groups used for rate measurements before being hybridised with group specific probes. A high majority of DAPI positive cells from each sorted cell group were hybridised with the EUBI-III probe (between 74 and 100 %; Fig. 6.15). The majority of cells could be hybridised with group

specific probes in the LNA cell group only (Fig. 6.15). In this group, in surface waters between 55 and 81 % (mean 70 ± 2.0 %; n = 12) of DAPI positive cells hybridised with the SAR11-441R probe (targeting the majority of SAR11 cells) and between 37 and 69 % (mean 49 ± 2.4 %; n = 12) of DAPI positive cells hybridised with a more specific SAR11 probe, targeting the SAR11-A1 subgroup.

In both the HNA I and HNA II sorted cell groups, the highest proportion of cells that could be hybridised with group specific probes were in the southern temperate region (ST) at 31 and 38 ºS where approximately 40 % of DAPI positive cells hybridised with the *Cytophagales-Flavobacteria* probe (CF319a; Fig. 6.15). Over 20 % of DAPI positive cells in the HNA II group were *Prochlorococcus* (405 Pro) in all three stations in the equatorial province (EQ) and one station in the ST whereas *Prochlorococcus* were not found in any of the HNA I sorted cells. *Roseobacter* cells were found at less than 10 % of the total DAPI positive cells in the HNA II cell group but none were found in the HNA I group (Fig. 6.15). SAR 11 cells were also found in the HNA I and II cell groups at a few stations, although these were generally at low concentrations. A small percentage of SAR 86 cells were also found in the northern (NT) and southern (ST) temperate regions in the HNA I cell group. Probes targeting the SAR 406 and SAR 116 cell groups were also tested with no positive signals in any of the sorted cell groups. In all samples from each cell group, less than 1 % of the total DAPI stained cells hybridised with the NON-EUB probe.

There was no clear relationship between methionine uptake rates for each sorted cell group and community composition (Fig. 6.15). Due to the dominance of SAR 11 and the failure to detect any other groups of bacterioplankton in the LNA group, the uptake of methionine by this group can be ascribed to SAR 11. Cells from the HNA I and HNA II groups belonged to several different phylogenetic groups and in most samples less than 50 % of the cells could be identified using the group specific probes used in this study. Therefore it is more difficult to link the uptake of methionine in each flow sorted group to specific bacterial clades.

Figure 6.15: Community composition and methionine (met) uptake rates (where available) of each sorted cell group in surface waters; LNA (a); HNA I (b) and HNA II (c). Methionine uptake rates are based on incubations at saturating concentrations except from the samples marked with a * where the *in situ* uptake rates are shown. Error bars represent the standard error of counting calculated from duplicate counts.

a. LNA

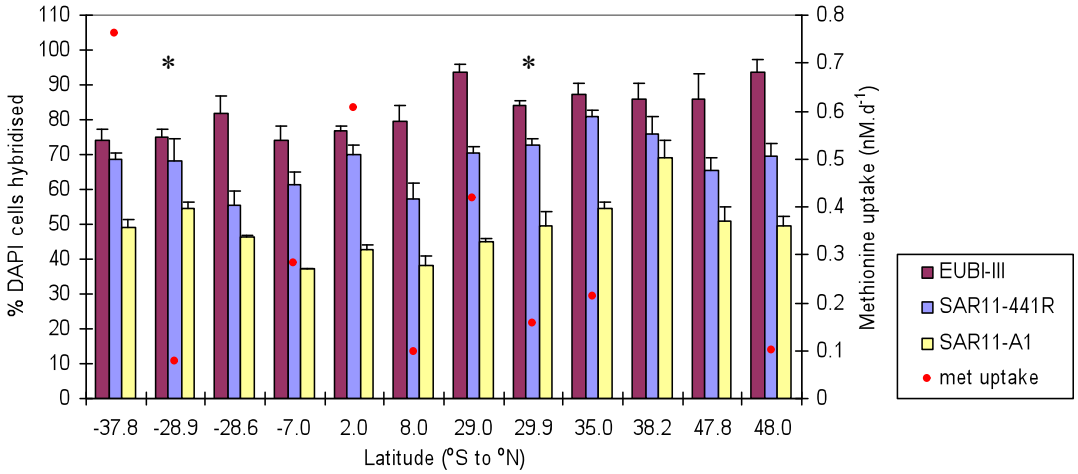

b. HNA I

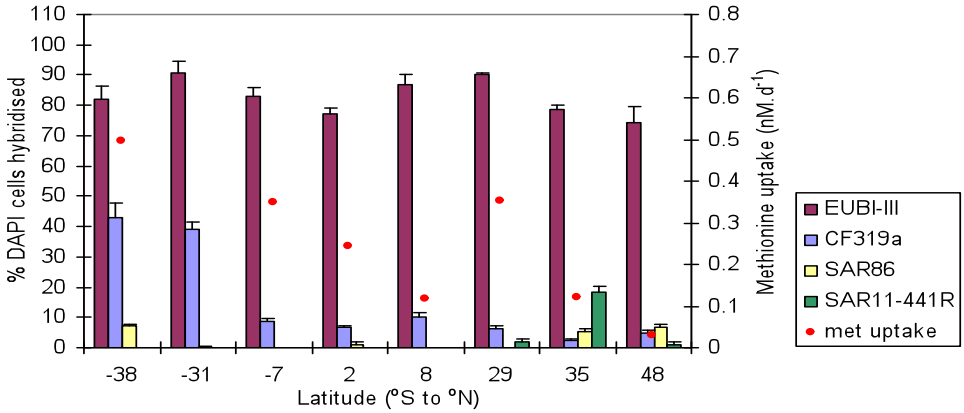

c. HNA II

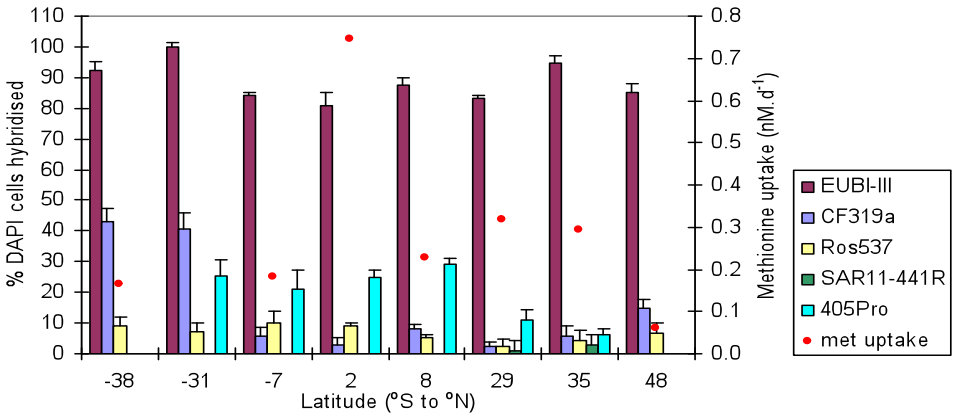

The concentrations of bacterial groups in each sample were calculated by multiplying the percentages of cells hybridised with each probe by the concentration of each sorted cell group (LNA, HNA I and HNA II) determined by flow cytometry. The number of cells that hybridised with the group specific probes constituted between 35 and 49 % of the total abundance of bacterioplankton (mean 40.3 ± 2.2 %).

The SAR 11 clade was the most abundant group in all provinces. The highest concentrations were found in the southern (ST) and northern (NT) temperate regions and the southern gyre (SAG) with lower concentrations in the northern gyre (NAG) and equatorial provinces (EQ). *Cytophaga-Flavobacterium-Bacteroides* were the next most abundant group with the highest concentration in the SAG and the lowest in the NAG (Table 6.5). The concentrations of *Prochlorococcus* calculated from hybridisations with the 405Pro probe following cell sorting were approximately 10 % of the concentrations determined by flow cytometry (chapter 4). *Prochlorococcus* cells can be found in both the HNA I or HNA II cell groups, therefore the 90 % of the *Prochlorococcus* cells not hybridised with the 405Pro probe may account for the large proportion of unidentified cells in the groups of cells with high nucleic acid.

Table 6.5: Mean concentration of SAR 11, *Cytophaga-Flavobacterium-Bacteroides* (CF), *Roseobacter* (Rsb), *Prochlorococcus* (Pro) and SAR 86 bacteria in surface waters in different provinces. Where the number of samples (n) > 1, the standard error of the mean (S.E.M.) is also shown.

	Cell concentration ± S.E.M. (x 10^3 cells.ml^{-1})				
Province	SAR 11	CF	Rsb	Pro	SAR 86
NT	332.6 ± 31.7 (n = 2)	32.2 (n = 1)	8.1 (n = 1)	0 (n = 1)	21.2 (n = 1)
NAG	156.4 ± 16.1 (n = 2)	10.3 ± 3.3 (n = 2)	2.0 ± 1.2 (n = 2)	4.8 ± 1.0 (n = 2)	4.0 ± 4.0 (n = 2)
SAG	327.0 (n = 1)	76.6 (n = 1)	1.8 (n = 1)	6.4 (n = 1)	0.7 (n = 1)
EQ	185.6 ± 13.8 (n = 3)	29.2 ± 5.9 (n = 3)	10.2 ± 2.5 (n = 3)	33.6 ± 7.4 (n = 3)	0.6 ± 0.6 (n = 3)
ST	426.5 (n = 1)	-	-	-	-

6.4 Discussion

6.4.1 Is the uptake of amino acids concentration dependent?

Ambient concentrations of methionine and leucine calculated from concentration series bioassays agree with other reported values for the southern Atlantic gyre estimated using the same method. Zubkov et al. (2004) reported an average methionine concentration in surface waters of the southern gyre (SAG) of 0.40 nM compared to 0.34 nM in this study. The lower average leucine concentration of 0.16 nM in surface waters of the SAG was also comparable to the concentration reported in Zubkov et al (2004; 0.19 nM).

The higher estimated concentrations of leucine and methionine at the chlorophyll maximum compared to the surface waters is consistent with previous studies (Zubkov et al., 2004). Correlation between methionine concentration and uptake rates during AMT-14 suggests that uptake of these amino acids is limited by the ambient concentration. However, this was not the case during AMT-15. In some samples, high amino acid uptake rates were associated with low ambient concentrations. In the equatorial upwelling region and the northern temperate region, the pool of leucine molecules was actively cycled with the amount of leucine incorporated per day into bacterioplankton more than double the concentration. High amino acid uptake rates may act to maintain a low ambient concentration in these regions.

It would be tempting to suggest that a high rate of turnover of the amino acid pool occurs in regions with a high rate of organic nutrient supply, thus sustaining high uptake rates. This explanation is valid for the equatorial and northern temperate regions, where increased inorganic nutrient supply supports a higher rate of primary production and increased biomass relative to the oligotrophic gyres. However, during AMT-15 in the northern gyre, leucine was taken up at a rate of 0.30 $nM.d^{-1}$ despite a low ambient concentration of 0.06 nM. In the oligotrophic gyres, biomass and rates of primary production are low, resulting in a reduced supply of dissolved organic matter (DOM) compared to the more dynamic upwelling and temperate regions. Therefore it would be expected that the pool of amino acids would by cycled at a lower rate in the oligotrophic gyres with the uptake of amino acids lower in comparison to the ambient concentration.

Previous research has highlighted the importance of mesoscale eddies in the finescale upwelling of nitrate to support phytoplankton growth in the North Atlantic gyre (Mahaffey et al., 2004; McGillicuddy et al., 1998). Isolated hotspots of increased DOM resulting from eddy-induced increases in primary production could cause a temporary increase in the activity of heterotrophic bacterioplankton thus explaining the high turnover of the leucine pool in the northern gyre. The higher turnover of the leucine pool compared to the methionine pool in the gyres indicates the differential cycling rates of different dissolved free amino acids.

6.4.2 Methionine uptake rates of cells with high and low nucleic acid content

The lowest cellular activities were found in each sorted cell group in the southern gyre. At *in situ* methionine concentrations in surface waters the HNA cell group was more active than the LNA group but at saturating methionine concentrations the LNA group were more active than the HNA group. This indicates that the LNA group is more successful in higher amino acid concentrations. The LNA group is comprised mainly of cells from the SAR 11 clade and previous research indicates that these cells are more successful in oligotrophic environments (Morris et al., 2002 and Giovannoni et al., 2005). This contrasts with the results presented here. The comparison between uptake rates at *in situ* and saturating methionine concentrations were made on different cruises. It has been demonstrated that cellular and community methionine uptake is variable within provinces along and between each of the three transects. The upwelling region is a physically dynamic region with high variation in nutrient concentrations over relatively small spatial scales. Therefore the difference observed between activity in the LNA and HNA groups at differing met saturation levels may be due to the cells being in different conditions on the different cruises.

Methionine uptake rates for each sorted cell group did not relate to changes in community composition detected in this study. The CARD-FISH technique is more sensitive at detecting small cells with low rRNA content than the standard FISH technique (Pernthaler et al., 2002) however, with the suite of probes used here a large proportion of the community (approximately 60 %) remained uncharacterised. The Alpha and Gamma-Proteobacteria probes did not hybridise with all the cells in these groups as demonstrated by the higher hybridisation percentages observed with probes targeting only certain groups within the Alpha and Gamma-Proteobacteria clades. The probes were replaced with new probes, however lower values were still obtained. It could be that the more specific probes, such as the SAR 11 probes hybridised with

additional cells outside of the Alpha-Proteobacteria clade. However, as the results were consistent between two different SAR 11 probes it is more likely that the Alpha-Proteobacteria probe failed to hybridise to all the cells in this clade. This could be either due to either too high stringency of hybridisation conditions or failure to target all the Alpha-Proteobacteria, although the probe is complimentary to the majority of known Alpha-Proteobacterial 16S rRNA sequences found in databases. Therefore the values obtained from the Alpha and Gamma-Proteobacteria probes were not included in the comparison between community composition for the flow sorted cell groups.

The separation of bacterioplankton into the three flow cytometrically defined groups; LNA, HNAI and HNAII was a useful tool to examine the community structure in the Atlantic Ocean. There was little overlap of different bacterial clades between the different flow sorted groups thus indicating the validity of using side scatter and nucleic acid content for defining distinct phylogenetic groups. SAR11 dominance of the LNA group has been reported previously (Mary et al., 2006) and the low nucleic acid content of these cells measured by SYBR Green I fluorescence indicates their small genome size (Giovannoni et al., 2005).

Both HNA sorted cells groups contained cells from the *Cytophaga-Flavobacterium-Bacteroides* in similar proportions. From the flow cytometry dotplots, there was generally a good separation between the HNAI and HNAII groups and so the occurrence of these bacteria in both sorted groups may be due to different species within this clade. Another explanation is that the *Cytophaga-Flavobacterium-Bacteroides* are actively dividing and the cells in the HNAII group are the larger cells prior to cell division after which they would be smaller and located within the HNAI group. *Roseobacter* sp. and *Prochlorococcus* sp. cells were only found in the HNAII sorted cell group, indicating relatively large cell sizes.

The uncharacterised sorted and unsorted bacterioplankton cells in this study may have been dormant or less active cells with low amounts of rRNA. The probes chosen for this study were based on clone libraries carried out previously on AMT-6 samples and samples from the Arabian Sea in conjunction with other published studies of oceanic bacterioplankton community composition. If more time was available, further clone libraries could be constructed from various stations along the transect and more probes specific to these samples designed. In particular it would be useful to optimise probe design and hybridisation of *Prochlorococcus* sp. to gain a better correlation of abundance with flow cytometric counting.

Chapter 7

General Discussion

Bacterioplankton play an important role in the recycling of organic nutrients in the upper ocean via the microbial loop. The activity and composition of bacterioplankton in the Atlantic Ocean was studied within three main objectives as follows:

1. To determine the microbial community composition and how this varies both vertically in the water column and latitudinally along each transect.
2. To examine the flow of carbon through the microbial loop.
3. To determine the metabolic activities of dominant bacterial groups in order to assess the influence of microbial community composition on biogeochemical cycles.

Flow cytometric analysis of the bacterioplankton along seven transects of the Atlantic Ocean and in the Scotia Sea enabled the identification of distinct provinces with characteristic abundances and biomass of bacterioplankton groups. The photic zone of the oligotrophic northern and southern gyres had a high abundance of *Prochlorococcus* and the lowest abundances of heterotrophic bacteria in the Atlantic Ocean. The equatorial region was characterised by similarly high surface abundances of *Prochlorococcus* but also much higher concentrations of *Synechococcus* and heterotrophic bacteria. The northern and southern temperate regions of the Atlantic Ocean typically contained the highest abundance of *Synechococcus*, relatively high concentrations of heterotrophic bacteria and little or no *Prochlorococcus*.

The location of some stations sampled in the Scotia Sea were relatively close to the southern temperate region sampled on the AMT cruises, however the bacterioplankton community was distinctly different. The autotrophic microbial community was dominated by larger eukaryotic picoplankton with very few *Synechococcus* and the concentration of heterotrophic bacteria in the offshore region was almost half of that in the southern temperate region of the Atlantic Ocean.

There was little overall inter-annual variability in bacterioplankton abundances and biomass in the oligotrophic gyres and the equatorial region of the Atlantic Ocean indicating the stability of these large-scale biomes.

The relationship between bacterial production and primary production was used to quantify and compare the importance of the microbial loop in different provinces of the Atlantic Ocean. Bacterial production was highest in the more nutrient rich waters of the temperate, equatorial and North-West African upwelling regions and lowest in the oligotrophic northern and southern gyres, however this was not a function of heterotrophic bacterial abundance. It was hypothesised that the role of the microbial loop in recycling nutrients would be greater in the oligotrophic gyres due to a lower rate of primary production. This was true for the northern Atlantic gyre although not the case in the southern Atlantic gyre. It may be that a larger proportion of the heterotrophic bacterioplankton were dormant or less active in the southern gyre compared to the northern gyre.

Under objective three of this study, the metabolic activities of defined bacterioplankton groups and the effect of community composition were quantified using a combination of flow cytometric sorting and radiotracer uptake or CARD-FISH.

One major outcome of this project is the quantification and linking of bacterioplankton metabolic activity with community composition. It would be expected that the small genome and cell size (Giovannoni et al., 2005) of the SAR11 clade of bacterioplankton would result in a reduced requirement for DOM compared to the larger bacterioplankton such as *Roseobacter* sp. It has been shown that the LNA group of flow sorted cells are almost entirely comprised of SAR11 bacteria which has made it possible to quantify the rate of DOM cycling in this dominant group of bacterioplankton. Previous research has indicated that SAR11 are responsible for up to 50 % of total amino acid turnover (Malmstrom et al., 2004). Unlike the previous estimations of SAR11 activity, this project has enabled more precise estimates of amino acid turnover rates for this group and shows that they are as active as an average bacterioplankton cell and are responsible for between 30 and 50 % of the total methionine turnover.

Difficulty in characterising the community composition of the remaining fraction of the bacterioplankton using CARD-FISH may reflect a large proportion of the HNA cell group containing dormant or less active cells with low numbers of ribosomes. Over most of the Atlantic Ocean, the majority of methionine uptake was due to cells from the HNA group, however, it is likely that only a few cells in this sorted group were actively cycling methionine and that many of the sorted cells were dormant or had low metabolic rates . Due to the usually larger cells size and higher DNA content of

these cells compared to the LNA group, it is expected that these cells would have a greater requirement for methionine and other amino acids. The oligotrophic conditions over much of the Atlantic Ocean may inhibit the activity of many of these larger cells, thus reducing their ribosomal content.

Bacterioplankton abundances and biomass have been characterised for the major Atlantic Ocean regions. In addition the role of the microbial loop has been found to be more significant in the northern oligotrophic gyre compared to the other Atlantic Ocean provinces examined. An important role for SAR11 bacteria in the oceanic cycling of amino acids has been demonstrated and this clade has been shown to be proportionally as important in oligotrophic as well as more mesotrophic environments. This provides valuable insight into ecosystem functioning in these regions and when combined with studies of grazing rates and export rates from the photic layer helps to further understand biogeochemical cycles in the ocean.

Appendix A: Amino acid uptake rates in 50 % diluted cultures from surface water taken from the UP (i), NAG (ii) and SAG (iii).

i.

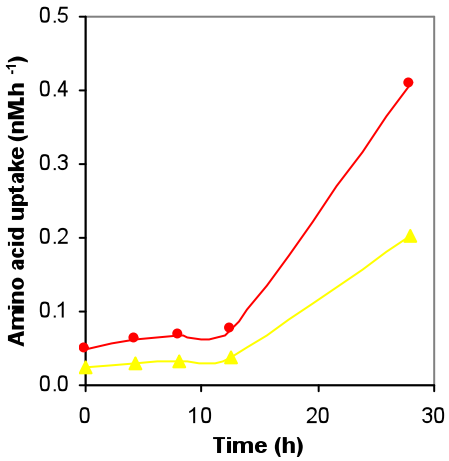

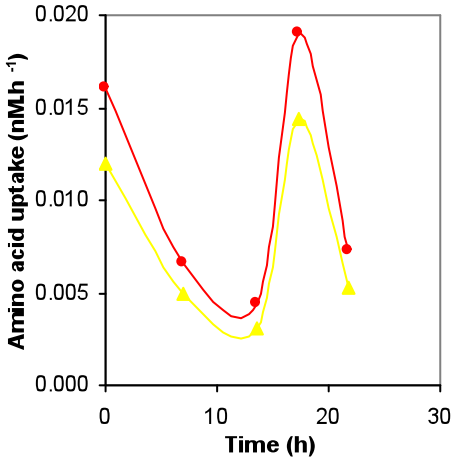

iii.

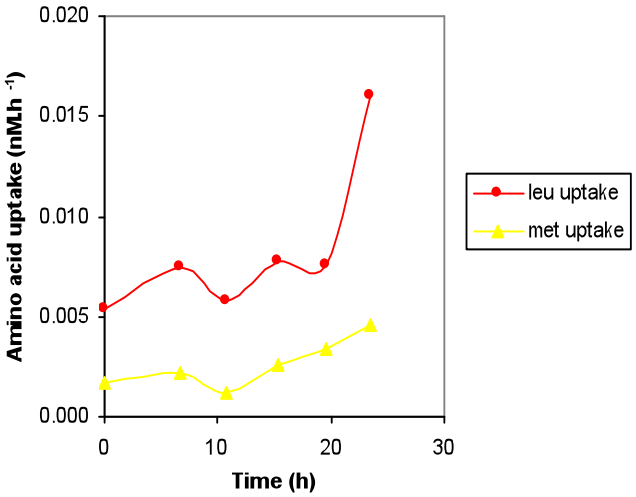

Appendix B: Biomass-normalised bacterial production (BP) at different depths along the AMT-15 transect.

a. Surface (n = 15)

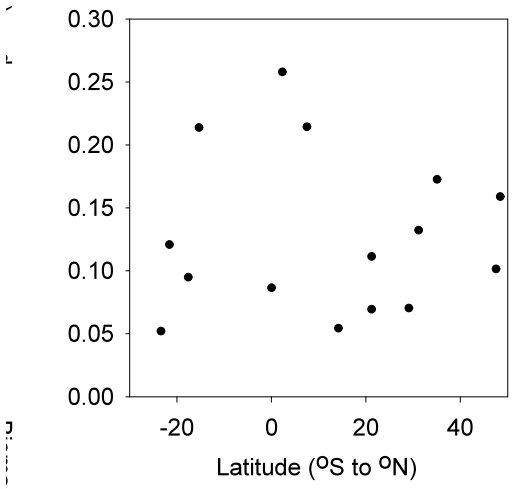

b. F_{max} (n = 15)

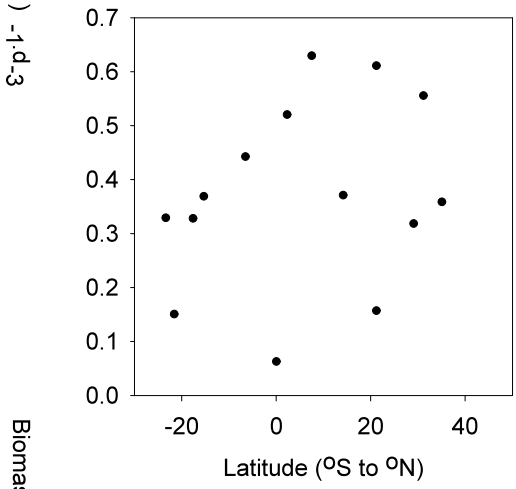

c. 0.1 % Light level (n = 11)

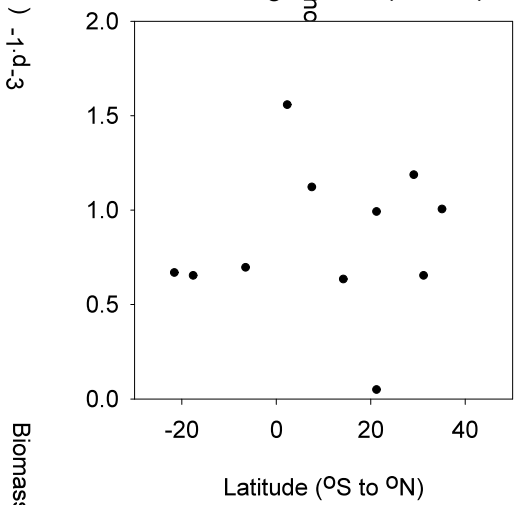

Appendix C: Bacterial production as a percentage of Primary production (BP/PP) as calculated using methionine uptake on AMT-14 (a) and AMT-15 (b) and calculated using leucine uptake on AMT-15 (c). Note the different scale used for AMT-14.

a.

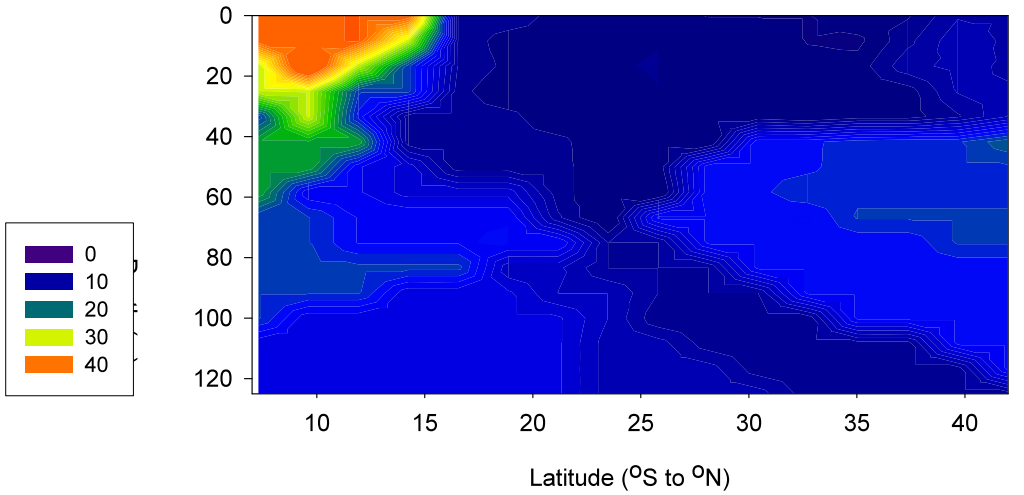

b.

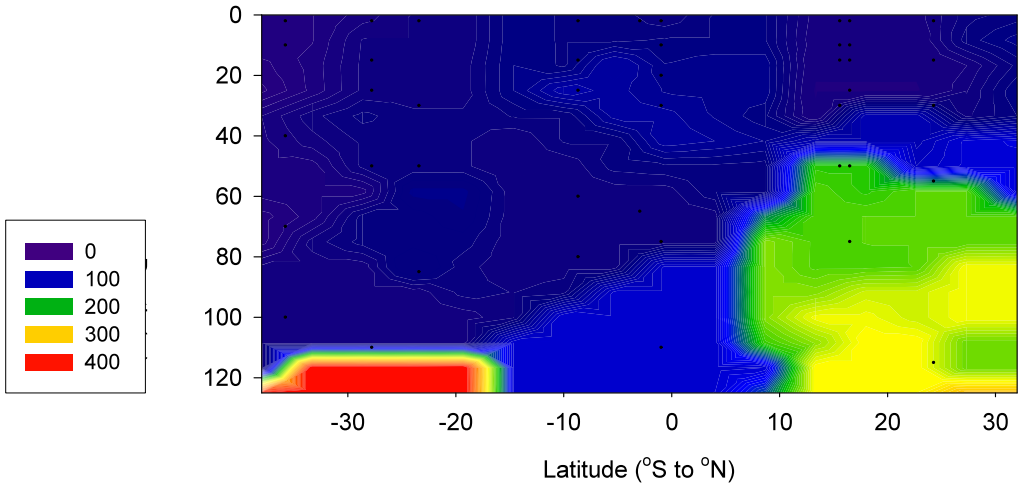

c.

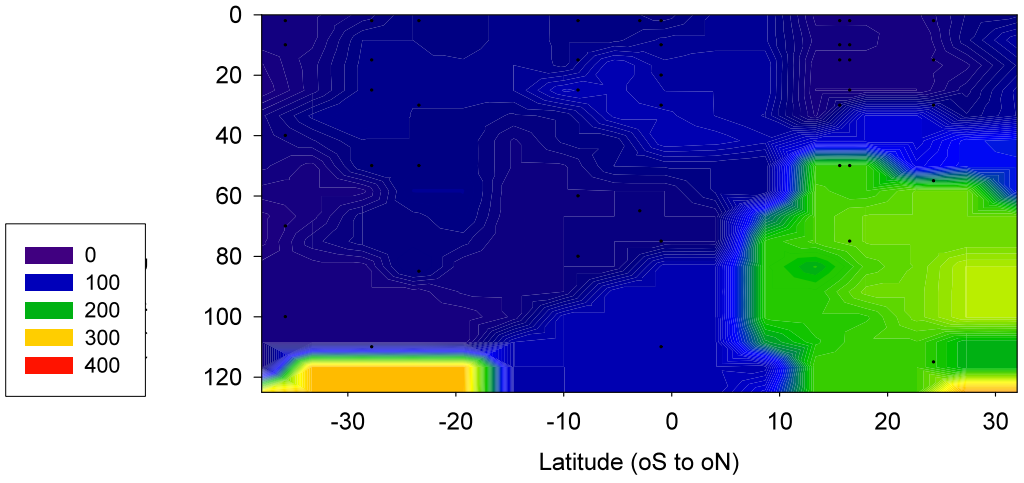

References

Acinas, S. G., Rodriguez-Valera, F. and Pedros-Alio, C. (1997). Spatial and temporal variation in marine bacterioplankton diversity as shown by RFLP fingerprinting of PCR amplified 16S rDNA. *FEMS Microbiology Ecology* **24,** 27-40.

Ahlgren, N. A., Rocap, G., and Chisholm, S. W. (2006). Measurement of *Prochlorococcus* ecotypes using real-time polymerase chain reaction reveals different abundances of genotypes with similar light physiologies. *Environmental Microbiology* **8,** 441-454.

Alonso, C., and Pernthaler, J. (2005). Incorporation of glucose under anoxic conditions by bacterioplankton from coastal North Sea surface waters. *Applied and Environmental Microbiology* **71,** 1709-1716.

Alonso, C., and Pernthaler, J. (2006). Concentration-dependent patterns of Leucine incorporation by coastal picoplankton. *Applied and Environmental Microbiology* **72,** 2141-2147.

Amann, R. I., Krumholz, L., and Stahl, D. A. (1990). Fluorescent-oligonucleotide probing of whole cells for determinative, phylogenetic, and environmental studies in microbiology. *Journal of Bacteriology* **172,** 762-770.

Amann, R. I., Ludwig, W., Schleifer, K.-H. (1995). Phylogenetic identification and in situ detection of individual microbial cells without cultivation. *Microbiological reviews* **59,** 143-169.

Ammerman, J. W. (1993). Microbial cycling of inorganic and organic phosphorus in the water column. *In* "Handbook of methods in microbial ecology" (P. F. Kemp, B. F. Sherr, E. B. Sherr, and J. J. Cole, Eds.), pp. 649-659. Lewis Publishers.

Andrade, L., Gonzalez, J. M., Paranhos, V., and Paranhos, R. (2004). Bacterial abundance and production in the southwest Atlantic Ocean. *Hydrobiologia* **511,** 103-111.

Arrigo, K. R. (2005). Marine microorganisms and global nutrient cycles. *Nature* **437,** 349-355.

Auman, A. J., Speake, C. C. and Lidstrom, M. E. (2001). *nifH* sequences and nitrogen fixation in Type I and Type II methanotrophs. *Applied and Environmental Microbiology* **67,** 4009-4016.

Azam, F. (1998). Microbial control of oceanic carbon flux: the plot thickens. *Science* **280,** 694-695.

Azam, F., Fenchel, T., Field, J. G., Gray, J. S., Meyer-Reil, L. A., and Thingstad, F. (1983). The ecological role of water-column microbes in the sea. *Marine Ecology Progress Series* **10,** 257-263.

Azam, F., and Worden, A. Z. (2004). OCEANOGRAPHY: microbes, molecules, and marine ecosystems. *Science* **303,** 1622-1624.

Barbeau, K., Rue, E. L., Bruland, K. W., and Butler, A. (2001). Photochemical cycling of iron in the surface ocean mediated by microbial iron(iii)-binding ligands. *Nature* **413,** 409-413.

Bates, T. S. (1994). The cycling of sulfur in surface seawater of the northeast Pacific. **99,** 7835-7843.

Behrenfeld, M. J., O'Malley, R. T., Siegel, D. A., McClain, C. R., Sarmiento, J. L., Feldman, G. C., Milligan, A. J., Falkowski, P. G., Letelier, R. M., and Boss, E. S. (2006). Climate-driven trends in contemporary ocean productivity. *Nature* **444,** 752-755.

Beja, O., Spudich, E. N., Spudich, A. L., Leclerc, M. and DeLong, E. F. (2001). Proteorhodopsin phototrophy in the ocean. *Nature* **411,** 786-789.

Bell, W. H., and Sakshaug, E. (1980). Bacterial utilization of algal extracellular products. A kinetic study of natural populations. *Limnology and Oceanography.* **25,** 1021-1033.

Beman, M. J., Arrigo, K. R., and Matson, P. A. (2005). Agricultural runoff fuels large phytoplankton blooms in vulnerable areas of the ocean. *Nature* **434,** 211-214.

Bjornsen, P. K. and Kuparinen, J. (1991). Determination of bacterioplankton biomass, net production and growth efficiency in the Southern Ocean. *Marine Ecology Progress Series* **71,** 185-194.

Brandon, M. A., Naganobu, M., Demer, D. A., Chernyshkov, P., Trathan, P. N., Thorpe, S. E., Kameda, T., Berezhinskiy, O. A., Hawker, E. J., and Grant, S. (2004). Physical oceanography in the Scotia Sea during the CCAMLR 2000 survey, austral summer 2000. *Deep Sea Research Part II: Topical Studies in Oceanography* **51,** 1301-1321.

Brewer, P. G., and Riley, J. P. (1965). The automatic determination of nitrate in seawater. *Deep-Sea Research* **12,** 765-772.

Buck, K. R., Chavez, F. P. and Campbell, L. (1996). Basin-wide distributions of living carbon components and the inverted trophic pyramid of the central gyre of the North Atlantic Ocean, summer 1993. *Aquatic Microbial Ecology* **10,** 283-298.

Button, D. K., and Robertson, B. R. (2001). Determination of DNA content of aquatic bacteria by flow cytometry. *Applied and Environmental Microbiology* **67,** 1636-1645.

Campbell, L. and Vaulot, D. (1993). Photosynthetic picoplankton community structure in the subtropical North Pacific Ocean near Hawaii (station ALOHA). *Deep Sea Research I* **40,** 2043-2060.

Capone, D. G., Zehr, J. P., Paerl, H., Bergman, B., and Carpenter, E. J. (1997). Trichodesmium, a globally significant marine Cyanobacterium. *Science* **276,** 1221-1229.

Carlson, C. A., Ducklow, H. W., and Sleeter, T. D. (1996). Stocks and dynamics of bacterioplankton in the northwestern Sargasso Sea. *Deep-Sea Research II* **43,** 491-516.

Carrero-Colon, M., Nakatsu, C. H., and Konopka, A. (2006). Effect of nutrient periodicity on microbial community dynamics. *Applied and Environmental Microbiology* **72,** 3175-3183.

Cavender-Bares, K. K., Karl, D. M. and Chisholm, S. W. (2001). Nutrient gradients in the western North Atlantic Ocean: relationship to microbial community structure and comparisons to patterns in the Pacific Ocean. *Deep Sea Research I* **48,** 2373-2395.

Cherrier, J., and Bauer, J. E. (2004). Bacterial utilization of transient plankton-derived dissolved organic carbon and nitrogen inputs in surface ocean waters. *Aquatic Microbiology Ecology* **35,** 229-241.

Chisholm, S.W. (2000). Stirring times in the Southern Ocean. *Nature* **407,** 685-687.

Chisholm, S. W., Olson, R. J., Zettler, E. R., Goericke, R., Waterbury, J. and Welschmeyer, N. (1988). A novel free-living prochlorophyte abundant in the oceanic euphotic zone. *Nature* **334,** 340-343.

Choi, J. W., Sherr, E. B. and Sherr, B. F. (1996). Relation between presence-absence of a visible nucleoid and metabolic activity in bacterioplankton cells. *Limnology and Oceanography* **41,** 1161-1168.

Christian, J. R., and Karl, D. M. (1994). Microbial community structure at the U.S.-Joint Global Ocean Flux study station ALOHA: Inverse methods for estimating biochemical indicator ratios. *Journal of Geophysical Research* **99,** 14269-14276.

Clarke, K. R., Warwick, R. M. (2001). Change in marine communities: an approach to. statistical analysis and interpretation. PRIMER-E, Plymouth, U.K. 38pp.

Coffin, R. B., Connolly, J. P., and Harris, P. S. (1993). Availability of dissolved organic carbon to bacterioplankton examined by oxygen utilisation. *Marine Ecology Progress Series* **101,** 9-22.

Cole, J. J., Pace, M. L., and S, F. (1988). Bacterial production in fresh and saltwater ecosystems: a cross-system overview. *Marine Ecology Progress Series* **43,** 1-10.

Coleman, M. L., Sullivan, M. B., Martiny, A. C., Steglich, C., Barry, K., DeLong, E. F., and Chisholm, S. W. (2006). Genomic islands and the ecology and evolution of *Prochlorococcus*. *Science* **311,** 1768-1770.

Curtis, T. P., Sloan, W. T. and Scannell, J. W. (2002). Estimating prokaryotic diversity and its limits. *Proceedings of the National Academy of Sciences* **99,** 10494-10499.

Dandonneau, Y., Deschamps, P.-Y., Nicolas, J.-M., Loisel, H., Blanchot, J., Montel, Y., Thieuleux, F., and Becu, G. (2004). Seasonal and interannual variability of ocean color and composition of phytoplankton communities in the North Atlantic, equatorial Pacific and South Pacific. *Deep Sea Research Part II: Topical Studies in Oceanography* **51,** 303-318.

Del Giorgio, P. A., Cole, J. J., and Cimbleris, A. (1997). Respiration rates in bacteria exceed plankton production in unproductive aquatic systems. *Nature* **385,** 148-151.

Del Giorgio, P. A., and Duarte, C. M. (2002). Respiration in the open ocean. *Nature* **420,** 379-384.

DeLong, E. F. (1992). Archaea in coastal marine environments. *Proceedings of the National Academy of Sciences* **89,** 5685-5689.

Duarte, C. M. and Vaque, D. (1992). Scale dependence of bacterioplankton patchiness. *Marine Ecology Progress Series* **84,** 95-100.

Duarte, C. M., and Agusti, S. (1998). The CO_2 balance of unproductive aquatic systems. *Science* **281,** 234-236.

Ducklow, H. W., Kirchman, D. L., Quinby, H. L., Carlson, C. A. and Dam, H. G. (1993). Stocks and dynamics of bacterioplankton carbon during the spring phytoplankton bloom in the eastern North Atlantic Ocean. *Deep-Sea Research II* **40,** 245-263.

Ducklow, H. W. (1999). The bacterial component of the oceanic euphotic zone. *FEMS Microbiology Ecology* **30,** 1-10.

Ducklow, H. W. (2000). Bacterial production and biomass in the oceans. *In* "Microbial ecology of the oceans" (D. L. Kirchman, Ed.), pp. 85-120. John Wiley and Sons, New York.

Ducklow, H. W. (2003). Biogeochemical Provinces: Towards a JGOFS Synthesis. Pp. 3-18 In: M. J. R. Fasham, Ed., Ocean Biogeochemistry: A New Paradigm. New York. Springer-Verlag.

Dufresne, A., Salanoubat, M., Partensky, F., Artiguenave, F., Axmann, I. M., Barbe, V., Duprat, S., Galperin, M. Y., Koonin, E. V., Le Gall, F., Makarova, K. S., Ostrowski, M., Oztas, S., Robert, C., Rogozin, I. B., Scanlan, D. J., Tandeau de Marsac, N., Weissenbach, J., Wincker, P., Wolf, Y. I., and Hess, W. R. (2003). Genome sequence of the cyanobacterium *Prochlorococcus marinus* SS120, a nearly minimal oxyphototrophic genome. *Proceedings of the National Academy of Sciences* **100,** 10020-10025.

DuRand, M. D., Olson, R. J., and Chisholm, S. W. (2001). Phytoplankton population dynamics at the Bermuda Atlantic Time-series station in the Sargasso Sea. *Deep-Sea Research II* **48,** 1983-2003.

Edwards, K. J., Bond, P. L., Gihring, T. M., and Banfield, J. F. (2000). An Archaeal iron-oxidizing extreme acidophile important in acid mine drainage. *Science* **287,** 1796-1799.

Eilers, H., Pernthaler, J., Peplies, J., Glockner, F. O., Gerdts, G., and Amann, R. (2001). Isolation of novel pelagic bacteria from the German Bight and their seasonal contributions to surface picoplankton. *Applied and Environmental Microbiology* **67,** 5134-5142.

Elifantz, H., Malmstrom, R. R., Cottrell, M. T., and Kirchman, D. L. (2005). Assimilation of polysaccharides and glucose by major Bacterial groups in the Delaware estuary. *Applied and Environmental Microbiology* **71,** 7799-7805.

Field, C. B., Behrenfeld, M. J., Randerson, J. T. and Falkowski, P. (1998). Primary production of the biosphere: integrating terrestrial and oceanic components. *Science* **281,** 237-240.

Fuhrman, J. A., and Azam, F. (1982). Thymidine incorporation as a measure of heterotrophic bacterioplankton production in marine surface waters. *Marine Biology* **66,** 109-120.

Fuhrman, J. A., McCallum, K., and Davis, A. A. (1992). Novel major archaebacterial group from marine plankton. *Nature* **356,** 148-149.

Gallagher, J. M., Carton, M. W., Eardly, D. F., Patching, J. W. (2004). Spatio-temporal variability and diversity of water column prokaryotic communities in the eastern North Atlantic. *FEMS Microbiology Ecology* **47,** 249-262.

Gasol, J. M., Doval, M. D., Pinhassi, J., Calderon-Paz, J. I., Guixa-Boixereu, N., Vaque, D., and Pedros-Alio, C. (1998). Diel variations in bacterial heterotrophic activity and growth in the north-western Mediterranean sea. *Marine Ecology Progress Series* **164,** 107-124.

Giovannoni, S., and Rappe, M. (2000). Evolution, diversity, and molecular ecology of marine prokaryotes. In: Microbial Ecology of the Oceans. Ed. Kirchman, D. L. Wiley-Liss, 47-84.

Giovannoni, S. J. and Sting, U. (2005). Molecular diversity and ecology of microbial plankton. *Nature* **437,** 343-348.

Giovannoni, S. J., Tripp, H. J., Givan, S., Podar, M., Vergin, K. L., Baptista, D., Bibbs, L., Eads, J., Richardson, T. H., Noordewier, M., Rappe, M. S., Short, J. M., Carrington, J. C., and Mathur, E. J. (2005). Genome streamlining in a cosmopolitan oceanic Bacterium. *Science* **309,** 1242-1245.

Glockner, F. O. (2003). Complete genome sequence of the marine planctomycete Pirellula sp. strain 1. *Proceedings of the National Academy of Sciences* **100,** 8298-8303.

Grasshoff, K. (1976). "Methods of seawater analysis." Weinheim, Verlag Chemie.

Hanson, R. S. and Hanson, T. E. (1996). Methanotrophic bacteria. *Microbiological Reviews* **60,** 439-471.

Haugland, R. P. (1992). "Handbook of fluorescent probes and research chemicals." Molecular Probes Inc., Eugene, Oregon,

Heywood, K. J., Naveira Garabato, A. C., and Stevens, D. P. (2002). High mixing rates in the abyssal Southern Ocean. *Nature* **415,** 1011-1014.

Hobbie, J. E., Daley, R. J. and Jasper, J. (1977). Use of Nuclepore filters for counting bacteria by fluorescence microscopy. *Applied and Environmental Microbiology* **33**, 1225-1228.

Honda, D., Yokota, A., and Sugiyama, J. (1999). Detection of seven major evolutionary lineages in cyanobacteria based on the 16S rRNA gene sequence analysis with new sequences of five marine *Synechococcus* strains. *Journal of Molecular Evolution* **48,** 723-739.

Hoppe, H.-G., Gocke, K., Koppe, R., and Begler, C. (2002). Bacterial growth and primary production along a north-south transect of the Atlantic Ocean. *Nature* **416,** 168-171.

Hutchinson, C. A. III, Smith, H. O., Pfannkoch, C., Venter, J. C. (2005). Cell-free cloning using φ29 DNA polymerase. *Proceedings of the National Academy of Sciences* **102,** 17332-17336.

Jannasch, H. W. and Jones, G. E. (1959). Bacterial populations in sea water as determined by different methods of ennumeration. *Limnology and Oceanography* **4,** 128-139.

Karl, D. (1997). The role of nitrogen fixation in biogeochemical cycling in the subtropical North Pacific Ocean. *Nature* **388,** 533-538.

Karl, D. M. (1999). A sea of change: biogeochemical variability in the North Pacific subtropical gyre. *Ecosystems* **2,** 181–214.

Karl, D. M., Bidigare, R. R., and Letelier, R. M. (2001). Long-term changes in plankton community structure and productivity in the North Pacific subtropical gyre: the domain shift hypothesis. *Deep-Sea Research II* **48,** 1449-1470.

Karl, D. M., and Lukas, R. (1996). The Hawaii Ocean Time-series (HOT) Program: Background, rationale and field implementation. *Deep-Sea Research II* **43,** 129-156.

Kiene, R. P., Linn, L. J., Gonzalez, J., Moran, M. A., and Bruton, J. A. (1999). Dimethylsulfoniopropionate and methanethiol are important precursors of methionine and protein-sulfur in marine bacterioplankton. *Applied and Environmental Microbiology* **65,** 4549-4558.

Kirchman, D., Ducklow, H., and Mitchell, R. (1982). Estimates of bacterial growth from changes in uptake rates and biomass. *Applied and Environmental Microbiology* **44,** 1296-1307.

Kirchman, D. L. (1993). Leucine incorporation as a measure of biomass production by heterotrophic bacteria. *In* "Handbook of methods in microbial ecology" (P. F. Kemp, B. F. Sherr, E. B. Sherr, and J. J. Cole, Eds.), pp. 509-512. Lewis Publishers.

Kirchman, D. L., and Ducklow, H. W. (1993). Estimating conversion factors for the thymidine and leucine methods for measuring bacterial production. *In* "Handbook of methods in microbial ecology" (P. F. Kemp, B. F. Sherr, E. B. Sherr, and J. J. Cole, Eds.), pp. 513-517. Lewis Publishers.

Kolber, Z. S., Plumley, F. G., Lang, A. S., Beatty, J. T., Blankenship, R. E., VanDover, C. L., Vetriani, C., Koblizek, M., Rathgeber, C. and Falkowski, P. G. (2001). Contribution of aerobic photoheterotrophic bacteria to the carbon cycle in the ocean. *Science* **292,** 2492-2495.

Konopka, A. (2000). Bacterioplankton community diversity in a series of thermally stratified lakes. *Microbial ecology* **38,** 321-329.

Korb, R. E., Whitehouse, M. J., Thorpe, S. E., and Gordon, M. (2005). Primary production across the Scotia Sea in relation to the physico-chemical environment. *Journal of Marine Systems* **57,** 231-249.

Kuypers, M. M. M., Sliekers, A. O., Lavik, G., Schmid, M., Barker Jorgensen, B., Kuenen, J. G., Sinninghe Damste, J. S., Strous, M. and Jetten, M. S. M. (2003). *Nature* **422,** 608-611.

Lalli, C. M., and Parsons, T. R. (1997). "Biological oceanography: an introduction." Butterworth-Heinemann Press.

LaRoche, J., and Breitbarth, E. (2005). Importance of the diazotrophs as a source of new nitrogen in the ocean. *Journal of Sea Research* **53,** 67-91.

Larsson, U., and Hagström, A. (1982). Fractionated phytoplankton primary production, exudate release and bacterial production in a Baltic eutrophication gradient. *Marine Biology* **67,** 57-70.

Lebaron, P., Servais, P., Agogue, H., Courties, C., and Joux, F. (2001). Does the high nucleic acid content of individual bacterial cells allow us to discriminate between active cells and inactive cells in aquatic systems? *Applied and Environmental Microbiology* **67,** 1775-1782.

Legendre, L., and Fevre, J. L. (1995). Microbial food webs and the export of biogenic carbon in oceans. *Aquatic Microbiology Ecology* **9,** 69-77.

Legendre, L., and Rassoulzadegan, F. (1996). Food-web mediated export of biogenic carbon in oceans: hydrodynamic control. *Marine Ecology Progress Series* **145,** 179-193.

Li, W. K. W. (1994). Primary production of prochlorophytes, cyanobacteria and eucaryotic ultraphytoplankton: measurements from flow cytometric sorting. *Limnology and Oceanography* **39,** 169-175.

Li, W. K. W. (1995). Composition of ultraphytoplankton in the Central North Atlantic. *Marine Ecology Progress Series* **122,** 1-8.

Li, W. K. W., and Harrison, W. G. (2001). Chlorophyll, bacteria and picophytoplankton in ecological provinces of the North Atlantic. *Deep-Sea Research II* **48,** 2271-2293.

Li, W. K. W., Jellett, J. F., and Dickie, P. M. (1995). DNA distributions in planktonic bacteria stained with TOTO or TO-PRO. *Limnology and Oceanography* **40**, 1485-1495.

Long, R. A. and Azam, F. (2001). Antagonistic interactions among marine pelagic bacteria. *Applied and Environmental Microbiology* **67,** 4975-4983.

Longhurst, A. R. (1995) Seasonal cycles of pelagic production and consumption. *Progress in Oceanography* **36,** 77-167.

Longnecker, K., Sherr, B. F., and Sherr, E. B. (2005). Activity and phylogenetic diversity of bacterial cells with high and low nucleic acid content and electron transport system activity in an upwelling system. *Applied and Environmental Microbiology* **71,** 7737-7749.

Longnecker, K., Sherr, B. F., and Sherr, E. B. (2006). Variation in cell-specific rates of leucine and thymidine incorporation by marine bacteria with high and low nucleic acid content off the Oregon coast *Aquatic Microbiology Ecology* **43,** 113-125.

Lopez-Amoros, R., Comas, J., Garcia, M. a. T., and Vives-Rego, J. (1998). Use of the 5-cyano-2,3-ditolyl tetrazolium chloride reduction test to assess respiring marine bacteria and grazing effects by flow cytometry during linear alkylbenzene sulfonate degradation. *FEMS Microbiology Ecology* **27,** 33-42.

Madigan, M. T., and Martinko, J. M. (2006). Biosynthesis of amino acids and nucleotides. *In* "Brock biology of microorganisms", pp. 131. Pearson Prentice Hall, Upper Saddle River, New Jersey.

Mahaffey, C., Williams, R. G., Wolff, G. A., and Anderson, W. T. (2004). Physical supply of nitrogen to phytoplankton in the Atlantic Ocean. *Global Biogeochemical Cycles* **18**.

Malmstrom, R. R., Cottrell, M. T., Elifantz, H., and Kirchman, D. L. (2005). Biomass production and assimilation of dissolved organic matter by SAR11 Bacteria in the Northwest Atlantic Ocean. *Applied and Environmental Microbiology* **71,** 2979-2986.

Malmstrom, R. R., Kiene, R. P., Cottrell, M. T., and Kirchman, D. L. (2004). Contribution of SAR11 Bacteria to dissolved dimethylsulfoniopropionate and amino acid uptake in the North Atlantic Ocean. *Applied and Environmental Microbiology* **70,** 4129-4135.

Maranon, E., Behrenfeld, M. J., Gonzalez, N., Mourino, B., and Zubkov, M. V. (2003). High variability of primary production in oligotrophic waters of the Atlantic Ocean: uncoupling from phytoplankton biomass and size structure. *Marine Ecology Progress Series* **257,** 1-11.

Maranon, E., Holligan, P. M., Barciela, R., Gonzalez, N., Mourino, B., Pazo, M. J., and Varela, M. (2001). Patterns of phytoplankton size structure and productivity in contrasting open-ocean environments. *Marine Ecology Progress Series* **216,** 43-56.

Maranon, E., Holligan, P. M., Varela, M., Mourino, B., and Bale, A. J. (2000). Basin-scale variability of phytoplankton biomass, production and growth in the Atlantic Ocean. *Deep Sea Research Part I: Oceanographic Research Papers* **47,** 825-857.

Marie, D., Partensky, F., Jacquet, S., and Vaulot, D. (1997). Enumeration and cell cycle analysis of natural populations of marine picoplankton by flow cytometry using the nucleic acid stain SYBR Green I. *Applied and Environmental Microbiology* **63,** 186-193.

Mary, I., Heywood, J. L., Fuchs, B., Amann, R., Tarran, G. A., Burkill, P. H., and Zubkov, M. V. (2006). SAR11 dominance among metabolically active low

nucleic acid bacterioplankton in surface waters along an Atlantic meridional transect. *Aquatic Microbiology Ecology* **45,** 107-113.

Massana, R., Murray, A. E., Preston, C. M., and DeLong, E. F. (1997). Vertical distribution and phylogenetic characterization of marine planktonic *Archaea* in the Santa Barbara Channel. *Applied and Environmental Microbiology* **63,** 50-56.

McClain, C. R., Feldman, G. C., and Hooker, S. B. (2004). An overview of the SeaWiFS project and strategies for producing a climate research quality global ocean bio-optical time series. *Deep Sea Research Part II: Topical Studies in Oceanography* **51,** 5-42.

McGillicuddy, D. J., Jr., Robinson, A. R., Siegel, D. A., Jannasch, H. W., Johnson, R., Dickey, T. D., McNeil, J., Michaels, A. F., Knap, A. H., Mcgillicuddy, D., and Jannasch, H. e. a. (1998). Influence of mesoscale eddies on new production in the Sargasso Sea. *Nature* **394,** 263-266.

McGowan, J. A., and Hayward, T. L. (1978). Mixing and oceanic productivity. *Deep-Sea Research* **25,** 771-793.

Michaels, A. F. (1994). Seasonal patterns of ocean biochemistry at the U. S. JGOFS Bermuda Atlantic Time Series study site. *Deep-Sea Research* **41,** 1013-1038.

Michaels, A. F. (1996). Inputs, losses and transformations of nitrogen and phosphorus in the pelagic North Atlantic Ocean. *Biogeochemistry* **35,** 181-226.

Mitchell, G. J. and Fuhrman, J. A. (1989). Centimeter scale vertical heterogeneity in bacteria and chlorophyll a. *Marine Ecology Progress Series* **54,**141-148.

Mojzsis, S. J., Arrhenius, G., McKeegan, K. D., Harrison, T. M., Nutman, A. P., and Friend, C. R. L. (1996). Evidence for life on Earth before 3,800 million years ago. *Nature* **384,** 55-59.

Moore, L. R., and Chisholm, S. W. (1999). Photophysiology of the marine cyanobacterium Prochlorococcus: Ecotypic differences among cultured isolates. *Limnology and Oceanography* **44,** 628-638.

Moore, L. R., Goericke, R., and Chisholm, S. W. (1995). Comparative physiology of Synechococcus and Prochlorococcus: Influence of light and temperature on growth, pigments, fluorescence and absorptive properties. *Marine Ecology Progress Series* **116,** 259-275.

Moore, L. R., Rocap, G., and Chisholm, S. W. (1998). Physiology and molecular phylogeny of coexisting Prochlorococcus ecotypes. *Nature* **393,** 464-467.

Morris, R. M., Rappe, M. S., Connon, S. A., Vergin, K. L., Siebold, W. A., Carlson, C. A., and Giovannoni, S. J. (2002). SAR11 clade dominates ocean surface bacterioplankton communities. *Nature* **420,** 806-810.

Neveux, J., Lanfoine, F., Vaulot, D., Marie, D. and Blanchot, J. (1999). Phycoerythrins in the southern tropical and equatorial Pacific Ocean: evidence for new cyanobacterial types. *Journal of Geophysical Research* **104,** 3311–3321.

Niiler. (2001). The global flow field. *In* "ocean circulation and climate" (G. Siedler, J. Church, and J. Gould, Eds.). Elsevier.

Olsen, Y., Jensen, A., Reinertsen, H., Borsheim, K. Y., Heldal, M. and Langeland, A. (1986). Dependence of the rate of release of phosphorus by zooplankton on the P:C ratio in the food supply, as calculated by a recycling model. *Limnology and Oceanography* **31,** 34-44.

Olson, R. J., Chisholm, S. W., Zettler, E. R., Altabet, M. A., and Dusenberry, J. A. (1990). Spatial and temporal distributions of prochlorophyte picoplankton in the North Atlantic Ocean. *Deep Sea Research* **37,** 1033-1051.

Olson, R. J., Zettler, E. R., and DuRand, M. D. (1993). Phytoplankton analysis using flow cytometry. *In* "Handbook of methods in aquatic microbial ecology" (P. F. Kemp, B. F. Sherr, E. B. Sherr, and J. J. Cole, Eds.), pp. 777. Lewis.

Orsi, A. H., Nowlin Jr, W. D., and Whitworth III, T. (1995). On the meridional extent and fronts of the Antarctic Circumpolar Current. *Deep Sea Research I: Oceanographic Research Papers* **42,** 641-673.

Oschlies, A., and Garcon, V. (1998). Eddy-induced enhancement of primary production in a model of the North Atlantic Ocean. *Nature* **394,** 266-269.

Ouverney, C. C., and Fuhrman, J. A. (1999). Combined microautoradiography-16S rRNA probe technique for determination of radioisotope uptake by specific microbial cell types in situ. *Applied and Environmental Microbiology* **65,** 1746-1752.

Palter, J. B., Lozier, M. S., and Barber, R. T. (2005). The effect of advection on the nutrient reservoir in the North Atlantic subtropical gyre. *Nature* **437,** 687-692.

Partensky, F., Blanchot, J., Lantoine, F., Neveux, J., and Marie, D. (1996). Vertical structure of picophytoplankton at different trophic sites of the tropical northeastern Atlantic Ocean. *Deep-Sea Research I* **43,** 1191-1213.

Pedros-Alio, C., Vaque, D., Guixa-Boixereu, N., and Gasol, J. M. (2002). Prokaryotic plankton biomass and heterotrophic production in western Antarctic waters during the 1995-1996 Austral summer. *Deep-Sea Research II* **49,** 805-825.

Perez, V., Fernandez, E., Maranon, E., Serret, P., Varela, R., Bode, A., Varela, M., Varela, M. M., Moran, X. A. G., and Woodward, E. M. S. (2005). Latitudinal distribution of microbial plankton abundance, production, and respiration in the Equatorial Atlantic in autumn 2000. *Deep Sea Research Part I: Oceanographic Research Papers* **52,** 861-880.

Pernthaler, A., Pernthaler, J., Schattenhofer, M. and Amann, R. (2002a). Identification of DNA-synthesising bacterial cells in coastal North Sea plankton. *Applied and Environmental Microbiology* **68,** 5728-5736.

Pernthaler, A., Pernthaler, J., and Amann, R. (2002b). Fluorescence in situ hybridization and catalyzed reporter deposition for the identification of marine bacteria. *Applied and Environmental Microbiology* **68,** 3094-3101.

Pernthaler, A., Pernthaler, J., Eilers, H., and Amann, R. (2001). Growth patterns of two marine Isolates: adaptations to substrate patchiness? *Applied and Environmental Microbiology* **67,** 4077-4083.

Pomroy, A., and Joint, I. (1999). Bacterioplankton activity in the surface waters of the Arabian Sea during and after the 1994 SW monsoon. *Deep-Sea Research II* **46,** 767-794.

Pomeroy, L. R. (1974). The ocean's food web, a changing paradigm. *Bioscience* **24,** 499-504.

Poulton, A.J., Holligan, P.M., Hickman, A., Kim, Y.-N., Adey, T.R., Stinchcombe, M.C., Holeton, C., Root, S., Woodward, E.M.S. (2006). Phytoplankton carbon fixation, chlorophyll-biomass and diagnostic pigments in the Atlantic Ocean. *Deep-Sea Research II* **53,** 1593-1610.

Rappe, M. S., Vergin, K. and Giovannoni, S. J. (2000). Phylogenetic comparisons of a coastal bacterioplankton community with its counterparts in open ocean and freshwater systems. *FEMS Microbiology Ecology* **33,** 219-232.

Richardson, T. L., and Jackson, G. A. (2007). Small Phytoplankton and Carbon Export from the Surface Ocean. *Science* **315,** 838-840.

Riebesell, U., Zondervan, I., Rost, B., Tortell, P. D., Zeebe, R. E., and Morel, F. M. M. (2000). Reduced calcification of marine plankton in response to increased atmospheric CO2. *Nature* **407,** 364-367.

Rintoul, S., Hughes, C., and Olbers, D. (2001). The Antarctic Circumpolar Current system. *In* "Ocean circulation and climate" (G. Siedler, J. Church, and J. Gould, Eds.), pp. 271-302. Academic Press, London.

Robinson, C., Poulton, A. J., Holligan, P. M., Baker, A. R., Forster, G., Gist, N., Jickells, T. D., Mailin, G., Upstill-Goddard, R., Williams, R. G., Woodward, E. M. S., and Zubkov, M. V. (2006). The Atlantic Meridional Transect (AMT)

Programme: A contextual view 1995-2005. *Deep Sea Research Part II: Topical Studies in Oceanography* **53,** 1485-1515.

San Martin, E., Irigoien, X., Harris, R. P., Lopez-Urrutia, A., Zubkov, M. V. and Heywood, J. L. (2006). Variation in the transfer of energy in marine plankton along a productivity gradient in the Atlantic Ocean. *Limnology and Oceanography* **51,** 2084-2091.

Sarthou, G., Baker, A. R., Kramer, J., Laan, P., Laes, A., Ussher, S., Achterberg, E. P., de Baar, H. J. W., Timmermans, K. R., and Blain, S. (2007). Influence of atmospheric inputs on the iron distribution in the sub-tropical North-East Atlantic Ocean. *Marine Chemistry* **104,** 186-202.

Schonhuber, W., Zarda, B., Eix, S., Rippka, R., Herdman, M., Ludwig, W., and Amann, R. (1999). In Situ Identification of Cyanobacteria with Horseradish Peroxidase-Labeled, rRNA-Targeted Oligonucleotide Probes. *Applied and Environmental Microbiology* **65,** 1259-1267.

Schut, F. (1993). Isolation of typical marine bacteria by dilution culture: growth, maintenance, and characteristics of isolates under laboratory conditions. *Applied and Environmental Microbiology* **59,** 2150-2160.

Servais, P., Casamayor, E. O., Courties, C., Catala, P., Parthuisot, N., and Lebaron, P. (2003). Activity and diversity of bacterial cells with high and low nucleic acid content. *Aquatic Microbial Ecology* **33,** 41-51.

Seymour, J. R., Mitchell J. G., Pearson L., and Waters R. L. (2000) Heterogeneity in bacterioplankton abundance from 4.5 millimetre resolution sampling. *Aquatic Microbial Ecology* **22,**143-153.

Shalapyonok, A., Olson, R. J., and Shalapyonok, L. S. (1998). Ultradian growth in *Prochlorococcus* spp. *Applied and Environmental Microbiology* **64,** 1066-1069.

Shalapyonok, A., Olson, R. J., and Shalapyonok, L. S. (2001). Arabian Sea phytoplankton during Southwest and Northeast monsoons 1995: composition, size structure and biomass from individual cell properties measured by flow cytometry. *Deep-Sea Research II* **48,** 1231-1261.

Sherry, N. D., and Wood, M. A. (2001). Phycoerythrin-containing picocyanobacteria in the Arabian Sea in February 1995: diel patterns, spatial variability, and growth rates. *Deep-Sea Research II* **48,** 1263-1283.

Sieracki, M. E., Cucci, T. L., and Nicinski, J. (1999). Flow Cytometric Analysis of 5-Cyano-2,3-Ditolyl Tetrazolium Chloride Activity of Marine Bacterioplankton in Dilution CultuResearch *Applied and Environmental Microbiology* **65,** 2409-2417.

Sintes, E., and Herndl, G. J. (2006). Quantifying substrate uptake of individual cells of marine bacterioplankton by MICRO-CARD-FISH. *Applied and Environmental Microbiology***,** 763-806.

Snaidr, J., Amann, R., Huber, I., Ludwig, W., and Schleifer, K.-H. (1997). Phylogenetic analysis and insitu identification of bacteria in activated sludge. *Applied and Environmental Microbiology* **63,** 2884-2896.

Staley, J. T. and Konopka, A. (1985). Measurement of in situ activities of nonphotosynthetic microorganisms in aquatic and terrestrial habitats. *Annual Reviews in Microbiology* **39,** 321-346.

Stepanauskas, R. and Sieracki, M. E. (2007). Matching phylogeny and metabolism in the uncultured marine bacteria, one cell at a time. *Proceedings of the National Academy of Sciences* **104,** 9052-9057.

Tarran, G. A., Heywood, J. L., and Zubkov, M. V. (2006). Latitudinal changes in the standing stocks of nano- and picoeukaryotic phytoplankton in the Atlantic Ocean. *Deep-Sea Research II* **53,** 1516-1529.

Thomas, D. N., and Dieckmann, G. S. (2002). Antarctic Sea Ice-a Habitat for Extremophiles. *Science* **295,** 641-644.

Thurman, E. M. (1985). "Organic geochemistry of natural waters." Kluwer Academic Publishers, Dordrecht, The Netherlands.

Tomczak, M., and Godfrey, S. J. (2003). The Atlantic Ocean. *In* "Regional Oceanography: an introduction", pp. 229-252. Daya publishing house, Delhi.

Topping, J.N., Heywood, J.L., Ward, P. and Zubkov, M.V. (2006) Bacterioplankton composition in the Scotia Sea, Antarctica, during the austral summer of 2003. *Aquatic Microbial Ecology* **45,** 229-235.

Tyndall, R. L., Hand, R. E., Jr., Mann, R. C., Evans, C., and Jernigan, R. (1985). Application of flow cytometry to detection and characterization of Legionella spp. *Applied and Environmental Microbiology* **49,** 852-857.

Unanue, M., Ayo, B., Agis, M., Slezak, D., Herndl, G. J., and Iriberri, J. (1999). Ectoenzymatic activity and uptake of monomers in marine bacterioplankton described by a biphasic kinetic model. *Microbial ecology* **37,** 36-48.

Vaque, D., Guixa-Boixereu, N., Gasol, J. M., and Pedros-Alio, C. (2002). Distribution of microbial biomass and importance of protists in regulating prokaryotic assemblages in three areas close to the Antarctic Peninsula in spring and summer 1995/96. *Deep-Sea Research II* **49,** 847-867.

Vaulot, D., and Marie, D. (1999). Diel variability of photosynthetic picoplankton in the equatorial Pacific. *Journal of Geophysical Research* **104,** 3297-3310.

Vaulot, D., Marie, D., Olson, R. J. and Chisholm, S. W. (1995). Growth of *Prochlorococcus*, a photosynthetic prokaryote, in the equatorial Pacific Ocean. *Science* **268,** 1480-1482.

Veldhuis, M. J. W., Cucci, T. L. and Sieracki, M. E. (1997). Cellular DNA content of marine phytoplankton using two new fluorochromes: taxonomic and ecological implications. *Journal of Phycology* **33,** 527-541.

Veldhuis, M. J. W., and Kraay, G. W. (2004). Phytoplankton in the subtropical Atlantic Ocean: towards a better assessment of biomass and composition. *Deep-Sea Research I* **51,** 507-530.

Venter, J. C., Remington, K., Heidelberg, J. F., Halpern, A. L., Rusch, D., Eisen, J. A., Wu, D., Paulsen, I., Nelson, K. E., Nelson, W., Fouts, D. E., Levy, S., Knap, A. H., Lomas, M. W., Nealson, K., White, O., Peterson, J., Hoffman, J., Parsons, R., Baden-Tillson, H., Pfannkoch, C., Rogers, Y.-H., and Smith, H. O. (2004). Environmental genome shotgun sequencing of the Sargasso Sea. *Science* **304,** 66-74.

Vila, M., Simo, R., Kiene, R. P., Pinhassi, J., Gonzalez, J. M., Moran, M. A., and Pedros-Alio, C. (2004). Use of microautoradiography combined with fluorescence in situ hybridization to determine dimethylsulfoniopropionate incorporation by marine bacterioplankton taxa. *Applied and Environmental Microbiology* **70,** 4648-4657.

Wallner, G., Amann, R., and Beisker, W. (1993). Optimizing fluorescent in situ hybridization of suspended cells with rRNA-targeted oligonucleotide probes for the flow cytometric identification of microorganisms. *Cytometry* **14,** 136-143.

Walter, J. M., Greenfield, D., Bustamante, C., and Liphardt, J. (2007). Light-powering Escherichia coli with proteorhodopsin. *Proceedings of the National Academy of Sciences* **104,** 2408-2412.

Ward, P., Whitehouse, M. J., Shreeve, R. S., Thorpe, S. E., Atkinson, A., Pond, D. W. and Cunningham, N. (2006). Plankton community structure and variability in the Scotia Sea: austral summer 2003. *Marine Ecology Progress Series* **309,** 75-91.

West, N. J., Schonhuber, W. A., Fuller, N. J., Amann, R. I., Rippka, R., Post, A. F., and Scanlan, D. J. (2001). Closely related *Prochlorococcus* genotypes show remarkably different depth distributions in two oceanic regions as revealed by

in situ hybridisation using 16S rRNA-targetted oligonucleotides. *Microbiology* **147,** 1731-1744.

Whitman, W. B., Coleman, D. C., and Wiebe, W. J. (1998). Prokaryotes: The unseen majority. *Proceedings of the National Academy of Sciences* **95,** 6578-6583.

Williams, P. J. I. (1981). Microbial contribution to overall marine plankton metabolism: direct measurements of respiration. *Oceanolog. Acta* **4,** 359-364.

Williams, P. J. I. (1998). The balance of plankton respiration and photosynthesis in the open ocean. *Nature* **394,** 55-57.

Williams, R. G., Roussenov, V., and Follows, M. J. (2006). Nutrient streams and their induction into the mixed layer. *Global Biogeochemical Cycles* **20,** GB1016.

Woese, C. R., Kandler, O., and Wheelis, M. L. (1990). Towards a natural system of organisms: proposal for the Domains Archaea, Bacteria, and Eucarya. *Proceedings of the National Academy of Sciences* **87,** 4576-4579.

Woodward, E. M. S., and Rees, A. P. (2001). Nutrient distributions in an anticyclonic eddy in the northeast Atlantic Ocean, with reference to nanomolar ammonium concentrations. *Deep-Sea Research II* **48,** 775-793.

Wright, R., and Hobbie, J. E. (1966). Use of glucose and acetate by bacteria and algae in aquatic ecosystems. *Ecology* **47,** 447-464.

Yurkov, V. V., and Beatty, J. T. (1998). Aerobic anoxygenic phototrophic bacteria. *Microbiology Molecular Biology Review* **62,** 695-724.

Zehr, J. P. (2001). Unicellular cyanobacteria fix N_2 in the subtropical North Pacific Ocean. *Nature* **412,** 635-638.

Zehr, J. P., and Ward, B. B. (2002). Nitrogen cycling in the ocean: new perspectives on processes and paradigms. *Applied and Environmental Microbiology* **68,** 1015-1024.

Zengler, K., Toledo, G., Rappe, M., Elkins, J., Mathur, E. J., Short, J. M. and Keller, M. (2002). Cultivating the uncultured. *Proceedings of the National Academy of Sciences* **99,** 15681-15686.

ZoBell, C.E. (1946) Marine Microbiology. In Chronica Botanica Co., Waltham, Massachusetts, xv, 240 pp.

Zubkov, M. V., Fuchs, B. M., Archer, S. D., Kiene, R. P., Amann, R., and Burkill, P. H. (2001a). Linking the composition of bacterioplankton to rapid turnover of dissolved dimethylsulphoniopropionate in an algal bloom in the North Sea. *Environmental Microbiology* **3,** 304-311.

Zubkov, M. V., Fuchs, B. M., Burkill, P. H., and Amann, R. (2001b). Comparison of cellular and biomass specific activities of dominant bacterioplankton groups in

stratified waters of the Celtic Sea. *Applied and Environmental Microbiology* **67,** 5210-5218.

Zubkov, M. V., Fuchs, B. M., Eilers, H., Burkill, P. H., and Amann, R. (1999). Determination of total protein content of bacterial cells by SYPRO staining and flow cytometry. *Applied and Environmental Microbiology* **65**, 3251-3257.

Zubkov, M. V., Mary, I., Woodward, E. M. S., Warwick, P. E., Fuchs, B. M., Scanlan, D. J., and Burkill, P. H. (2007). Microbial control of phosphate in the nutrient-depleted North Atlantic subtropical gyre. *Environmental Microbiology* **9,** 2079-2089.

Zubkov, M. V., Sleigh, M. A., and Burkill, P. H. (1998a). Measurement of bacterivory by protists in open ocean waters. *FEMS Microbiology Ecology* **27,** 85-102.

Zubkov, M. V., Sleigh, M. A., and Burkill, P. H. (2000). Assaying picoplankton distribution by flow cytometry of underway samples collected along a meridional transect across the Atlantic Ocean. *Aquatic Microbial Ecology* **21,** 13-20.

Zubkov, M. V., Sleigh, M. A., and Burkill, P. H. (2001c). Heterotrophic bacterial turnover along the 20^{o}W meridian between 59^{o}N and 37^{o}N in July 1996. *Deep-Sea Research II* **48,** 987-1001.

Zubkov, M. V., Sleigh, M. A., Tarran, G. A., Burkill, P. H. and Leakey, R. J. G. (1998b). Picoplankton community structure on an Atlantic transect from 50 ºN to 50 ºS. *Deep-Sea Research I* **45,** 1339-1355.

Zubkov, M. V., Tarran, G. A., and Fuchs, B. M. (2004). Depth related amino acid uptake by Prochlorococcus cyanobacteria in the Southern Atlantic tropical gyre. *FEMS Microbiology Ecology* **50,** 153-161.

Zweifel, U. L., and Hagström, A. (1995). Total counts of marine bacteria include a large fraction of non-nucleoid-containing bacteria (ghosts). *Applied and Environmental Microbiology* **61,** 2180-2185.